WIND TUNNEL MODEL STUDY OF DIFFUSION FROM A STEAM ELECTRIC GENERATING PLANT AT STOCK ISLAND, KEY WEST, FLORIDA

by

R. N. Meroney
J. E. Cermak
B. T. Yang
S. Veenhuizen
C. R. Symes

Prepared Under Contract to
R. W. Beck and Associates
Denver, Colorado

Fluid Dynamics and Diffusion Laboratory
College of Engineering
Colorado State University
Fort Collins, Colorado

August 1969
Revised December 1969

CER69-70RNM-JEC-BTY-SV-CRS14

ABSTRACT

Tests were conducted in a meteorological wind tunnel to determine the distribution of gas concentrations resulting from gaseous plumes released from stacks associated with the steam electric generating plant to be constructed at Key West, Florida, on Stock Island. The tests were conducted over a model of the generating station including all proposed future expansions. Data obtained included photographs of model smoke plume trajectories and contaminant concentrations along the plume centerline at elevated and ground level sampling positions. Effects of wind orientation and thermal stratification were also analyzed.

Evaluation of test results revealed the plant buildings did not appear to aggravate the pollution condition. However, a simple analysis suggests that SO_2 scrubbing equipment may seriously aggravate the already marginal situation.

TABLE OF CONTENTS

LIST OF FIGURES

LIST OF FIGURES - (Continued)

LIST OF FIGURES - (continued)

LIST OF FIGURES - (Continued)

LIST OF SYMBOLS

Symbol		Definition	
A	=	Area of the projection of the power station building on a plane transverse to the upstream flow direction	(L^2)
C	=	Entrainment parameter	(-)
C_p	=	Specific heat capacity	$(L^2T^{-2}\theta^{-1})$
d	=	Stack diameter	(L)
D	=	Dilution factor	(-)
$f(\theta,S,N)$	=	Frequency	(%)
F	=	Plume buoyancy parameter	(L^4/T^3)
g	=	Gravitational constant	(L/T^2)
h	=	Effective stack height $(h = h_s + \Delta h)$	(L)
Δh	=	Plume rise	(L)
H	=	Power station effective building height	(L)
K	=	Concentration isopleth	(-)
L	=	Reference length	(L)
M	=	Molecular weight	(-)
Q	=	Source strength	(conc/T)
R_e	=	Reynolds number $\frac{VL}{\nu}$	(-)
R_i	=	Richardson number $\frac{g\Delta TL}{V^2T}$	(-)
R_1	=	Critical velocity ratio at 300 m	(-)
R_2	=	Critical velocity ratio at 150 m	(-)
S	=	Stability parameter $\frac{g}{T}\frac{d\theta}{dz}$	$(1/T^2)$
T	=	Temperature	(θ)
ΔT	=	Temperature difference across some reference distance or layer	(θ)

LIST OF SYMBOLS - (Continued)

Symbol		Definition	
V	=	Velocity at stack height	(L/T)
W	=	Stack exit velocity	(L/T)
x,y,z	=	General coordinates - downwind, lateral, upward	(L)
z_o	=	Surface roughness parameter	(L)
χ	=	Local concentration	(conc/L^3)
τ	=	Sampling time	(T)
θ	=	Potential temperature	(θ)
or	=	Azimuth angle of upwind direction measured from plant north	(-)
σ	=	Standard deviation of either plume dispersion or wind angle fluctuations	(L)
ν	=	Kinematic viscosity	(L^2/T)
δ	=	Boundary layer thickness	(L)

Subscripts

s	=	Stack
S	=	Stability condition
N	=	Wind speed class
∞	=	Free stream
m	=	Model
p	=	Prototype
a	=	Axial
max	=	Maximum
c	=	Critical

I. INTRODUCTION

Commercial fossil fuel steam electric generating stations generally require an analysis of the potential behavior of gaseous effluents emitted to the atmosphere as a result of combustion processes. Current design practice incorporates processes to reduce particulate and gaseous chemical effluents to a minimum; however, it is generally still necessary to release some small quantity of residual wastes to the atmospheric environment. Used wisely the atmospheric reservoir permits disposal without damage or nuisance; used without due consideration for its widely varying dispersion capacity, pollutants may at times remain at sufficiently high concentrations near the ground to cause annoyance, illness, or even death.

A primary factor in determining whether these gaseous products are to be a nuisance is the stack design. Under certain hypothetical conditions, it may be necessary to make a release in meteorologically unfavorable situations. Hence, it is necessary to design gas exhaust systems such that adequate dispersal of gaseous materials will occur under any plausible condition.

It has been a traditional design technique to release the various gases through the top of a tall stack located near the power station, where the stack is at least two and one-half times taller than nearby buildings. Calculation of peak and mean ground concentrations of these gases are then based on some semi-empirical model which relates the release rate from an elevated point source to the concentration at some point downwind. Models have been suggested by Sutton, Hay and Pasquill, Roberts and Cramer.[1,2,3,4] These models require the assumptions of plane homogeneous atmospheric turbulence and constant mean lateral and mean vertical velocities. These assumptions are satisfied for a point release over a flat undisturbed terrain.

In addition, considerable effort has been made to determine the effects of vertical stack velocity and gas buoyancy on the effective stack release height. Recently Carson and Moses[5] have reviewed over 15 plume rise formulas constructed to calculate effective stack heights for conditions where there are no effects from local terrain or buildings. They concluded that no available plume rise equation can be expected to accurately predict short term plume rise.

Often it is necessary, due to aesthetic, cost, and public relation reasons, to utilize a shorter stack. Such is the case for the proposed station on Stock Island where local aviation restrictions require that vertical obstructions be less than 120 feet in height. In these cases plume dispersion is sufficiently modified by the presence of the local building structure or ground topography that the only approach available is one of wind tunnel model tests.[6,7]

A number of wind tunnel studies have considered the effects of variations in a single building geometry on plume entrainment and dispersion.[8,9,10,11] These studies have permitted the specification of pertinent scaling criteria for model studies of plume excursions near buildings. Model laws will be discussed in greater detail in Section II.

Since each arrangement of the power plant and auxiliary buildings or terrain may have separate effects on the generation of mechanical turbulence and mean flow movement, any specific gas dispersion problem will require individual tests. Hence, there exist in the literature descriptions of a variety of different model studies on reactor and industrial plants.[7,12,13,14,15,16,30,31] These studies are significant in that their results have been essentially confirmed by either direct prototype measurements or the absence of the gases or dusts the study was directed to remove.

References 12), 13), 15), and 16) incorporate such comparisons within their text. Reference 7) has recently been compared with prototype measurements at the National Reactor Testing Station in Southeast Idaho.[17] Agreement of the diffusion concentration results were very satisfactory. Martin favorably compared his wind tunnel study measurements about a model of the Ford Nuclear Reactor at the University of Michigan with prototype measurements.[16] Finally, Munn and Cole have taken diffusion measurements on a power station complex at the National Research Council, Ottawa, Canada, to confirm the general entrainment criteria suggested by the model studies of Davies and Moore.[13,18]

It is the purpose of this study to investigate the effect of the Stock Island Power Station complex on effluent releases from a short stack, to determine the wind direction configuration for maximum entrainment, and to determine the feasibility of increasing stack velocity and flow rate to elevate the plume to a level where entrainment into the building separation cavities and subsequent dispersion at ground level is absent.

In Section II the modeling criteria necessary to simulate atmospheric motions over such a site are listed. Section III describes the experimental equipment. Finally, Sections IV, and V discuss the results obtained and their significance.

II. SIMULATION OF ATMOSPHERIC MOTIONS

The use of wind tunnel for model tests of atmospheric gas diffusion is dependent on the expression of concentration results in a non-dimensional coefficient whose value is independent of the variations in scale between model and prototype. The concentration coefficients will only be independent of scale if certain similarity criteria are met by the modeled flows. These criteria are generally understood as a result of analysis or experience, and they are discussed in detail in References 8, 16, and 19. Basically, these model laws may be divided into the areas of geometric, dynamic, and kinematic similarity. In addition, one must specify equivalent upstream and ground boundary conditions.

For the present case of the Stock Island site, geometric similarity is satisfied by an undistorted model of size ratio 1:200. This scale ratio was chosen to optimize measuring scale and minimize wind tunnel blockage*. In addition, this scale ratio allowed the wind tunnel boundary layer to extend a distance above the model complex.

Dynamic similarity is dependent upon equivalence of the inertial to buoyancy force ratio from model to prototype. Normally, this is assumed by equivalence of the atmospheric Froude number (Richardson number) and the control of stack gas densities; however, since it was projected that the gaseous plume temperature would be in a saturated condition at 135 to 140°F as a result of a sulpher dioxide scrubbing system, it was assumed

---

*A consideration in the selection of model scale is the degree of blockage presented by the model. The ratio of projected model area to area of the wind tunnel cross-section should not exceed 1 to 2%. A scale of 1:200 for the Stock Island facility produces a blockage ratio of 2%.

the effluent was near ambient temperatures. This was considered to be a conservative assumption since the actual behavior of a wet saturated plume is impossible to simulate. When a wet plume is cooled by evaporation a condition of negative buoyancy may create downwash to the ground.[40,43,44] As far as the authors know there is no quantitative manner in which to predict this phenomena; hence, one usually corrects by intuition and decreases the effective release height during calculations.

Recent model measurements of flow over obstacles under stably stratified conditions have indicated that fumigation might occur downstream of an elevated gaseous source due to wave like motion set up in the "lee" of the structure (Reference 37). The effect of such large scale excursions on a diffusing plume have not been previously modeled. Studies by Martin (Reference 16) and Golden (Reference 32) involved examination of releases under stratified conditions; however, the gas plumes were emitted from very short stacks (~3 m from roof top) essentially directly into the cavity region; hence, one would expect their measurements to be dominated by the building geometry and not the stratification.

An examination of weather records for the Key West vicinity indicated the occurances of inversion conditions were low[42] since the warm waters of the gulf of Mexico tend to inhibit their development. However, it was considered important to examine the condition of a ground based inversion over the Stock Island model since these meteorological conditions are generally considered most unfavorable. Plume concentrations may remain extremely high over large distances and may be trapped underneath such a "lid" for extended periods.[38]

For stable thermal stratification (inversions) flow similarity requires equality of the Richardson number

$$R_i = \frac{g(\Delta T)L}{V^2 T}$$

for model and prototype flows. In this expression g is the gravitational acceleration, ΔT is the temperature difference between surface and a point at the elevation L (stack height); V is the wind speed at height L, and T is the mean temperature over the layer to elevation L in absolute degrees. The model Richardson number was adjusted to suspected prototype values by cooling the floor of the wind tunnel and by heating the tunnel air stream.

Hence, non-buoyant model plume densities and both neutral and stable stratification conditions were simulated.

Kinematic similarity requires the scaled equivalence of streamline movement of the air over prototype and model. It has been shown by Golden[7] that flow around geometrically similar sharp-edged buildings at ambient temperatures in a neutrally stratified atmosphere should be dynamically similar when the approaching flow is dynamically similar. This approach depends upon producing flows in which the flow characteristics become constant (independent of Reynolds number) if a lower limit of the Reynolds number is exceeded. For example, the resistance coefficient for flow in a sufficiently rough pipe as shown in Schlichting (20, p 521) is constant for a Reynolds number larger than 2×10^4. This implies that surface or drag forces are directly proportional to the mean flow speed squared. In turn, this condition is the necessary condition for mean turbulence statistics such as root-mean square value and correlation coefficient of the turbulence velocity components to be equal for the model and the prototype flow.[8,19]

Golden, as cited by Halitsky[7,8], found that for flow about a cube for Reynolds numbers above 11,000, there was no change in concentration

measurements. The minimum Reynolds number encountered in the present study was 30,000 based on the model width of 1.5 ft and a minimum velocity of 3 fps. Correlation tests of flow about the Rock of Gibralter, flow over Pt. Arguello, California, and flow over San Nicolas Island, California, may be cited as examples of large Reynolds number flows which have been modeled successfully in a wind tunnel.[21,22,23]

Buildings and building complexes produce nonuniform fields of flow which perturb the regular upstream atmospheric wind profiles. Around each building a boundary layer exists, where the velocity is zero at the surface but increases rapidly to a relatively constant value a short distance from the building wall. Outside of the boundary layer and downstream there exists a region of low velocities and pressures called the cavity. In this region circulations are such that flow may actually reverse with respect to the upstream winds. Surrounding the cavity but extending further downstream is a parabolic region called the wake in which the presence of the building is still evident in terms of deviations of velocity, turbulence, and pressure from conditions found in the upstream atmospheric boundary layer, (See Figure 3).

The formation of the wake and cavity regions are associated with a phenomena called boundary-layer separation. Under certain conditions the boundary layer actually detaches and enters the flow streaming about the building. This may occur at the corner of a sharp edged building or on a curved surface if the pressure increases due to a decelerating flow field. The separated boundary layer forms a sheet which completely surrounds the cavity region which contains relatively stagnant fluid. The extent of the cavity region for the Stock Island Power Station building may be

approximated by $5H \cong 250$ feet. Based on the measurements of Evans (Reference 10) the effect of alternate wind approach angles to an elongated rectangular complex may extend this to $6H \simeq 300$ feet.

The interaction of the emitted effluent with the wind is governed by the ratio of their respective momenta.[7,8,9,13,16] When the prototype and model plumes have the same density this reduces to a ratio of velocities. In this study the stack areas were geometrically scaled and the velocity ratios studied ranged from 0.5 to 10.9. The wind velocity was adjusted in a range from 3 to 60 feet per second.

Finally, the need for scaling of the atmospheric mean wind profile is demonstrated in Reference 11. Substitutions of a uniform velocity profile for a logarithmic profile results in three fold variation in the dimensionless pressure coefficient downstream of a model building. Such variance in the pressure fields indicates a strong effect of the upstream wind profile on the kinematic behavior of the fluid near the building complex. The only tunnel currently capable of generating a turbulent boundary layer thick enough for a 1:200 model scale is the Meteorological Wind Tunnel at Colorado State University. Other investigators have attempted to generate logarithmic profiles in short tunnels by inserting special grids upstream of the test section; however, this technique normally creates a nontypical turbulence field which decays rapidly downstream.

The length scale used for scaling the velocity profile is the roughness height z_o.[19] For the Stock Island site typical roughness lengths for land to sea breezes is assumed to be less than 3 feet, while sea to land winds may be typified by a length less than 1/2 inch.[24] This means

the critical sea to land wind velocities could be modeled in the wind tunnel by a roughness length of less than 1/400 inch, or essentially a smooth upstream surface. A turbulent boundary layer approximately 2 feet thick was produced by an upstream fetch of 40 feet in the wind tunnel.

III. TEST APPARATUS

A. Wind Tunnel

Tests were conducted on the Army Meteorological Wind Tunnel in the Fluid Dynamics and Diffusion Laboratory at Colorado State University. The tunnel, specifically designed to study fluid phenomena of the atmosphere, has a 6 foot square by 50 foot long test section with an adjustable ceiling to provide a zero pressure gradient over modeled terrain,[25] (See Figure 1). A trip fence, located just upstream from the test section serves to stabilize the flow pattern as well as provide a thicker turbulent boundary layer. Mean velocities may be adjusted between 0 to 100 fps, and boundary layers 2 feet thick may be obtained.

B. Model

The model consisted of the power station, the stack, and the auxiliary buildings constructed to a linear scale of 1:200. The basic flat topography was reproduced by maintaining the model complex on a large circular plywood sheet which could be rotated into various wind attack angles. The surface roughness was typically $\frac{1}{2}$ inch for the prototype and could be satisfactorily modeled by the smooth tunnel floor. Figure 2 shows two views of the model in the tunnel. Stack 1 is on the left in the plan view.

The model was built to dimensions taken from a R. W. Beck & Associates Drawing, 115-G-102C. The four stacks were constructed from lucite plastic and were scaled to an equivalent height of 110 feet. The chimney top was a truncated cone faired at an angle of 15° down to an equivalent exit diameter of 4.67 feet. This diameter was chosen based on the stipulation of a 120 ft/sec stack velocity, gaseous temperatures of 140°F, and saturated gaseous products emitted from the boiler at a rate of 400,000 lbs/hr.

C. Wind Profiles, Pressure, and Turbulence Measurement

A pitot-static tube was used to measure upstream velocity profiles and set mean tunnel speeds. Pitot-static tube output was analyzed by a Transonic Model A, Type 120 electronic pressure meter. Turbulence intensities were measured under several conditions to specify the range of eddy sizes in the approach flow. A hot-wire anemometer system was utilized for these measurements.

D. Visualization Techniques

Smoke was used to define plume behavior over the power plant complex. The smoke was produced by bubbling compressed air through a container of titanium-tetrachloride located outside the wind tunnel and transported through the tunnel wall by means of a tygon tube terminating at the stack inlet within the model complex. A visible record was obtained by means of pictures taken with a Speed-graphic camera utilizing Poloroid film for immediate examination.

Titanium-tetrachloride and water vapor combine in an exo-thermal reaction to form the smoke particulates as a result the smoke was ~+ 7°F hotter than ambient for the neutral tests and -10°F cooler than the ambient temperature at stack level for the $\Delta T = 100°F$ case. However, it is not expected that these differences had very strong influence in the model experiment.

E. Gas Tracer Technique*

After the flow in the tunnel was stabilized, a mixture of Kr-85 and air was released from the power plant stack,[3] and samples of air were withdrawn from the tunnel and analyzed. The flow rate of Kr-85 mixture was controlled by a pressure regulator at the bottle outlet and monitored by a Fisher and Porter flowmeter. Source concentration was varied from .203 to 1.760 μ-curie/cc of Kr-85, a beta emitter (half life - 10.3 years).

A sampling rake of eight probes was manufactured from 2 mm diameter hypodermic tubing and was mounted on a traversing carriage whose horizontal and vertical position was controlled remotely from outside the tunnel. Concentrations were measured at ground levels at various scaled distance from 200 to 400 feet downwind and at vertical elevations centered on plume maximum concentrations. Samples were aspirated at a constant rate of 500 cc/min into eight TGC-308 Tracerlab Geiger Mueller side wall cylindrical counters. Samples were flushed through the counting tubes for at least two minutes, valve A in Figure 5B was closed, and each sample was subsequently counted for one minute on a Nuclear Chicago Ultra-scaler Model 192A. All samples counted were adjusted for background radiation (See Figure 4a and 4b).

*This apparatus was developed under the Public Health Service, Contract No. DHEW, 5R01 AP00091-07.

IV. TEST PROGRAM AND RESULTS

A. Test Program

The test program consisted of (1) a qualitative study of the flow field around the power plant by visual observation of the smoke plume trajectory released from the stacks; and (2) a quantitative study of gas concentrations produced by the release of Kr-85 from the stacks. The test conditions are summarized in Tables 1 and 2. The test program was accomplished in two parts: Phase A involved neutral stratification and Phase B involved stable stratification.

Angular locations of the approach winds are referred to in terms of azimuth angles from magnetic north. Downwind distances refer to lengths as measured from the stack location. Unless otherwise noted, the term wind velocity refers to the velocity in the free stream above the tunnel boundary layer; however, a velocity at any reference height is available by referring to the velocity profiles (Figures 5 and 6).

B. Test Results: Visualization

The test results consist of photographs and sketches showing the general nature of air flow and diffusion in the vicinity of the power station, (Figure 7 to Figure 36). A general understanding of wake and cavity flows is necessary for an interpretation of the plume behavior (see Reference 8).

The sequence of photographs shown in Figure 7 shows side views of the behavior of a smoke plume released at various free stream velocities. At low wind speeds the plume breaks through the streamline separating the cavity and the displaced plume flows above the complex. Subsequently the gas behaves as a plume released at an elevated point and is convected

downstream. As the wind speed increases the stack effluent plume is bent over and behaves as though it were released at increasingly lower effective heights. At a sufficiently large free stream velocity the plume intermittently fails to penetrate the building cavity streamline, and gas is brought to the ground at points near the building. At even higher wind speeds the plume becomes completely entrained in the building cavity. Entrainment, as utilized herein, will be understood as the presence of any of the gas released from the stack in the power station cavity. A small amount of entrainment usually first occurs under conditions where the gas plume follows the cavity separation stream line to the downstream cavity stagnation point from which it diffuses upstream into the cavity proper. Downwash will be understood as severe entrainment where the plume does not penetrate the separation stream-line but rather ventilates directly into the cavity region. Figures 8 to 36 display typical outlines of the visual smoke plume for various wind speeds and wind approach angles and thermal stratification conditions for both Phases A & B of the program.

For most wind approach angles (0° to 300°) the building complex appears to have a similar effect on plume entrainment. Davies and Moore suggested quantitative criteria for the tendency of a building to draw a gaseous plume released from a stack into the separation cavity.[13] They suggested the specification of the ratios, R_1 and R_2, of stack velocity to reference wind speed at which continuous plume contact becomes evident at distances of 1000 ft and 500 ft downstream from the source position. The critical velocity ratio R_2 of efflux velocity to wind velocity at which the turbulent motions in the wake region were great enough to disrupt the plume and produce contact at an equivalent distance of 500 ft downstream was between 0.5 and 1.0.

In Phase B two conditions of stratification were utilized to determine if the effects of downwash on the effluent dispersion would be aggravated. No lee wave like behavior appears to occur as a result of the stratification; however, the damping behavior of the stratification does appear to limit vertical dispersal as the Richardson number increases.

C. Test Results: Concentration Measurements

Since the conventional point-source diffusion equations cannot be used for predicting diffusion near objects which cause the wind to be non-uniform and nonhomogeneous in velocity and turbulence, it is necessary to calculate gaseous concentrations on the basis of experimental data. It is convenient to report dilution results in terms of a nondimensional factor independent of model to prototype scale.

In References 8 and 16 the problem of similarity for diffusion plumes is discussed in detail. It is suggested that concentration measurements be transformed to K-isopleths by the formula

$$K = \frac{\chi}{Q/AV}$$

where χ = sample volume concentration

A = frontally projected area of power plant complex

V = mean wind velocity at some reference height

Q = gas source release rate.

This expression is specifically suitable for measurements within the near-wake and cavity region. Data reported herein, however, represent measurements made at equivalent distances of 4,000 ft from the power plant. In this case it was considered more suitable to interpret results in terms of a different dimensionless parameter - D , a dilution factor, where

$$D = \frac{\chi}{\chi_s} = \left(\frac{\chi}{\chi_{max_x}}\right) \times \left(\frac{\chi_{max_x}}{\chi_s}\right)$$

and

χ = sample volume concentration

χ_s = concentration of source gas at release

χ_{max_x} = maximum concentration at downstream location of x .

The Kr-85 source strength utilized for this series of measurements varied from 1.760 to 0.203 μcuries/cc.

Concentration measurements were made at various downwind distances in the vertical and horizontal planes. Count rates were corrected to concentration in μμcuries and compensation was made for Geiger Mueller tube deadtime. The resulting profiles are typically displayed as Figures 49 to 58.

Since measurements were made at a variety of wind approach angles, wind velocities, and stack positions, the ground level concentration data is also reported in terms of the ratio $V\,\chi/Q$ which has units of length squared. For dispersion in a homogeneous flow this should produce similarity for various V values. The significance of all results are discussed in the following section (see Figure 59).

When interpreting model diffusion measurements it is important to remember that there can be considerable difference between the instantaneous concentration in a plume and the average concentration due to horizontal meandering. The average dilution factors near a building complex will correlate well with wind tunnel dilution factors since the mechanical turbulence of the wake and cavity region dominate the dispersion. In the wind tunnel a plume does not generally meander due to the absence of large scale eddies. Thus, it is found that field measurements of peak

concentrations, which effectively eliminate horizontal meandering, should correlate with the wind tunnel data.[16] In order to compare downwind measurements of dispersion to predict average field concentrations it is necessary to use data on peak-to-mean concentration ratio as gathered by Singer, et al.. Their data is correlated in terms of the gustiness categories suggested by Pasquill for a variety of terrain conditions.[27] It is possible to determine the frequency of different gustiness categories for a specific site.[28] Direct use of wind-tunnel data at points removed from the building cavity region may underestimate the dilution capacity of a site by a factor of 4 unless these adjustments are considered.[16]

An alternate technique has also been suggested by Hino who argues the relationship between the maximum of time-mean ground concentration χ_{max} and the sampling time is $\chi_{max} \sim \tau^{-\frac{1}{2}}$.[45] Field experiments may be compared with wind-tunnel data by the formula:

$$(\chi_a)_p = \frac{(\chi_a)_m \, Q_p \, V_p^{-1} \, h_p^{-2}}{Q_m \, V_m^{-1} \, h_m^{-2}} \left(\frac{\tau_p}{\tau_m}\right)^{-1/2}$$

where χ_a is the maximum axial concentration, Q discharge rate of gases from a stack, V wind speed, h effective height of stack, τ sampling time, and subscripts p and m represent values for a prototype and model respectively.[46] One may assume that τ_m corresponds to 3 to 5 minutes in the atmosphere for the wind tunnel experiment.[46] Pasquill's suggested values for the standard deviations σ_z and σ_y correspond to ten minute averages.[44] Hence tunnel concentrations could be high by a factor of 1.7

V. DISCUSSION OF RESULTS

Industrial designers must rely upon generalized dispersion formulae to predict concentrations in the vicinity of pollutant releases from tall stacks. Unfortunately one cannot depend upon the accuracy of such relations when nearby buildings are tall enough to cause aerodynamic perturbations upon the theoretical plume behavior. Hence, it is considered good practice to utilize wind-tunnel model studies to determine the range of validity of particular formulae and the necessity for correction coefficients for a particular application. It is with these thoughts in mind that the measurements over the Stock Island complex are interpreted. Corrections applied to plume rise near the source may provide a more reliable prediction of contamination at extended distances downstream by means of analytical expressions.[32,35,38,39,40,41]

The latest publications summarizing the "state of the art" for atmospheric diffusion estimates are very similar in detail.[32,41,44] There are some reasons however, to prefer some calculation methods over others; thus some of the relations will be discussed in detail below.

Effective Plume Height

While a smoke plume quickly attains the wind speed in the horizontal direction, its rise is determined by its vertical momentum and buoyancy. Numerous formulae have been published to correlate field measurements of plume rise; none is universally accepted, partially due to observational difficulties, and partially due to the fact that some plumes never really appear to level off.

Although Turner[44] recommends the use of Holland's plume rise formula it may be judged unnecessarily conservative. Stümke recommended the Holland formula be multiplied by a correction factor of 3.0. In addition more recent dimensional analysis formulas for buoyant sources give consistently good results for all source sizes and distances downwind and take into account atmospheric stability. The formulae below are conservative but not so severely conservative as other formulas. The A.E.C.-1968 monograph by Slade suggests the following expressions:

$$\text{Neutral} \quad \Delta h = 400 \frac{F}{V^3} + 1.5d \frac{W}{V} \tag{A}$$

$$\text{Stable with wind} \quad \Delta h = 2.6 \left(\frac{F}{VS}\right)^{1/2}$$

and

$$\text{Stable, calm} \quad \Delta h = 5.1 \, F^{1/4} S^{-3/8}$$

where

$$S = \frac{g}{T} \frac{d\theta}{dz}$$

$$F = \frac{T}{T_s} gW\left(\frac{d}{2}\right)^2 \left[\left(1 - \frac{M_s}{M}\right) + \left(\frac{T_s}{T} - 1\right) \left(\frac{(C_p)_s M_s}{C_p M}\right)\right]$$

$$\simeq \frac{\Delta T}{T_s} gW\left(\frac{d}{2}\right)^2$$

Figure 60 compares the analytical expression with the wind tunnel results for the Stock Island complex. A factor of 2.11 rather than 1.5 appears appropriate for the second term in equation A for neutral case; however, the effect of ground level inversion upon plume height is not strong until velocity ratios are less than two, a situation unlikely to occur. Figures

37 to 40 indicate the effects of wind approach angle upon plume behavior. Figures 41 to 43 compare the effect of velocity ratio variation for different wind approach angles. Figures 44 and 45 display stability effects. Figures 46 to 48 compare the effect of releasing from different stacks within the complex.

Finally, various formulae have been suggested to predict the transitional behavior of the smoke plume before it levels off. The curve in Figure 61 was suggested by Hoult, et al.[47] It is recommended that the height calculated from whichever of the formula above give the minimum rise in a given situation be utilized.

Maximum Ground Concentration

Often the limiting criteria for a particular stack release system is the maximum allowed ground concentration. Since the plume rise formulae recommended above incorporate the effect of atmospheric stability on plume rise it is possible to include their results in expressions which calculate the maximum probable concentration conditions directly. Again the A.E.C. monograph suggests:

$$\chi_{max} = 0.0065 \frac{Q}{F^{1/3} h_s^{5/3}}$$

at an actual velocity of:

$$V_c = 12.6 \, (F/h_s)^{1/3}$$

for a buoyant source in a neutral atmosphere. The corresponding equations for a nonbuoyant source are:

$$\chi_{max} = 0.01 \frac{Q}{W(\frac{d}{2})h_s}$$

and $V_c = 1.5 W\frac{d}{h_s}$. For the buoyant source in a stratified atmosphere, equation (5.33) in the A.E.C. monograph gives:

$$\frac{\chi_{max}}{Q} = \frac{0.05}{F^{1/2}S^{-1/4}(h_s + 5.1F^{1/4}S^{-3/8})} \quad .$$

The values for $\frac{\chi_{max}}{Q}$ in Table 3 were calculated by approximating,

$$S = \frac{g}{T_s} \frac{\Delta T}{h_s} \quad .$$

Table 3 compares the range of wind tunnel results with values obtained from the preceding equations. It is also possible to calculate the above information graphically as suggested by Turner (Problem 14, p. 49-50, Ref. 44).

Ground Level Concentration Distributions

Correct calculation of ground level dilution profiles depends, of course, on an accurate estimate of the effective stack height. Assuming such information is available the most popular expression is the Gaussian plume formulae:

$$\frac{\chi}{Q} = \frac{1}{\pi\sigma_y\sigma_z V} \exp\left[-\left(\frac{y^2}{2\sigma_y^2} + \frac{h^2}{2\sigma_z^2}\right)\right] \quad \text{where} \quad h = h_s + \Delta h \quad \text{and}$$

where the variance terms σ_y or σ_z are evaluated in terms of downwind distance and the stability condition. Authors such as Sutton, Calder,

Pasquill, Smith, and many others have suggested variance coefficient evaluation techniques.[32,41]

Probably the most convenient method currently is that developed by Pasquill where σ_y and σ_z figures have been prepared for simply defined stability categories. See Figures A.2 and A.3 and Table A.1 from the A.E.C. monograph.[32] Figures 3-2 through 3-9 in Turner's workbook also provide a convenient summary of ground level dilution for various height releases and atmospheric stability conditions. Figure 62 in this report incorporates the plume rise and plume dispersion formula into one graph for the case of a real stack height of 110 feet and neutral flow. Ground concentration profiles have been calculated for the conditions considered in the wind-tunnel study. Figures 59 and 62 compare analytical and wind tunnel concentrations. Table 3 compares corrected wind tunnel concentration measurements with some of the suggested prototype mathematical models. The wind tunnel results generally bracket the prototype prediction and in no case differ by even an order of magnitude. This accuracy is all that can be expected considering the stochastic nature of the diffusion phenomenon.

Negatively Buoyant Plume Effects

Recent practice in the air pollution control of fossil fuel power and heating plants frequently incorporate the use of wet flue gas-washing equipment to reduce particulate and SO_2 load levels. This equipment often saturates the flue gases and condenses water into cloud particles which are sufficiently small to avoid capture and emerge from the chimney top. After emission the effluent particles evaporate reducing the mean cloud temperature. Since wet washed plumes usually

emerge only slightly warmer than the surroundings, the cooling due to the condensed water usually far outweighs buoyancy due to initial excess temperature.[50] Such plumes with large negative buoyancy would effectively have a negative equivalent stack height and often reach the ground surface within a few hundred meters downwind. This awkward plume behavior may increase significantly the odor and toxicity at ground level, even beyond the values likely from the original unwashed flue gas. Scorer observed that on account of this effect, the plumes from the power plants at Battersea and Bankside in London usually reach the ground within a few hundred yards of the chimney when ambient turbulence is not large.[52]

The effect of evaporation on dense plumes has evidently not been taken into account in any of the published computations of pollution from power station chimneys emitting wet washed gases.[43] It is clear that computations based on the existing stack height formulas must fail since for the most part they produce complex numbers or ridiculous values for negative buoyancy conditions. This is not surprising since the most popular formulae represent regressions on experimental measurements confined to positively buoyant plumes.[32]

A number of authors have commented on the serious nature of the negatively buoyant plume.[32,41,43,48,49,50,51,52,53] None have proposed a rigorous correction procedure based on experimental evidence. Bodurtha made exploratory measurements of dense gas plume behavior in a wind tunnel utilizing visualization techniques. He concluded that "previously-existing atmospheric dispersion equations cannot be used with reliability to estimate the concentration of dense stack gases at the ground."[49] In addition, he recommended further tests in stable and unstable

atmosphere utilizing a tracer gas. Scorer emphasized that probable negative buoyancies obtained on an ordinary day are of sufficient magnitude to be of major importance.[43]

It is interesting to note that those involved in the design of SO_2 removal equipment are aware of this problem. As early as 1957, Field, et al.[54], commented on the probability of downwash with wet plumes in liquid scrubbing processes. In 1967 Katell justified the investment in dry removal processes which maintain flue gas temperatures of 200 to 900°F on the basis that additional dissipation may occur of the scrubbed gas.[53]

On the positive side of liquid scrubbing techniques Hawkins and Nonhebel argued that although the maximum or critical concentrations at ground level may be only slightly less than those obtained without scrubbing equipment the surface area affected by high concentrations is significantly reduced.[50] This conclusion holds however only if the maximum ground concentration with scrubbing is less than that obtained without scrubbing. In addition, gas washing removes most of any residual dust passing through the dust collector, and, consequently, little or no dust is visible in the path of the flue gases.

Potential values of concentration from a washed flue gas system are included in the typical set of calculations found in the next section.

Typical Concentration Results

Montgomery and Cain have compared the adherence of sulfur dioxide concentrations in the vicinity of a steam plant to plume dispersion models.[55] They concluded that general dispersion models cannot accurately predict specific pollutant concentrations that can be

expected to occur at a particular station at a specific time, but they can predict the range of concentrations likely to occur. Dispersion models generally incorporate a conservative bias, hence they also were found to successfully estimate maximum concentrations 93 to 99% of the time. Finally, the same mathematical model using different diffusion coefficients may yield very different results, hence the diffusion coefficients should be developed for the model at the particular site of application (if possible).

Keeping the above restraints and limitations of a prediction procedure in mind, dilutions obtained for the Key West configuration have been estimated for the input information shown in Table 4.

The equations presented in the previous sections have been utilized in their original form to calculate concentration levels as they might occur for the unscrubbed, scrubbed and neutrally buoyant, and scrubbed but negatively buoyant configurations. The lofting effect resulting from building geometry was not considered significant enough to incorporate in these results.

The effects of SO_2 pollutant on vegetation and human health are extensively reviewed in Volume 1 of Air Pollution edited by Stern.[51] It appears that it is desirable to maintain maximum 24 hour levels below 0.10 ppm and annual average levels below 0.02 ppm for a desirable environment. Criteria such as these must be utilized to evaluate the dispersion of gaseous wastes in the atmosphere. It should also be recognized that other sources exist in the environment not under the control of the power station.

Table 5 summarizes the results of the calculations discussed above. It is significant that if the washed plume does descend to the ground extremely hazardous situations may occur. The high concentrations

as a result of fumigation may be expected to be very transient; hence, dispersion in a neutral atmosphere may be a better criteria for selection of an optimum configuration.

A qualitative measurement of the aggravation of plume dispersion by the evaporation of entrained moisture is the potential decrease in plume temperature. Table 6.0 indicates the temperature depression as a result of from 2° to 10°F decrease in flue gas temperature as it travels up the stack. It is evident that even a slight temperature drop in the stack may cause an undesirable thermal situation.

Sea Breeze Effects on Atmospheric Dilution

Another factor which has not been previously discussed is the phenomena of the land-sea or sea-land circulation patterns. Recirculation may decrease the ability of the atmosphere to dilute the gaseous wastes. Differences in roughness between land and sea surfaces will cause wind shear and aerodynamic downwash effects. A complete site analysis should include an evaluation of the severity of such effects.[56]

VI. CONCLUSIONS AND RECOMMENDATIONS

Since specific maximum pollution levels were not known to the authors for the Florida power-station site, dimensionless prediction curves have been prepared in the manner of Pasquill for the Stock Island station configuration incorporating the modified effective plume rise formulae. Figure 62 displays ground concentration profiles versus longitudinal distance for a range of stack velocity ratios. If percent frequency of winds and stability conditions at various wind approach angles become available for the Stock Island site, average annual concentrations may be calculated in the manner of Hewson[38] or Sherlock and Lesher.[39]** If one desires to evaluate the concentrations expected during the meteorological significant situations such as looping, fanning, fumigation, or trapping one may combine the modified effective plume rise results with the expressions suggested by Bierly and Hewson[32] or Slade, Ch 3-3.5.[32]

Conclusion

1. Buildings have negligible influence on plume from 110' stack.
2. The effect of water vapor and plume cooling introduced by the scrubber may cause negative buoyancy.

**Note: See Appendix A for an approximation of the yearly average pollution levels based on simplified wind rose assumptions.

Recommendations

1. A complete air pollution analysis for the Stock Island Power Plant site should be performed utilizing the material discussed in Chapter V. An effort should be made to obtain more complete climatological data for the Key West area.
2. The qualitative anaysis reported herein is for only one stack; hence, pollution conditions should also be evaluated for future expansion to four stacks. It is recommended that the source strengths be added with no reduction for joint buoyancy effects.
3. It is suggested that a more concise estimate be obtained concerning the potential for release of a wet plume. The National Air Pollution Control Administration or the scrubber manufacturer should provide information concerning spray entrainment, subcooling of the flue gas, or potential condensation in the chimney stack itself.

REFERENCES

1. Sutton, O. G., "The Theoretical Distribution of Airborne Pollution from Factory Chimneys," Quar. J. R. Meteor. Soc. 73, p. 426 (1947).

2. Pasquill, F., Atmospheric Diffusion, D. Van Nostrand Co., London (1962).

3. Roberts, O. F. T., "The Theoretical Scaling of Smoke in a Turbulent Atmosphere," Proc. Roy. Soc., A. 104 , p. 640.

4. Cramer, H. E., "A Practical Method for Estimating the Dispersal of Atmospheric Contaminants," Proceedings, First Nat'l Conf. on Appl. Meteor, Amer. Meteor Soc., C. pp. 33-35. Hartford, Conn., (Oct. 1957).

5. Carson, J. E., and H. Moses, "Validity of Currently Popular Plume Rise Formulas," USAEC Meteorological Information Meeting, (September 11-14, 1967), Chalk River, Canada, AECL-2787, pp. 1-15.

6. Moses, H; G. H. Strom; and J. E. Carson, "Effects of Meteorological and Engineering Factors on Stack Plume Rise," Nuclear Safety, Vol. 6, No. 1, (Fall 1964), pp. 1-19.

7. Halitsky, J.; J. Golden; P. Halpern; and P. Wu, "Wind Tunnel Tests of Gas Diffusion from a Leak in the Shell of a Nuclear Power Reactor and from a Nearby Stack," Geophysical Sciences Laboratory Report No. 63-2, New York University, (April 1963).

8. Halitsky, J., "Gas Diffusion Near Buildings," Geophysical Science Laboratory Report No. 63-3, New York University, (February 1963).

9. Strom, G. H.; M. Hackman, and E. J. Kaplin, "Atmospheric Dispersal of Industrial Stack Gases Determined by Concentration Measurements in Scale Model Wind Tunnel Experiments," J. of APCA, Vol. 7, No. 3, pp. 198-204, (November 1957).

10. Evans, B. H., "Natural Air Flow Around Buildings," Research Report 59, Texas. Engineering Experiment Station, (1957).

11. Jensen, M., and N. Frank, "Model-Scale Test in Turbulent Wind, Part I," The Danish Technical Press, Copenhagen, (1963).

12. Kalinske, A. A., "Wind Tunnel Studies of Gas Diffusion in a Typical Japanese Urvan District," National Defense Res. Council OSCRD Informal Report No. 10.3A-48 and 48a, (1945).

13. Davies, P.O.A.L., and P. L. Moore, "Experiments on the Behavior of Effluent Emitted from Stacks at or Near the Roof Level of Tall Reactor Buildings," Int. Jour. Air Water Pollution. Vol. 8, pp. 515-533, (1964).

14. Sherlock, R. H., and E. A. Stalker, "The Control of Gases in the Wake of Smokestacks," Mechanical Engineering Vol. 62, No. 6, pp. 455-458, (June 1940).

15. Hohenleiten, H. L. von and E. Wolf, "Wind Tunnel Tests to Establish Stack Heights for the Riverside Generating Station," Trans ASME Vol. 64, pp. 671-683, (Oct. 1942).

16. Martin, J. E., "The Correlation of Wind Tunnel and Field Measurements of Gas Diffusion Using Dr-85 as a Tracer," Ph.D. Thesis, MMPP 272, University of Michigan, (June 1965).

17. Dickson, C. R., G. E. Start and E. H. Markee, Jr., "Aerodynamic Effects of the EBR-II Containment Vessel Complex on Effluent Concentrations," USAEC Meteorological Information Meeting, Chalk River, Canada, AECL-2787, pp. 87-104, (September 11-14, 1967).

18. Munn, R. E., and A. F. W. Cole, "Turbulence and Diffusion in the Wake of the Building" Atmospheric Environment, Vol. 1, pp. 34-43, (1967).

19. Cermak, J. E., et al., "Simulation of Atmospheric Motion by Wind-Tunnel Flows," Colorado State University, Report Number CER66-JEC-VAS-EJP-GJB-HC-RNM-SI-17

20. Schlichting, H., Boundary Layer Theory, McGraw Hill, New York, (1960).

21. Field, J. H., and R. Warden, "A Survey of the Air Currents in the Bay of Gibraltar, 1929-1930," Air Ministry, Geophys, Mem. No. 59, London (1933).

22. Cermak, J. E., and J. Peterka, "Simulation of Wind Fields Over Point Arguello, California, by Wind-Tunnel Flow Over a Topographical Model," Final Report, U. S. Navy Contract N 126(61756)34361 A(PMR), Colorado State University, Report Number CER65 JEC-JAP64, (December 1965).

23. Meroney, R. N., and J. E. Cermak, "Wind Tunnel Modeling of Flow and Diffusion Over San Nicolas Island, California," U. S. Navy Contract N123(61756)50192A(PMR), Colorado State University Report Number CER66-67RNM-JEC44, (September 1967).

24. Sutton, O. G., Micrometeorology, McGraw-Hill, 1953.

25. Plate, E. J., and J. E. Cermak, "Micro-Meteorological Wind-Tunnel Facility: Description and Characteristics," Fluid Dynamics and Diffusion Laboratory Report Number CER63EJP-JEC9, Colorado State University (1963).

26. Integrated Army Meteorological Wind-Tunnel Research Program, Eleventh Quarterly Progress Report, (1 November 1967 - 31 January 1968), 22 pages.

27. Singer, I. A., and I. Kazukiko, and G. D. Roman, "Peak to Mean Pollutant Concentration Ratios for Various Terrain and Vegetative Cover," Journal APCA, Vol. 13, No. 1, p. 40, (1963).

28. Singer, I. A., and M. E. Smith, "The Relation of Gustiness to Other Meteorological Parameters," Jour. Meteor. Vol. 10, No. 2, (1953).

29. Barry, P. J., "Estimation of Downwind Concentration of Airborne Effluents Discharged in the Neighborhood of Buildings," Atomic Energy of Canada, Limited, Report AECL-2043, (July 1964).

30. Meroney, R. N., Cermak, J. E., and Chaudhry, F. H., "Wind Tunnel Model Study of Shoreham Nuclear Power Station Unit 1, Long Island Lighting Company," Progress Report No. 1, FDDL Report CER68-69RNM-JEC-FHC-1, CSU, July 1968.

31. Meroney, R. N., Cermak, J. E., and Chaudhry, F. H., "Wind Tunnel Model Study of Shoreham Nuclear Power Station Unit 1, Long Island Lighting Company," Progress Report 2, CER68-69RNM-JEC-FHC-14, October, 1968.

32. Slade, D. H., Editor, "Meteorology and Atomic Energy, 1968," U. S. Atomic Energy Commission, TID-24190, July 1968.

33. Culkowski, W. M., "Estimating the Effect of Buildings on Plumes from Short Stacks," Nuclear Safety, Vol. 8, No. 3, Spring 1967, pp. 257-259.

34. Barry, P. J., "Estimation of Downwind Concentration of Airborne Efflients Discharged in the Neighborhood of Buildings," Canadian Report AECL-2043, July 1964.

35. Strom, G. H., "Atmospheric Dispersion of Stack Efflients," Air Pollution, Vol. I, Academic Press, New York, 1968, pp. 267-268.

36. Bryant, P. M., "Effect of Diluting Stack Gases on Downwind Concentration," Nuclear Safety, Winter 1966-67, Vol. 8, No. 2, pp. 161-164.

37. Lin, J. T.; and G. J. Binder, "Simulation of Mountain Lee Waves in a Wind Tunnel," Fluid Dynamics and Diffusion Laboratory Report, Colorado State University, CER67-68JTL-GJB24, (September 1967).

38. Hewson, E. W., "Stack Heights Required to Minimize Ground Concentrations," ASME Transaction, Vol. 77, 1955, pp. 1163-1172.

39. Sherlock, R. H. and E. J. Lesher, "Design of Chimneys to Control Downwash of Gases," ASME Transactions, Vol. 77, 1955, p. 1-9.

40. Bierly, E. W. and E. W. Hewson, "Some Restrictive Meteorological Conditions to be Considered in the Design of Stacks," Journal of Applied Meteorology, Vol. 1, 1962, pp. 383-390.

41. Smith, M., editor, "Recommended Guide for the Prediction of the Dispesion of Airborne Efflients," ASME, 1968.

42. Hosler, C. R. "Low-level Inversion Frequency in the Continuous United States," Monthly Weather Review, September 1961, pp. 319-339.

43. Scorer, Richard, Air Pollution, Pergamon Press, New York, 1968.

44. Turner, P. B. "Workbook of Atmospheric Dispersion Estimates," U. S. Dept. of Health, Education and Welfare, Public Health Service, Cincinnati, Ohio, 1969.

45. Hino, M. "Maximum Ground-Level Concentration and Sampling Time," Atmospheric Environment, Vol. 2, pp. 149-165, 1968.

46. Hino, M. "Computer Experiment on Smoke Diffusion Over a Complicated Topography," Atmospheric Environment, Vol. 2, pp. 541-558, 1968.

47. Hoult, D. P., et al. "A Theory of Plume Rise Compared with Field Observations," M.I.T. Fluid Lab. Pub. 68-2, March 1968 (PB 179 536).

48. Bosanquet, C. H., "The Rise of a Hot Waste Gas Plume," J. Inst. Fuel, Vol. 30, pp. 322f, (1957).

49. Bodurtha, F. T., Jr., "The Behavior of Dense Stack Gases," J. of APCA, Vol. 11, No. 9, pp. 431-437, (1961).

50. Hawkins, J. E., and G. Nonhebel, "Chimneys and the Dispersal of Smoke," J. of Inst. Fuel, pp. 530-545, (1955).

51. Stern, A. C., "Atmospheric Dispersion of Stack Effluents," Air Pollution, Vol. 1, Academic Press, New York, pp. 267-268, (1968).

52. Scorer, R. S., "The Behavior of Chimney Plumes," Int. J. Air Poll., Vol. 1, pp. 198-220 (1959).

53. Katell, S., "Removing Sulfer Dioxide from Flue Gases," Chemical Engineering Progress, Vol. 62, No. 10, pp. 67-73 (1966).

54. Field, J. H., L. M. Brunn, W. P. Haynes, and H. E. Bensen, "Cost Estimating of Liquid Scrubbing Processes for Removing of Sulfur Dioxide from Flue Gases," Journal of APCA, Vol. 7, No. 2, pp. 109-115 (1957).

55. Montgomery, T. L., and M. Cain, "Adherence of Sulfur Dioxide Concentrations in the Vicinity of a Steam Plant to Plume Dispersion Models," Journal of APCA, Vol. 17, No. 8, pp. 512-517 (1967).

56. Hewson, E. W., and L. E. Olsson, "Lake Effects on Air Pollution Dispersion," Journal of APCA, Vol. 17, No. 11, pp. 757-760 (1967).

Appendix A: Seasonal or Annual Concentrations at A Receptor from a Single Pollutant Source.[32,41,44]

For a source which emits at constant rate from hour to hour and day to day one may estimate an annual probability of dispersion based on stability wind "rose" data. A stability wind "rose" gives the frequency of occurrence for each wind direction (usually 16 points) of each wind speed class and stability category.

If the effluent is assumed uniformly distributed in each angular sector an appropriate equation for average concentration is then:

$$\frac{\chi(x,\theta)}{Q} = \sum_S \sum_N \left\{ \frac{2\, f\,(\theta,S,N)}{\sqrt{2\pi}\ \sigma_{zs}\ V_N\ (\frac{2\pi x}{16})} \exp\left[-\frac{1}{2} \left(\frac{h_V}{\sigma_{zs}}\right)^2 \right] \right\}$$

where $f(\theta,S,N)$ is the frequency during the period of interest that the wind is from the direction θ, for the stability condition, S, and wind speed class N.

$(\sigma_z)_S$ is the vertical dispersion parameter evaluated at the distance x for the stability condition S.

V_N is the representative wind speed for class N.

h_V is the effective height of release for the wind speed V_N.

When stability wind rose information is unavailable a first-order approximation may be made of annual concentrations by using the appropriate annual wind rose and assuming all releases occur in neutral stability class, Pasquill D.

Figure A-1 represents a representative annual wind rose for Key West, Florida calculated from data summary provided by the Data Processing Division, Climatic Center, USAF, Air Weather Service for Jan. 1949 to Dec. 1965.

Figures A-2 and A-3 are graphs on polar coordinates centered at the prospective Stock Island site of concentration in terms of $\chi/Q(\frac{sec}{ft^3})$. Effective stack heights were calculated assuming h_s = 110 feet and

$$\Delta h = 2.1\ d\ \frac{W}{V_\infty}\ ,\quad \text{where}\quad d = 4.67 \text{ feet.}$$

It is interesting to note that the annual concentrations are very symmetric despite the asymmetry of the annual wind rose. It is very probable that the patterns are dominated by those periods of high wind which occur somewhat uniformly in all wind sectors. The positions of the peak of the rather broad maximum have been indicated by stars in Figure A-3.

When two or more stacks are closely grouped they may have mutual influences. The plumes tend to merge into one but not with the same compactness as one plume. Plumes from multiple stacks will rise higher than from one of them but not as high as from one stack replacing all of them.[32] Near the power plant one finds release from two or more stacks may actually decrease the average concentration level; however, the vertical extent is usually limited by elevated inversions at some point, hence concentrations for a downwind are often a simple multiple of the single stack concentration.

TABLE 1

PROTOTYPE AND MODEL DIMENSIONS

	Prototype	Model
Stack Diameter	4.67 ft	0.28 in
Stack Area	17.13 ft^2	0.062 in^2
Stack Height	110.0 ft	6.60 in

TABLE 2

TEST CONDITIONS

Note: In last column, number in bracket refers to stack number and asterisk* signifies that smoke trace for this stack number is included in report.

θ°	ΔT(°F)	V	W	W/V	Max. Ground Conc. vs x	Vt. & Horiz. Conc. Profiles	Smoke Traces
40	0	55	33	0.6	Yes	No	No
		12	33	2.75	No	No	Yes (1,2,3,4)
	100	6	3	0.5	No	No	Yes (1,2,3,4)
		6	6	1	No	No	Yes (1,2,3,4*)
		6	12	2	No	No	Yes (1,2,3,4)
		6	8	3	No	No	Yes (1,2,3,4*)
		6	30	5	No	No	Yes (1,2,3,4*)
	100	6	3	0.5	No	No	Stacks 1,2,3 Operating Together
		6	6	1	No	No	
		6	12	2	No	No	
		6	18	3	No	No	
60	0	55	33	0.6	Yes	Yes	No
		Variable		0.95	No	No	Yes (1,2,3,4)
		"		2.75	No	No	Yes (1,2,3,4*)
		"		5.5	No	No	Yes (1,2,3,4)
80	0	Variable		0.95	No	No	Yes (1,2,3,4)
		"		2.75	No	No	Yes (1,2,3,4)
		"		5.5	No	No	Yes (1,2,3,4)
	50	3	3	1	Yes	No	Yes (1*,2,3,4)
		3	6	2	Yes	No	Yes (1*,2,3,4)
	100	6	3	0.5	Yes	Yes	Yes (1*,2*,3,4*)
		6	6	1	Yes	Yes	Yes (1*,2*,3,4*)
		6	12	2	No	No	Yes (1*,2*,3,4*)
		6	18	3	No	No	Yes (1,2,3,4)
		6	30	5	No	No	Yes (1,2,3,4)
100	0	55	33	0.6	Yes	No	No
				0.95	No	No	Yes (1*,2,3,4)
				2.75	No	No	Yes (1*,2,3,4)
				5.5	No	No	Yes (1,2,3,4)
	100	6	3	0.5	Yes	Yes	Yes (1*,2*,3,4*)
		6	6	1	Yes	Yes	Yes (1*,2*,3,4*)
		6	12	2	No	No	Yes (1*,2*,3,4*)

TABLE 2 – Continued

θ°	ΔT(°F)	V	W	W/V	Max. Ground Conc. vs x	Vt. & Horiz. Conc.Profiles	Smoke Traces
180	0			2.75	No	No	Yes (1,2,4)
				5.5	No	No	Yes (1,2,4)
				11	No	No	Yes (1,2,4)
				2.75	No	No	Yes (1-all, 4-all)
				5.5	No	No	Yes (1-all, 4-all)
				11	No	No	Yes (1-all, 4-all)
				2.75	No	No	Stacks 1,2,3 * operating together
				5.5	No	No	

Note: For the θ = 180° case, the effect of emission from stacks 2,3 and 4 on the smoke from stack 1 was examined. Smoke was emitted from stack 1, while air was emitted from stacks 2, 3 and 4. The abbreviation (1-all) implies this condition.

TABLE 3

DIFFUSION MODEL EQUATION COMPARISON WITH WIND TUNNEL RESULTS

	R_i	$(\frac{\chi_{max}}{Q})_{A.E.C.}$ (sec/ft^3)	$(\frac{\chi_{max}}{Q})_{wind\ tunnel}$ (sec/ft^3)	$(\frac{\chi_{max} V_c}{Q})_{A.E.C.}$ (ft^{-2})
Neutral Atmosphere Non-Buoyant Source	0	3.24×10^{-7}	1.63×10^{-7} to 5.0×10^{-7}	24.8×10^{-7}
Neutral Atmosphere Buoyant Source	0	1.96×10^{-7}	- -	68.1×10^{-7}
Stratified Atmosphere Buoyant Source $\Delta T = 50°F$, $(T_s)_m \simeq 86°F$	0.165	9.5×10^{-7}	10.4×10^{-7} to 28.2×10^{-7}	- -
Stratified Atmosphere Buoyant Source $\Delta T = 100°F$, $(T_s)_m \simeq 86°F$	0.083	14.3×10^{-7}	1.75×10^{-7} to 37.0×10^{-7}	- -

Note: Comparison of wind tunnel results with values calculated from A.E.C. concentration equations 5.28, 5.30 and 5.33. (All prototype units.) A correction factor of 4 has been applied to the wind tunnel results following the discussion of site dilution capacity in Chapter IV, Part C.

TABLE 4

DESIGN CRITERIA

Fuel burned	No. 6 Fuel Oil (Bunker C)
Firing rate	25,000 lbm/hr
Sulfur content	2.75% by weight, 1375 lbm/hr
Gas from boiler exit	
Temperature	350°F
Total pound-mole wet flue gas	55.22
Flow rate flue gas	426,000 lbm/hr 90,000 SCFM (wet basis)
SO_2 concentration	1375 lbm/hr (173.5 g/sec) 1556 ppm
Humidity	0.156 lbm moisture/lbm dry air
Gas from scrubber exit	
Temperature	150°F
Total pound-mole saturated flue gas	73.70
Flow rate flue gas	119,000 SCFM (wet basis)
SO_2 concentration	206 lbm/hr (26 g/sec)
(assume 85% removal)	175 ppm
Humidity	0.212 lbm moisture/lbm dry air
Gas from stack exit	
Temperature	140°F
Total pound-mole saturated flue gas	68.51
Flow rate flue gas	110,448 SCFM (wet basis)
SO_2 concentration	206 lbm/hr (26 g/sec) 188 ppm

TABLE 4 - Continued

Humidity	0.153 lbm moisture/lbm dry air
Suspended water droplets	0.059 lbm/lbm dry air
Velocity @ exit	120 ft/sec
Diameter exit	4.7 feet
Stack height	110 feet
Atmospheric environment conditions	
Temperature	80°F
Humidity	0.012 lbm moisture/lbm dry air (~50% humidity)
Pressure	14.7 psia

TABLE 5

MAXIMUM GROUND LEVEL CONCENTRATION FOR VARIOUS EXHAUST GAS CONFIGURATIONS

Configuration	T (°F)	W (ft/sec)	Q (lbm/hr)	d (ft)	F (ft^4/sec^3)	S ($1/sec^2$)	h_{eff} (ft)	χ_{max} ($\mu g/m^3$)	χ_{max} (ppm)	χ_{max} annual (ppm) (Fig. A-3)	V_c (ft/sec)
Unscrubbed flue gas (neutral atm)	350	120	1375	4.90	11,597	--	147	695	0.26	--	59.5
Unscrubbed flue gas (fumigation)	350	120	1375	4.90	11,597	0.00049	1032	409	0.15	--	--
Scrubbed flue gas (neutral buoyancy)	140	120	206	4.67	--	--	220	296	0.11	0.001	7.6
Scrubbed flue gas (fumigation)	140	120	206	4.67	2,226	0.00049	719	202	0.076	--	--
Scrubbed flue gas (negatively buoyant) (zero dilution)	140	120	206	4.67	--	--	0	498,673	188.0	--	--
	T effective after evaporation $\simeq$ 94°F										
Scrubbed flue gas (negatively buoyant) (dilution by 100)	140	120	206	4.67	--	--	0	4,986	1.88	--	--
	T effective after evaporation and dilution $\simeq$ 77.5°F										

TABLE 6

COOLING OF PLUME DUE TO EVAPORATION

Condition exhaust	T (°F)	ρ lbm moisture / lbm dry	r condensed	L @ T Btu/lbm	L @ 80°F Btu/lbm	ΔT of no dilution	ΔT of 100 dilution	T @ 100 dilution
Scrubber exhaust	150	.212	--	--	--	--	--	--
Stack exhaust	148	.198	.014	1009	1048.4	- 58.1	- .81	79.19
"	146	.186	.026	1010	"	-108	-1.12	78.88
"	144	.175	.037	1012	"	-154	-1.59	78.84
"	142	.162	.050	1013	"	-209	-2.15	77.85
"	140	.153	.059	1014	"	-246	-2.54	77.46

$\dot{m}$ = 421,000 lbm/hr flue gas dry

$\dot{m}$ = 426,000 lbm/hr flue gas wet

$$\Delta T = \frac{\dot{m}_{dry}(r)\ L\ @\ T}{\dot{m}_{wet}\ (C_{p_{air}})}$$

$C_{p_{air}}$ = 0.24 Btu/lbm°F

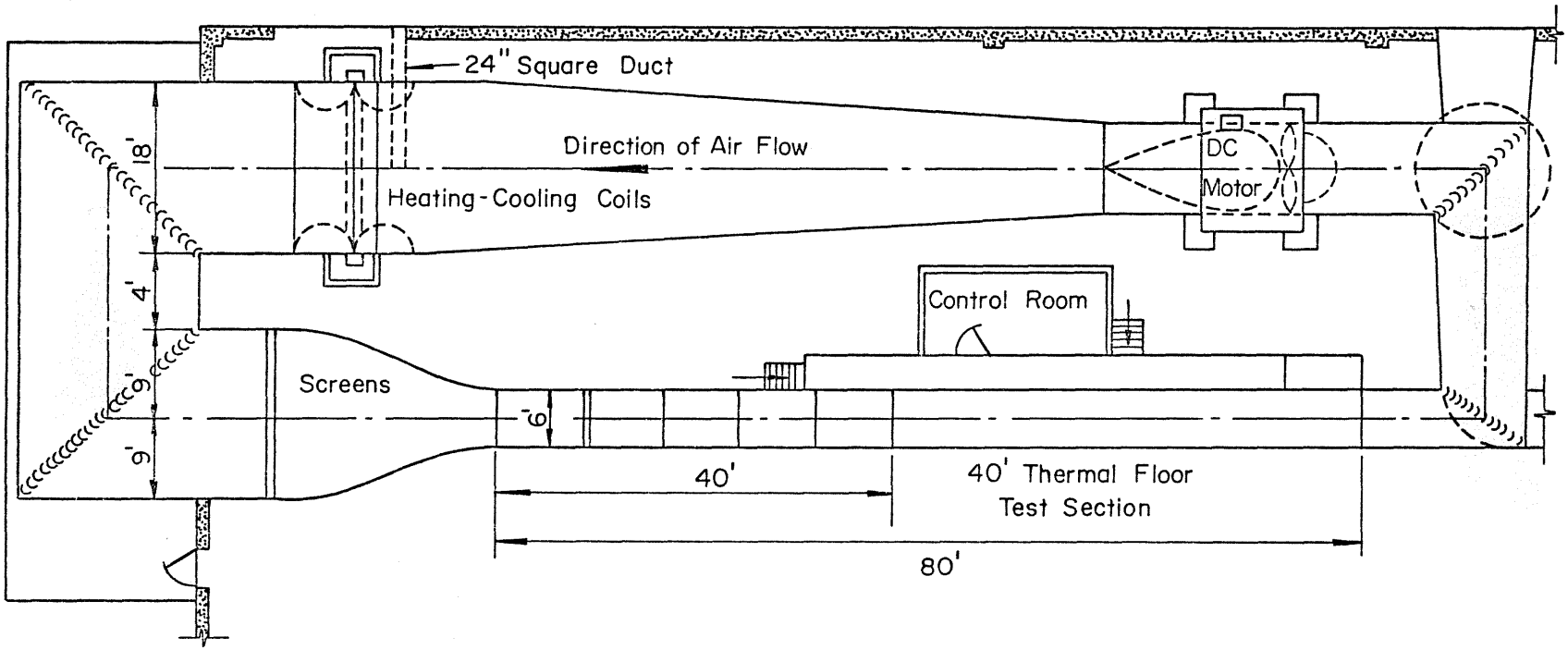

Figure 1. Army meteorological wind tunnel

Plan View

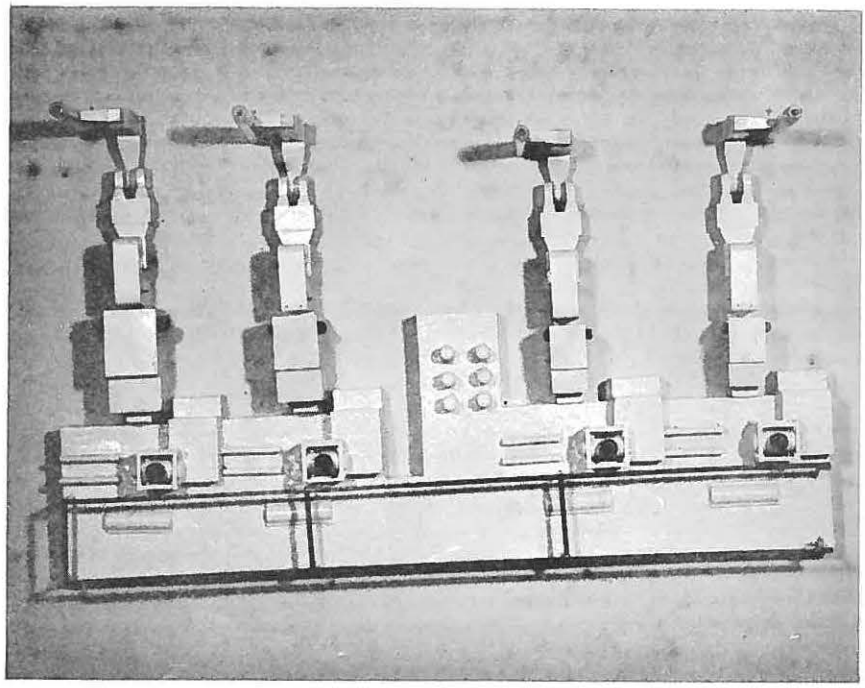

Elevated View

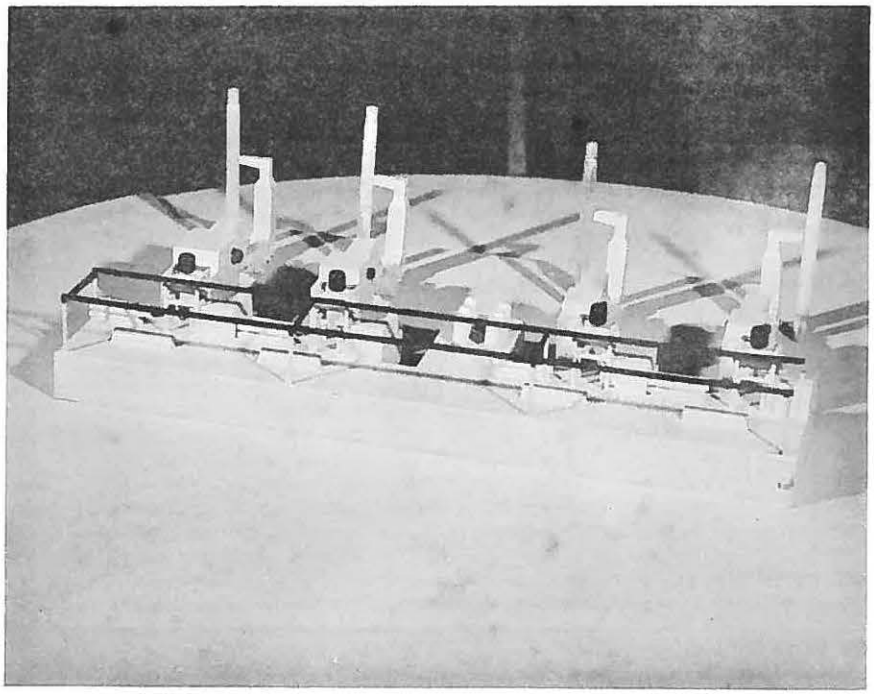

FIGURE 2 a. Stock Island power plant model

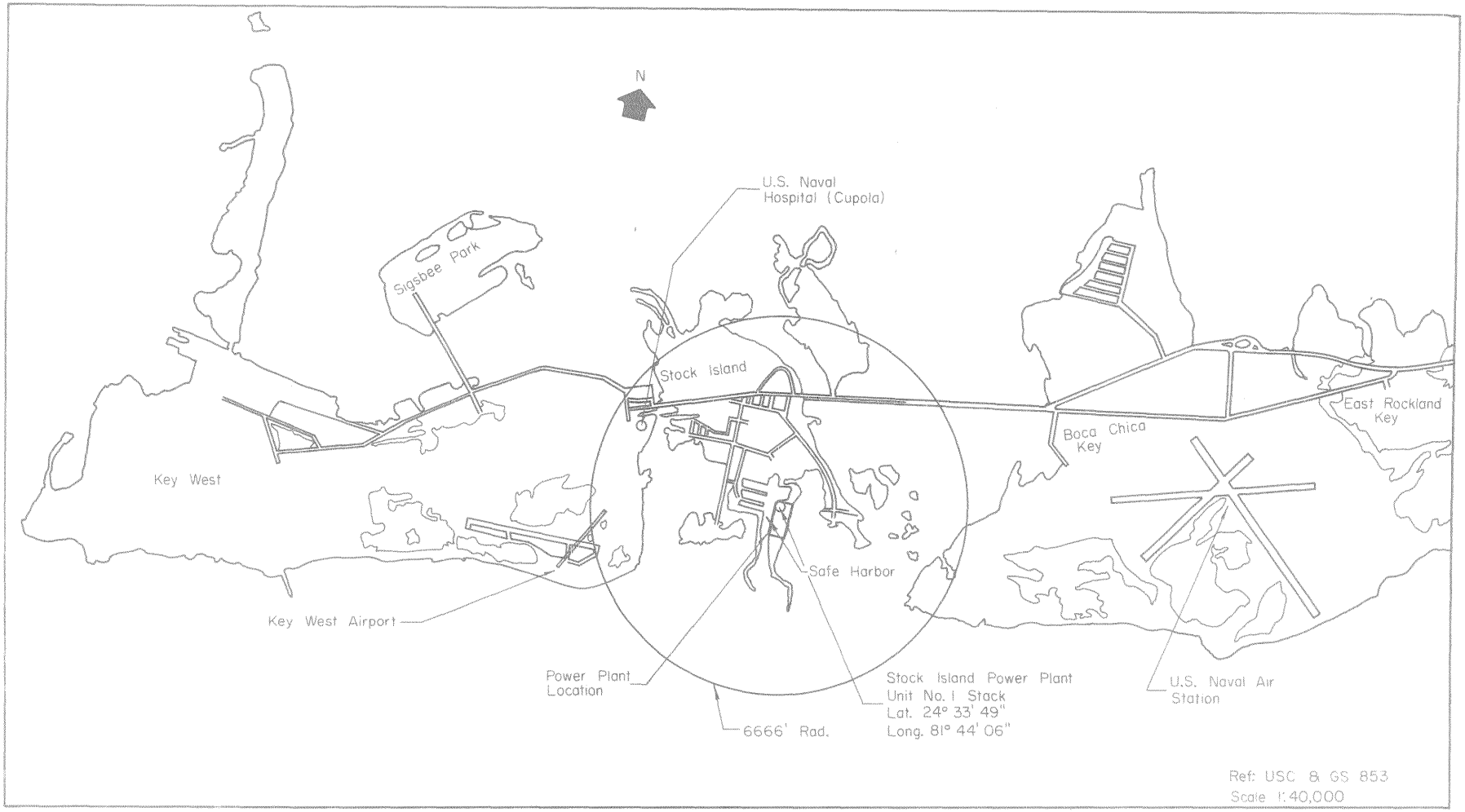

Figure 2b. Stock Island power plant vicinity location map

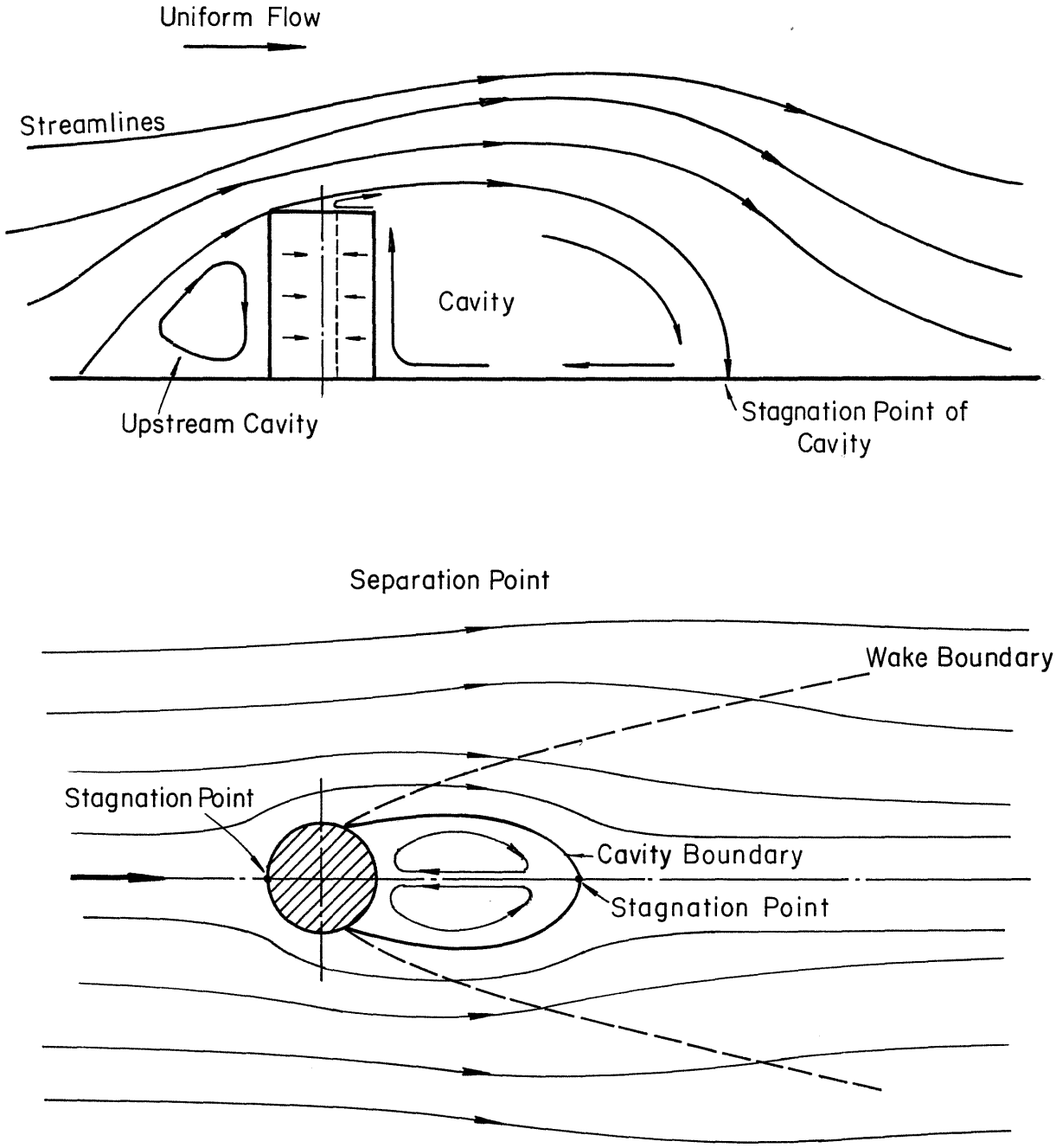

Figure 3. Cavity and wake downstream of a circular building

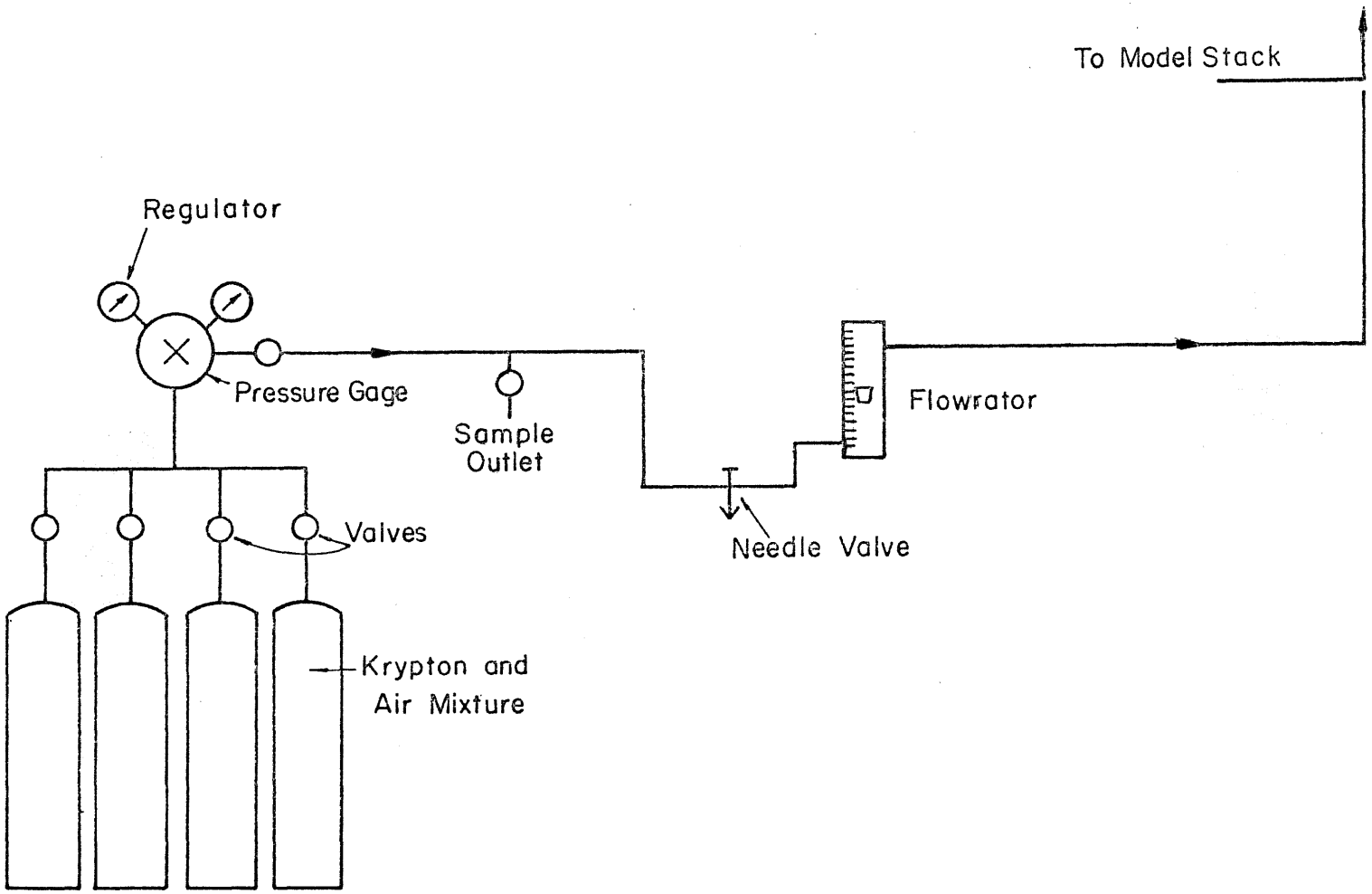

Figure 4a. Gas tracer apparatus - source

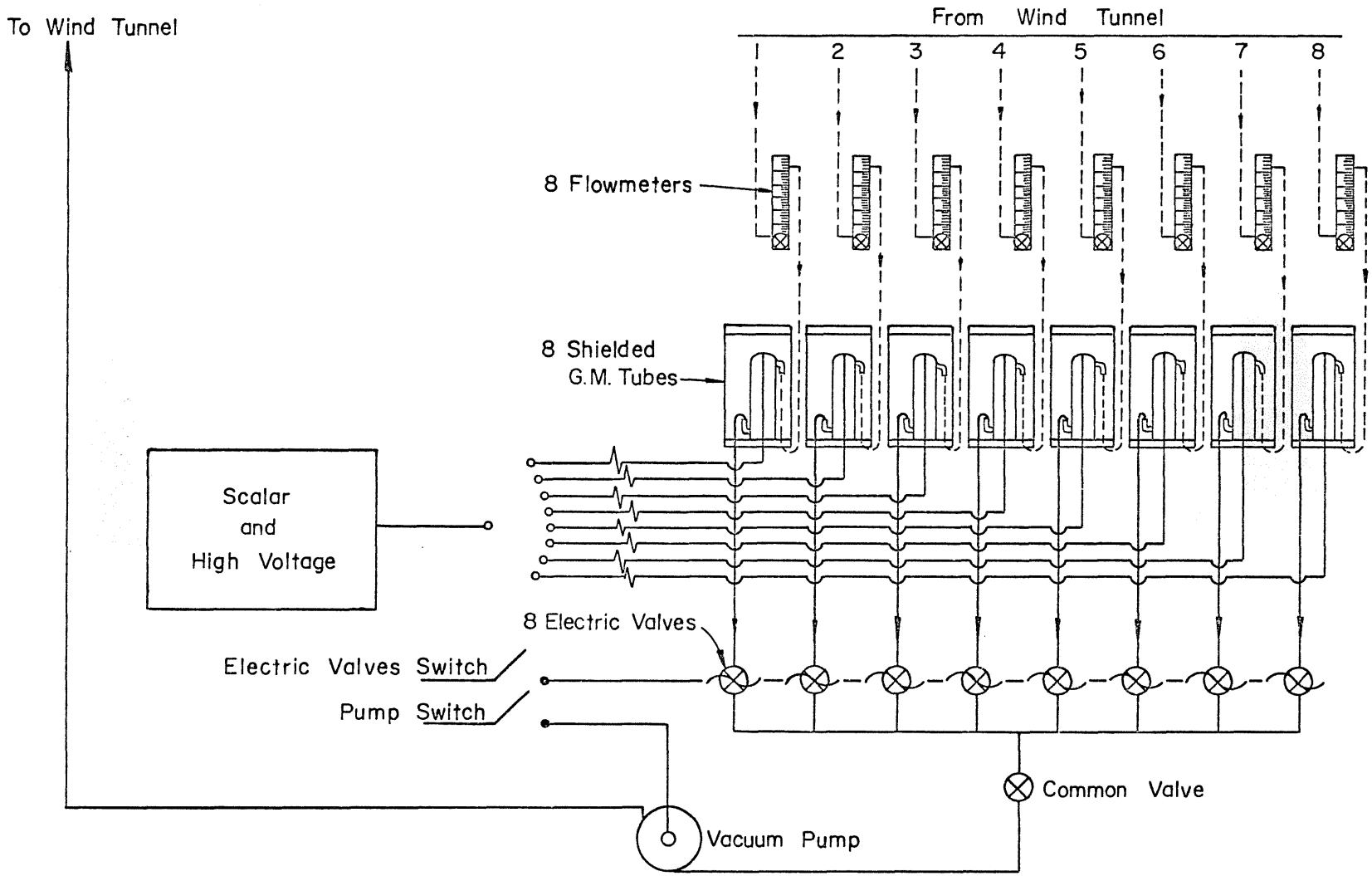

Figure 4b. Gas tracer apparatus - sampler

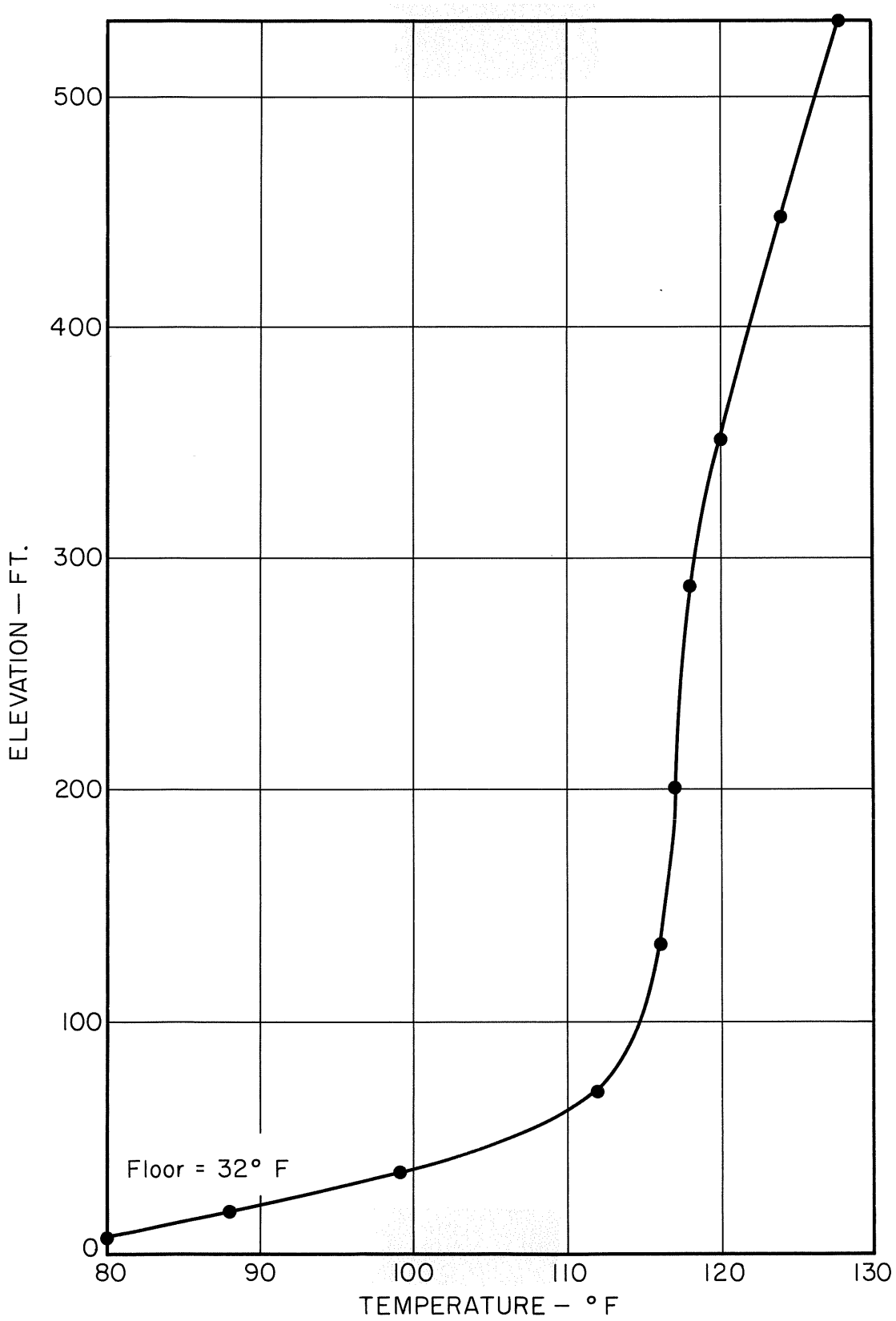

Figure 5. Temperature profile, V_∞ = 6 ft/sec

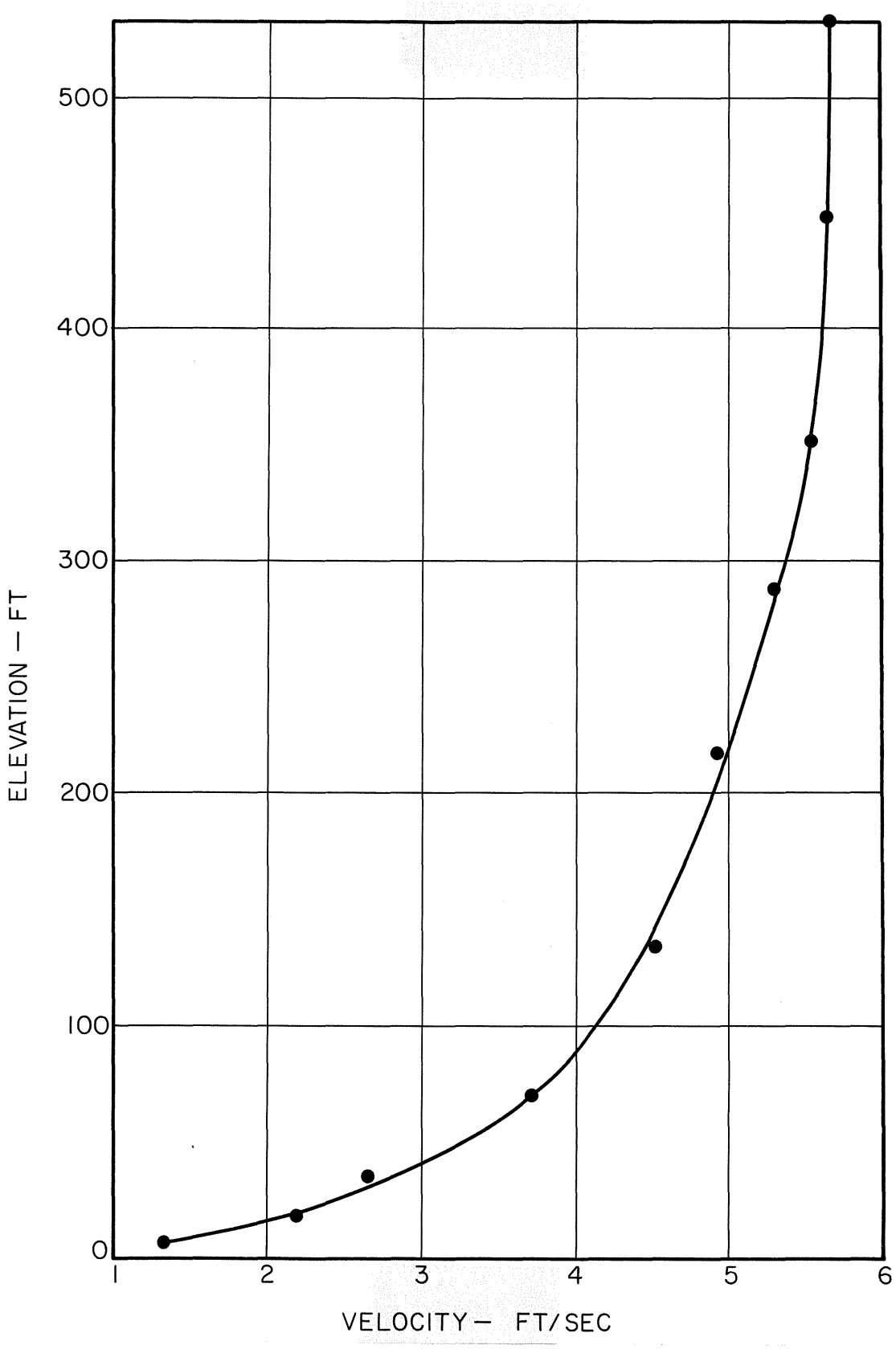

Figure 6a. Velocity profile, $\Delta T = 100^{\circ}F$

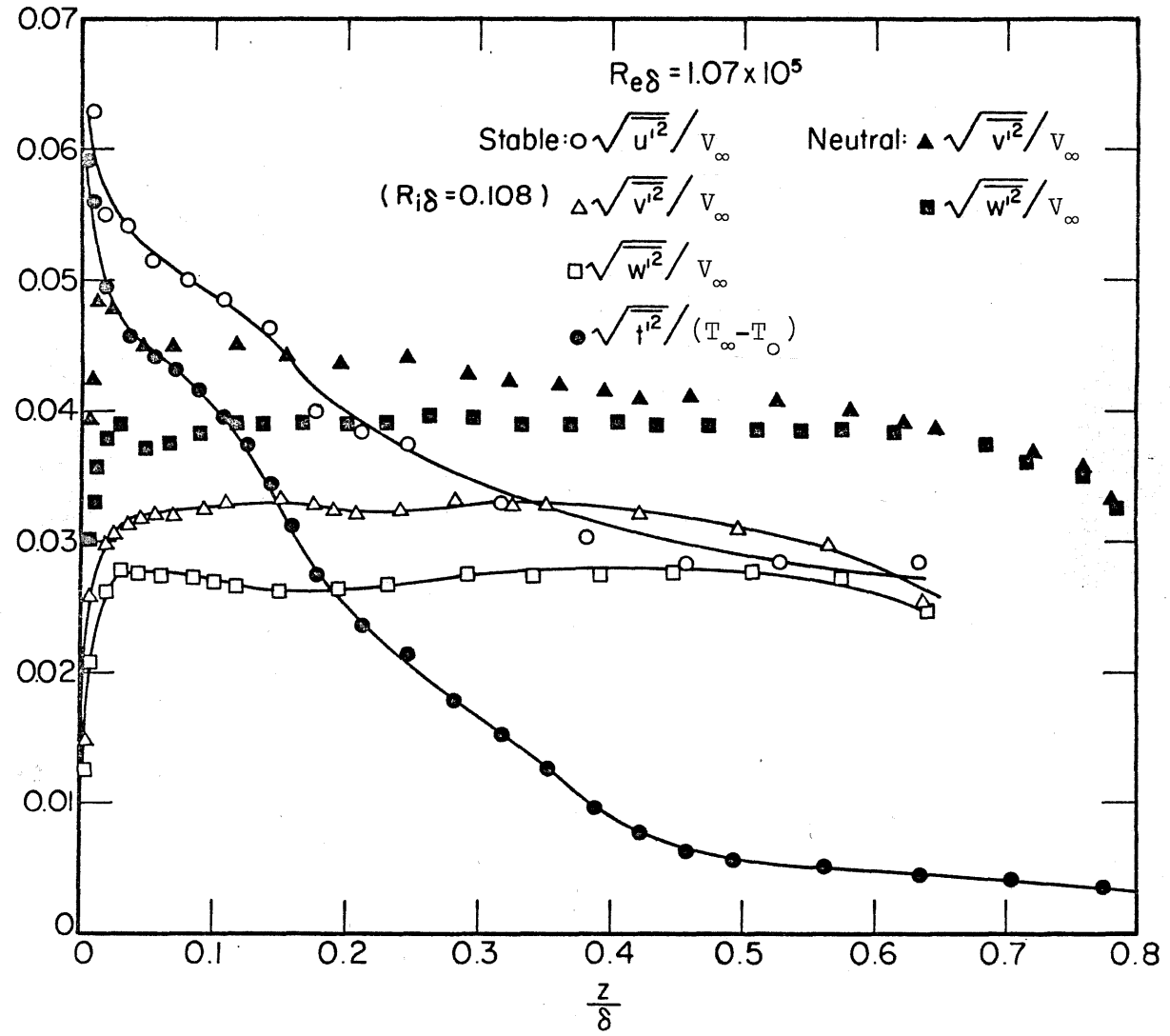

Figure 6b. Distribution of turbulent intensities; $R_{e_\delta} = 1.07 \times 10^5$ and $R_{i_\delta} = 0.108$

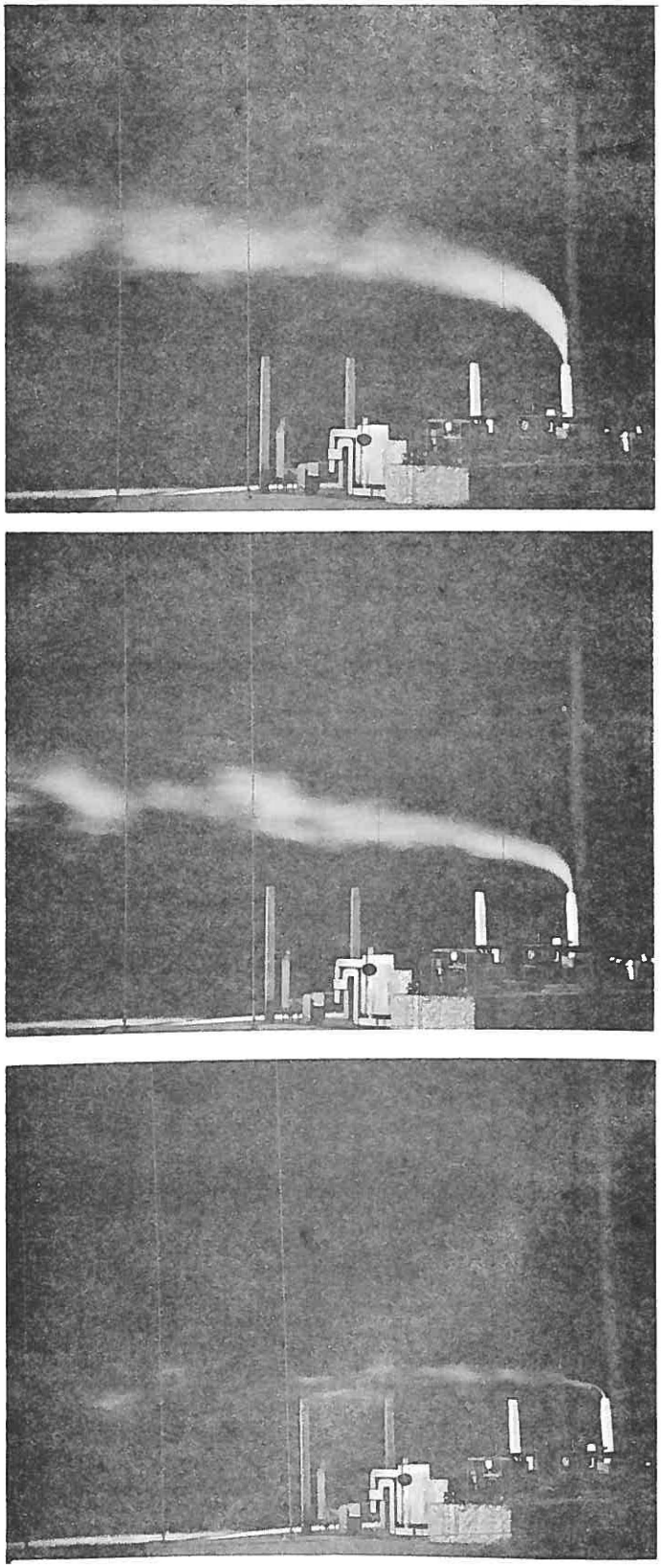

FIGURE 7 Typical smoke plume photographs $\theta = 40°$, $W/V = 1,3,5$, $\Delta T = 100°F$, stack 4

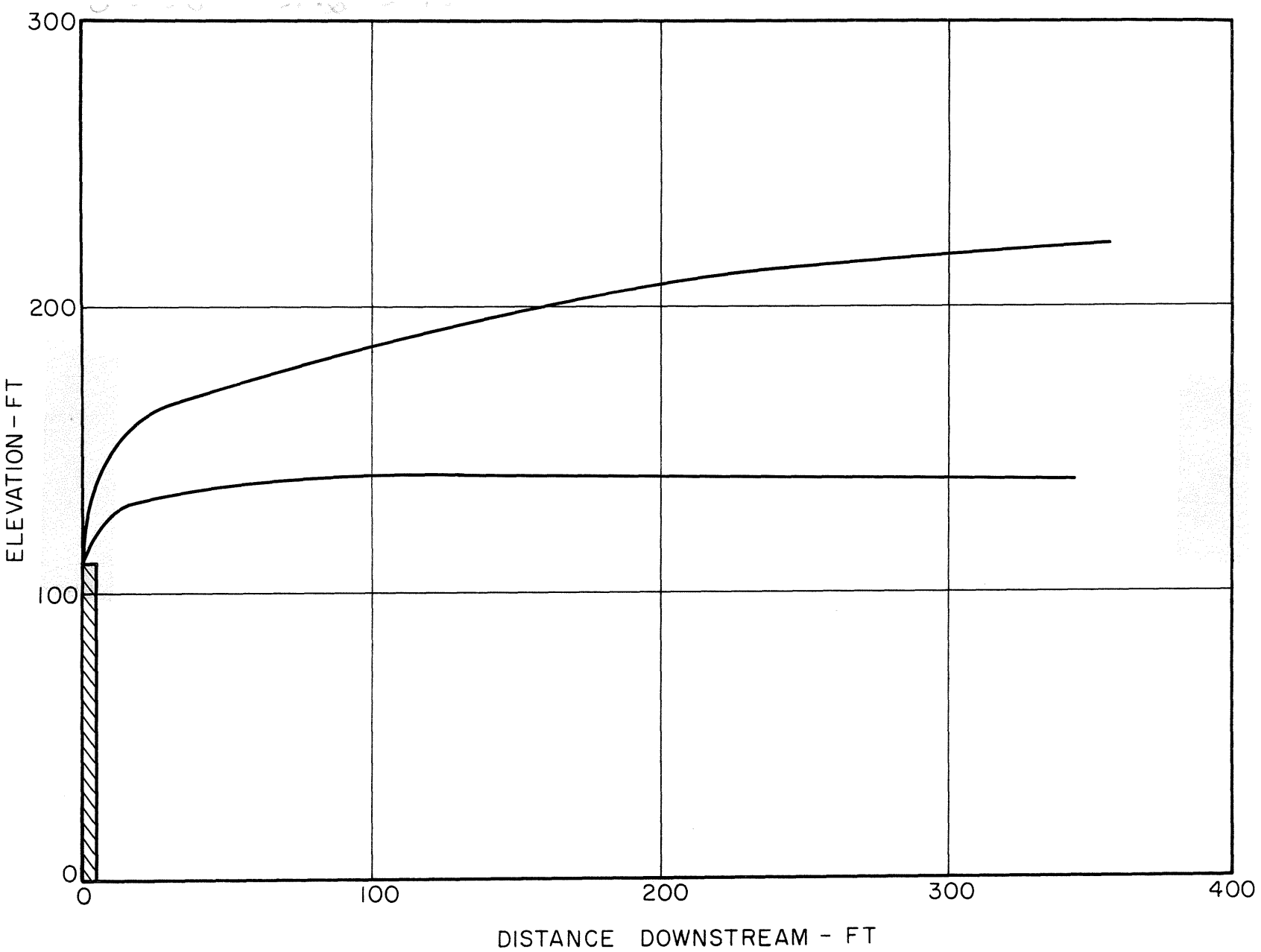

Figure 8 Stack 1, $\theta = 100°$, $W/V = 2.75$, $\Delta T = 0°F$

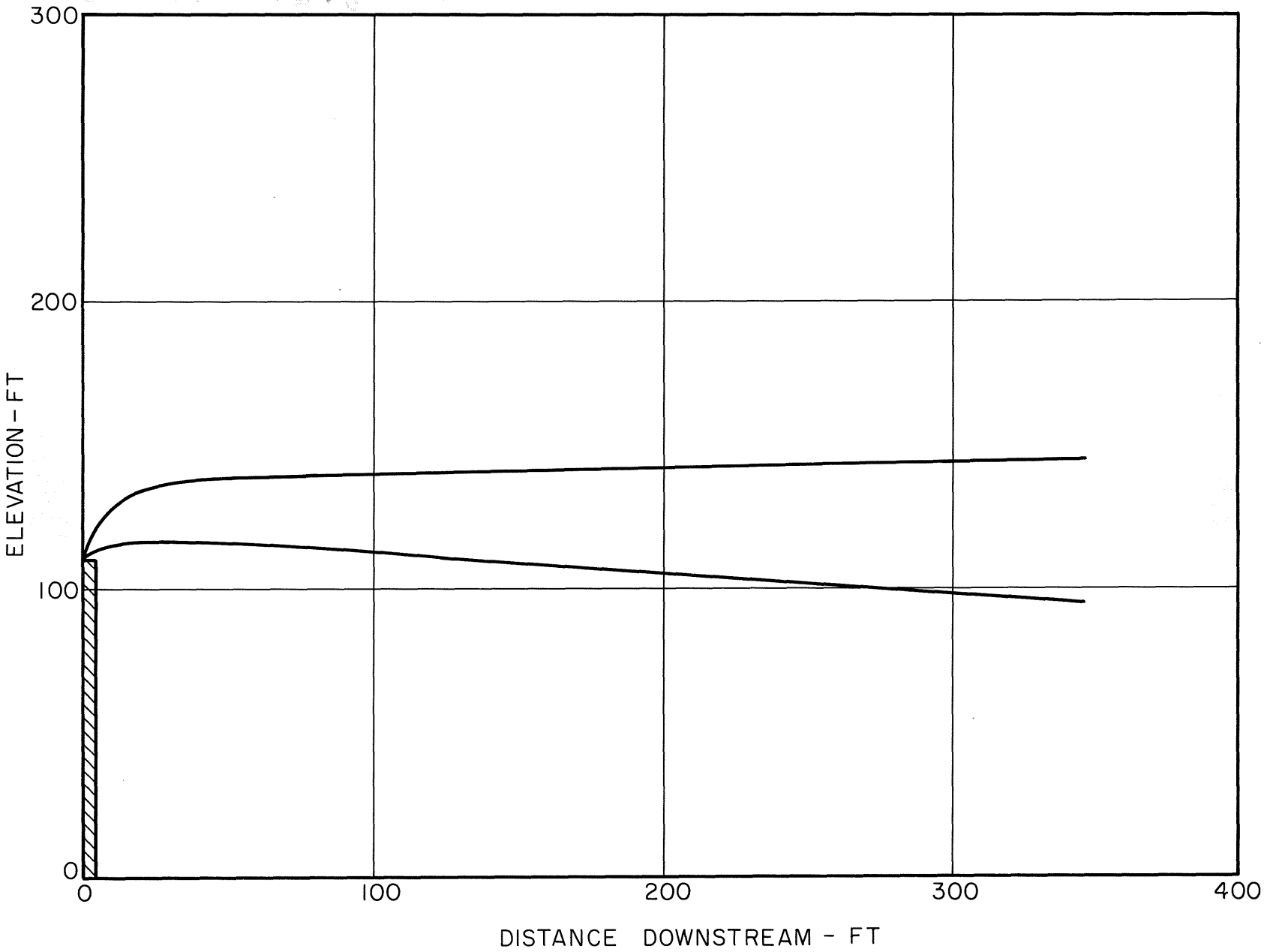

Figure 9 Stack 1, $\theta = 100°$, W/V = 0.95, $\Delta T = 0°F$

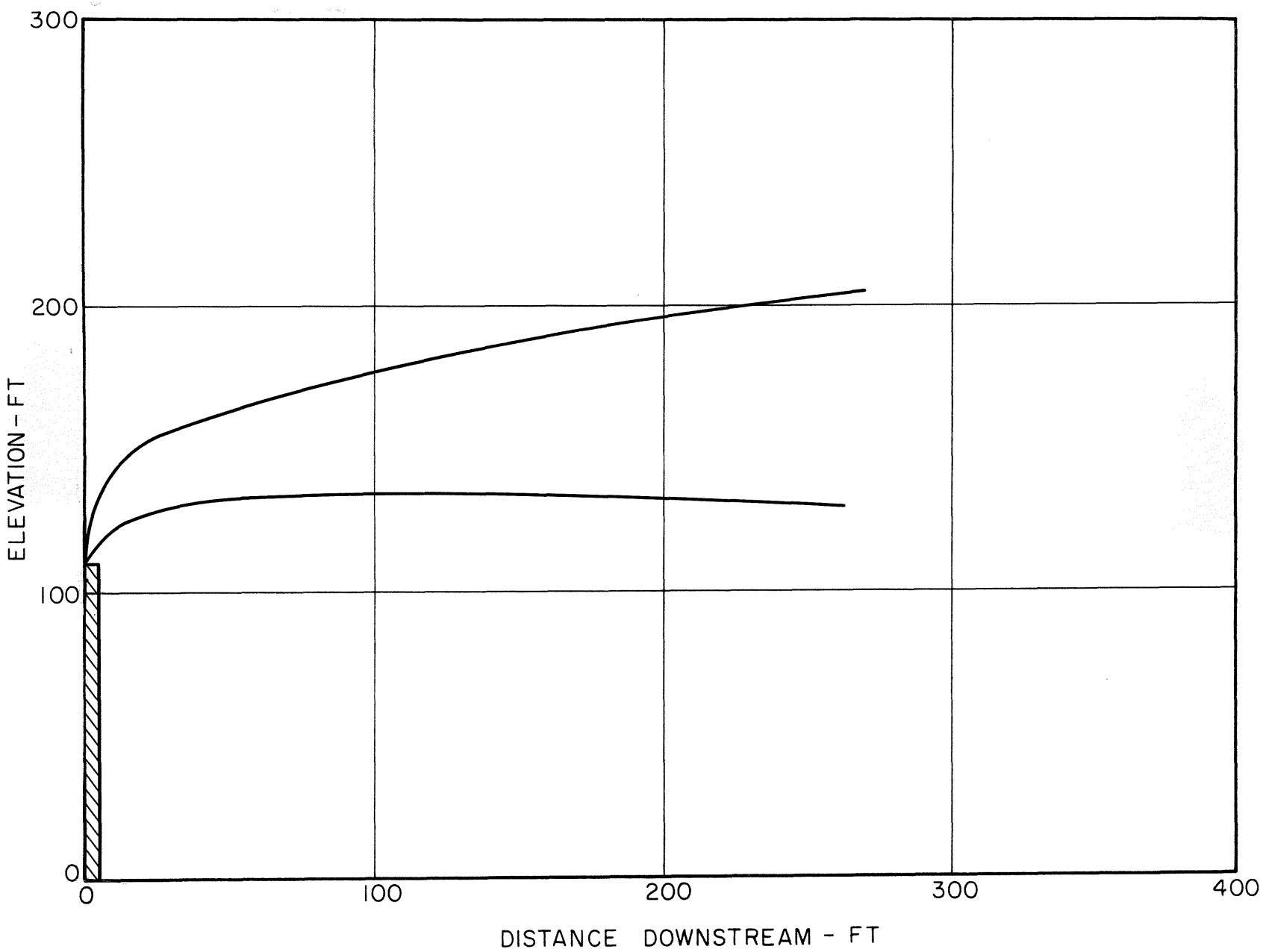

Figure 10 Stack 4, $\theta = 60°$, W/V = 2.75, $\Delta T = 0°F$

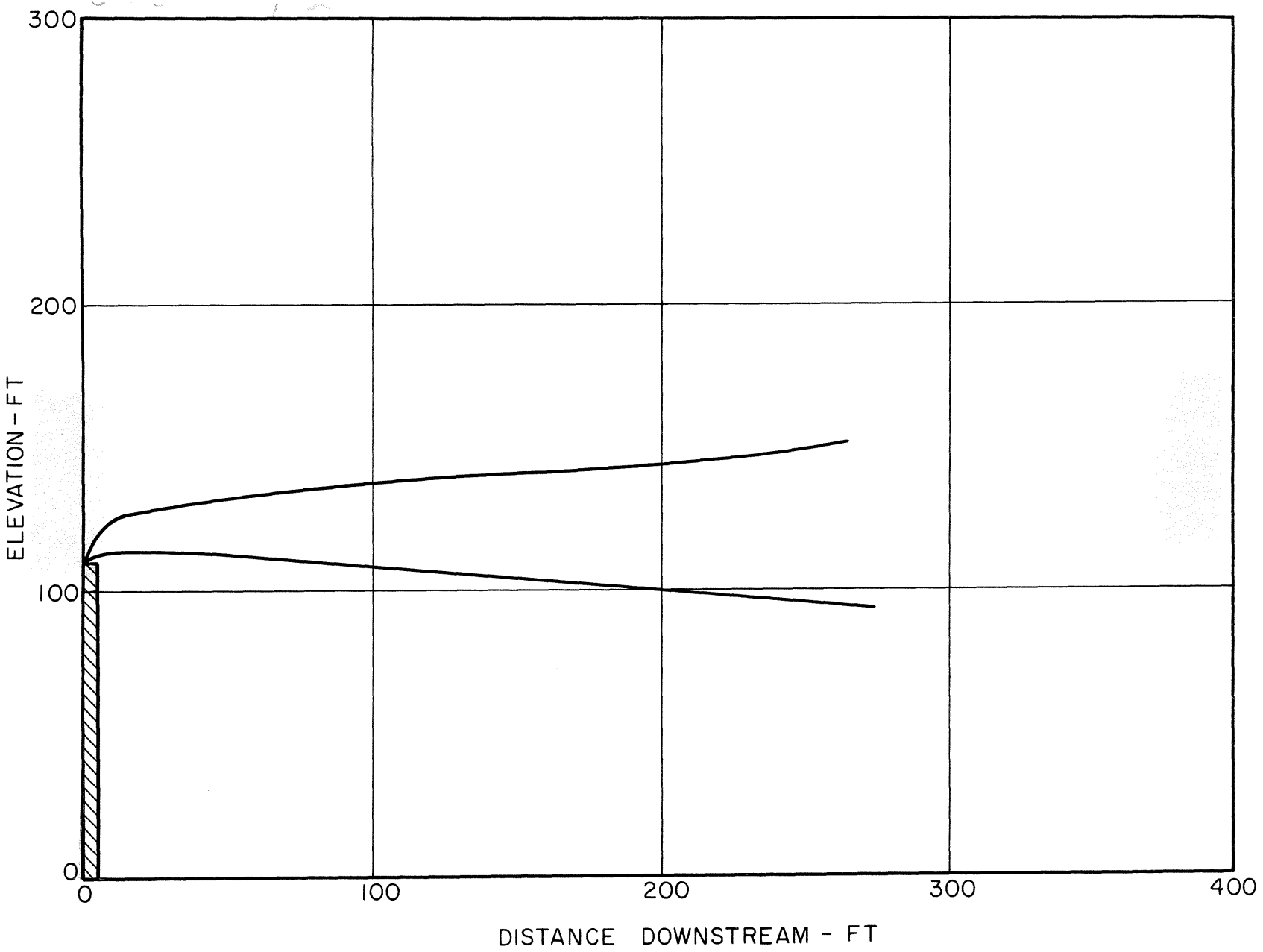

Figure 11 Stack 4, $\theta = 60°$, W/V = 0.95, $\Delta T = 0°F$

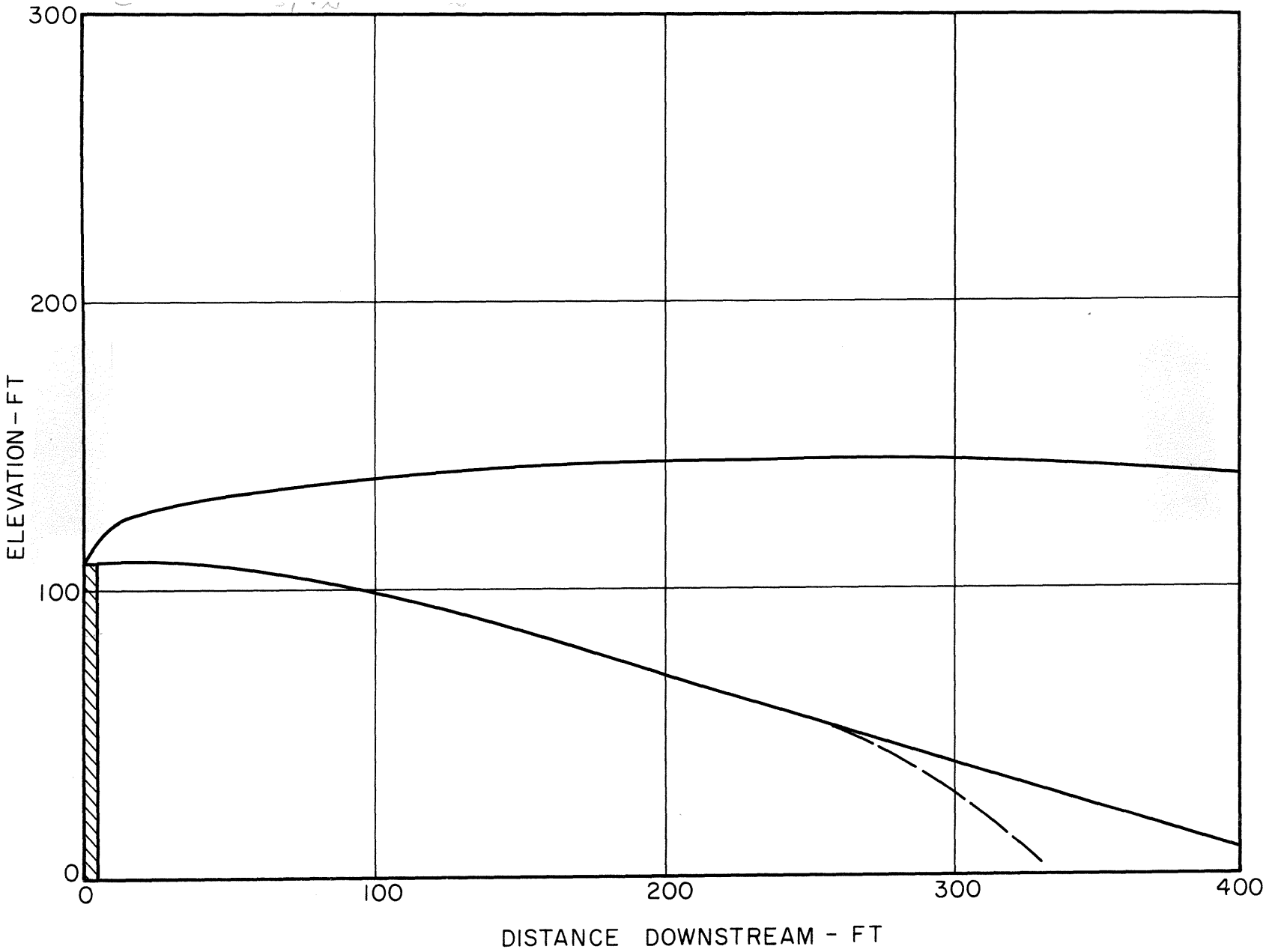

Figure 12 Stack 1, $\theta = 80^\circ$, W/V = 2 , $\Delta T = 50^\circ F$

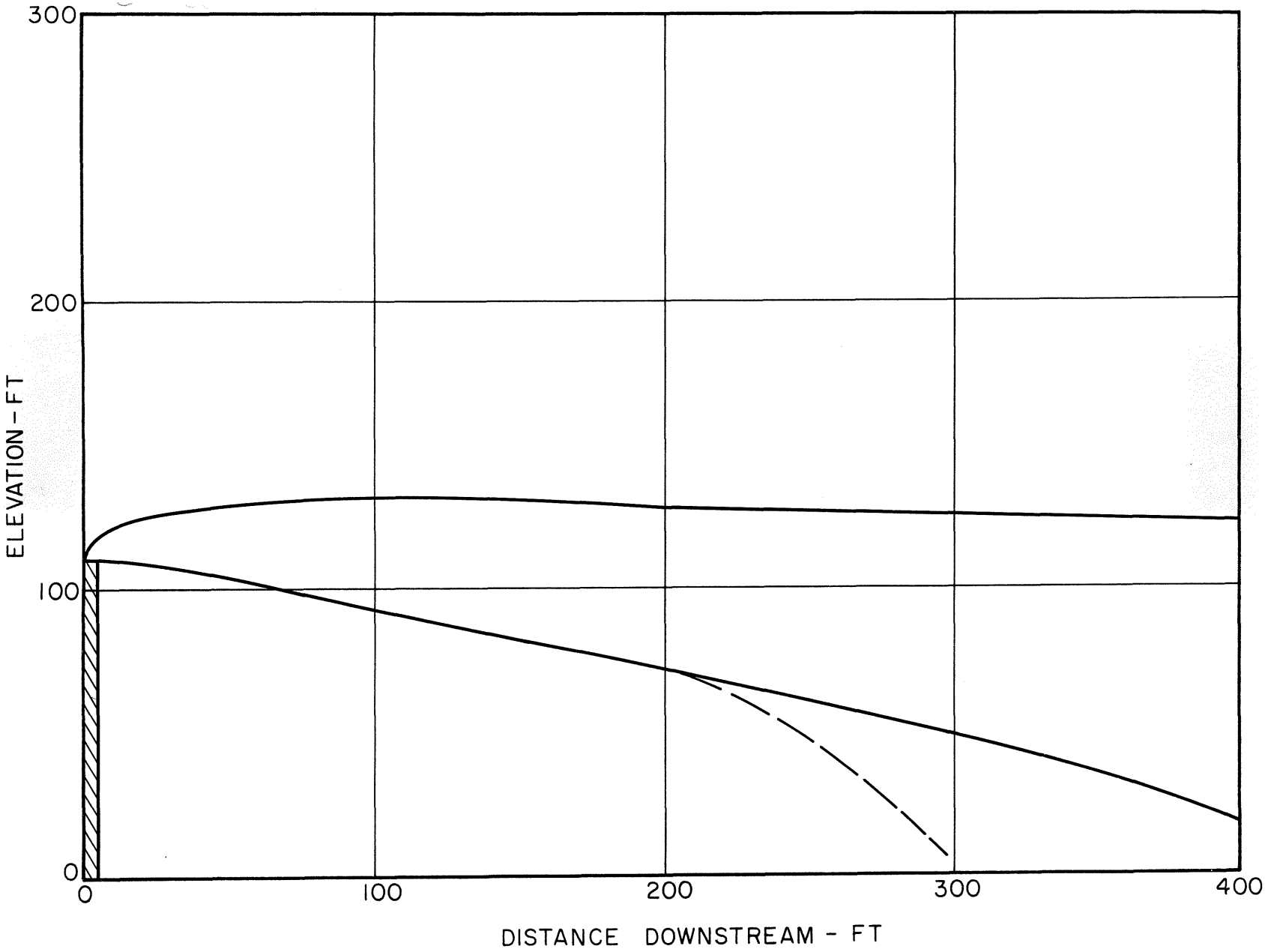

Figure 13 Stack 1, $\theta = 80^\circ$, W/V = 1 , $\Delta T = 50^\circ F$

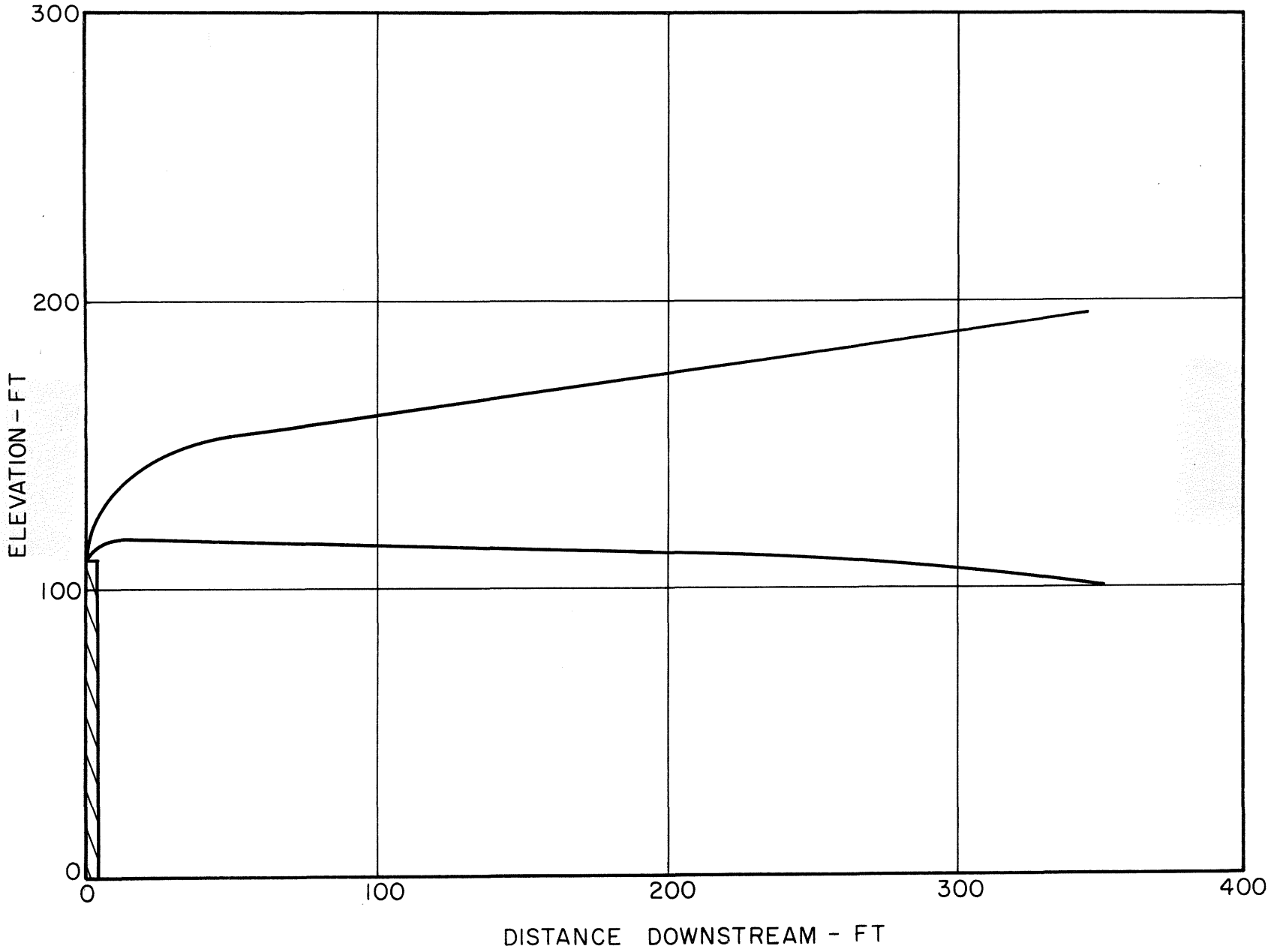

Figure 14 Stack 1, $\theta = 80°$, W/V = 2 , $\Delta T = 100°F$

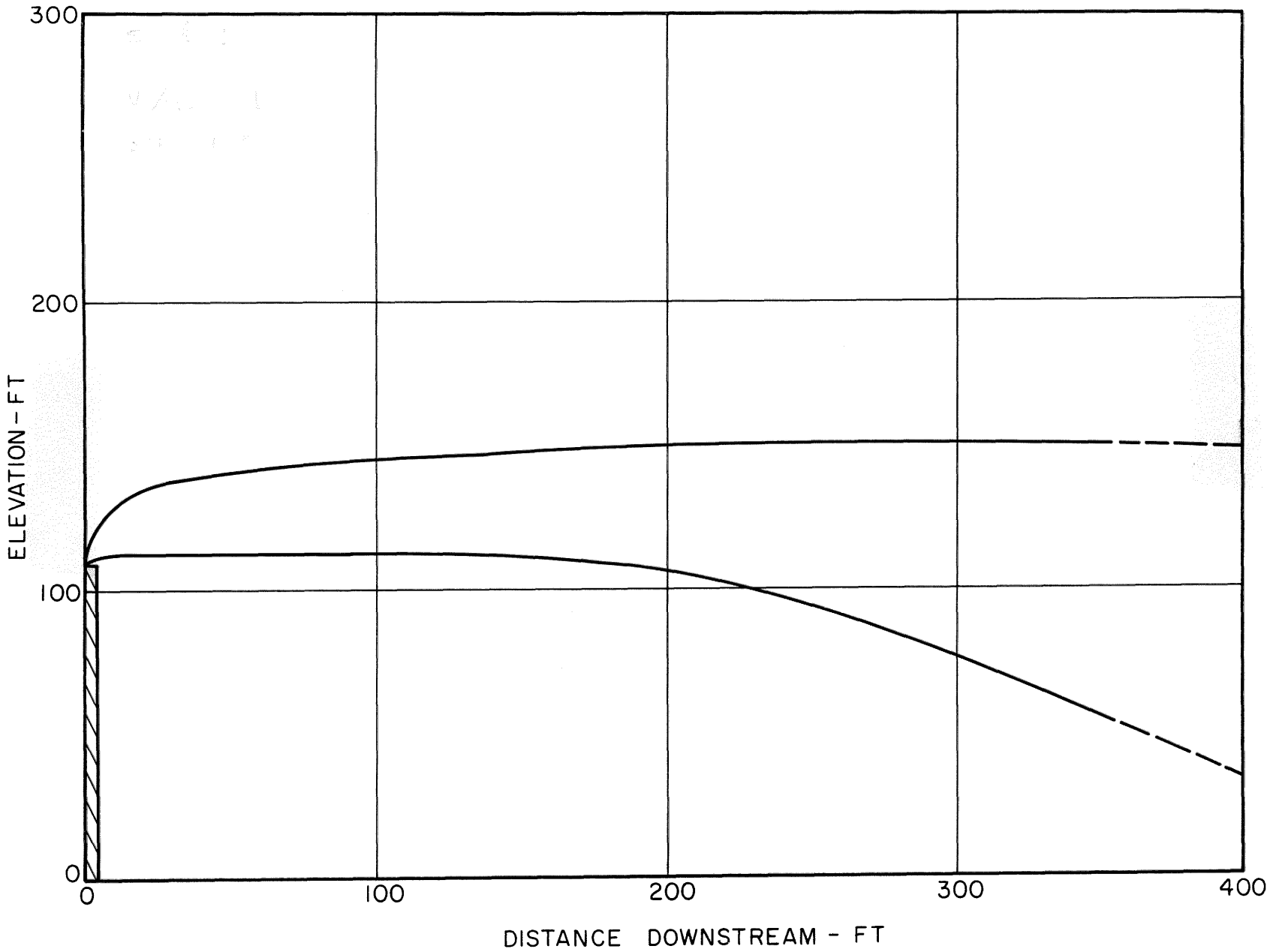

Figure 15 Stack 1, $\theta = 80°$, W/V = 1 , $\Delta T = 100°F$

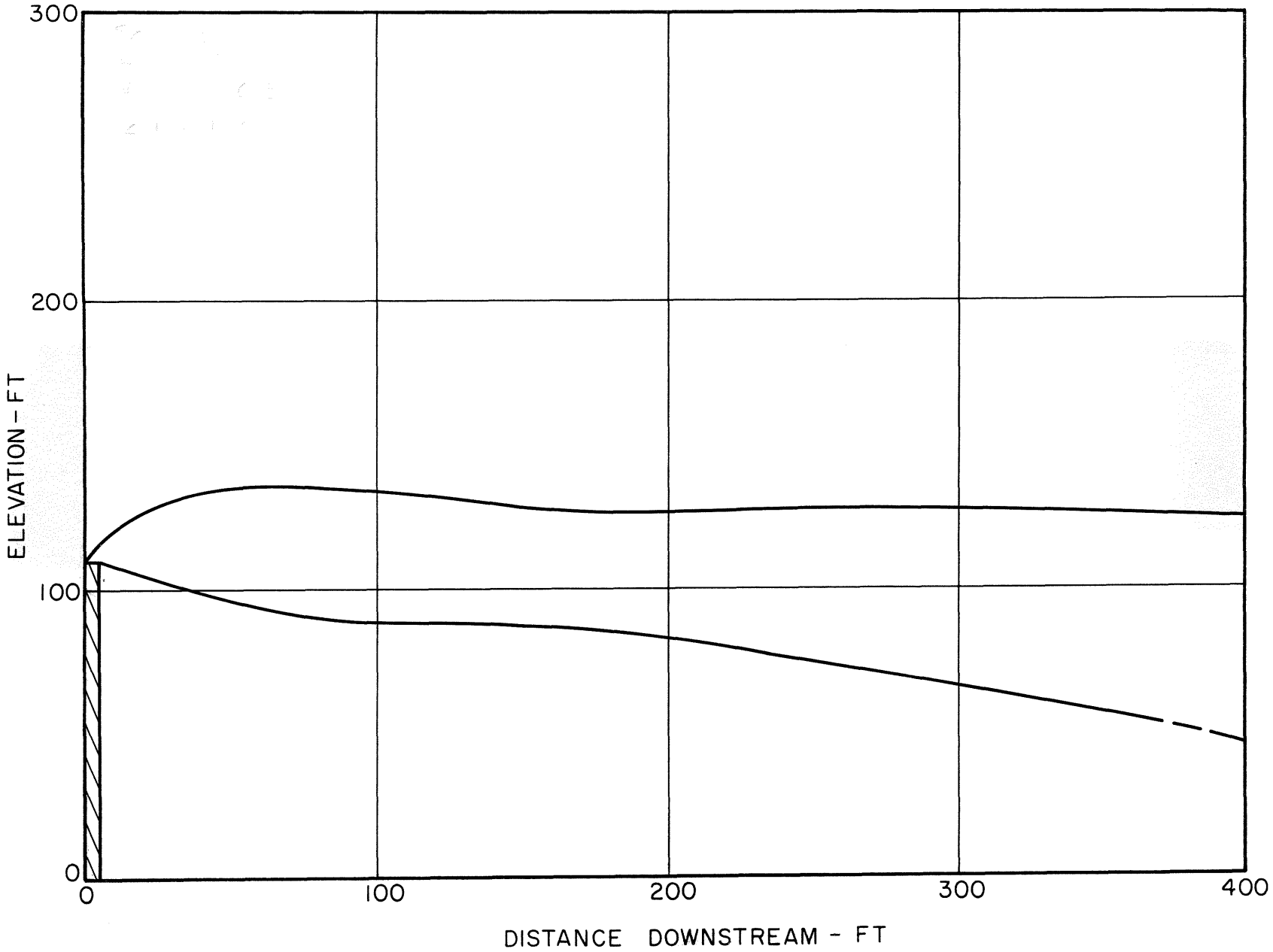

Figure 16 Stack 1, $\theta = 80°$, W/V = 0.5, $\Delta T = 100°F$

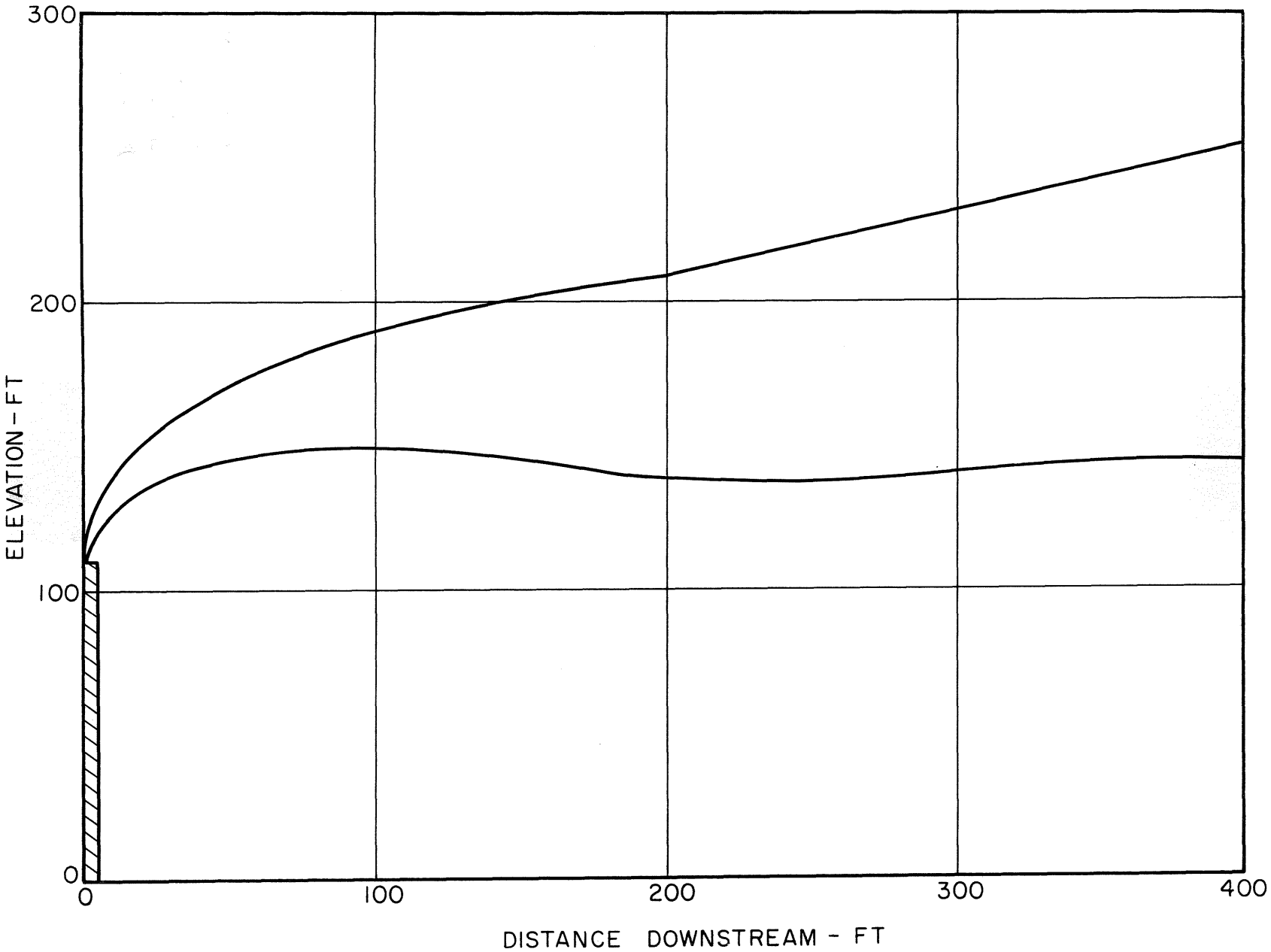

Figure 17 Stack 2, $\theta = 80°$, $W/V = 2$, $\Delta T = 100°F$

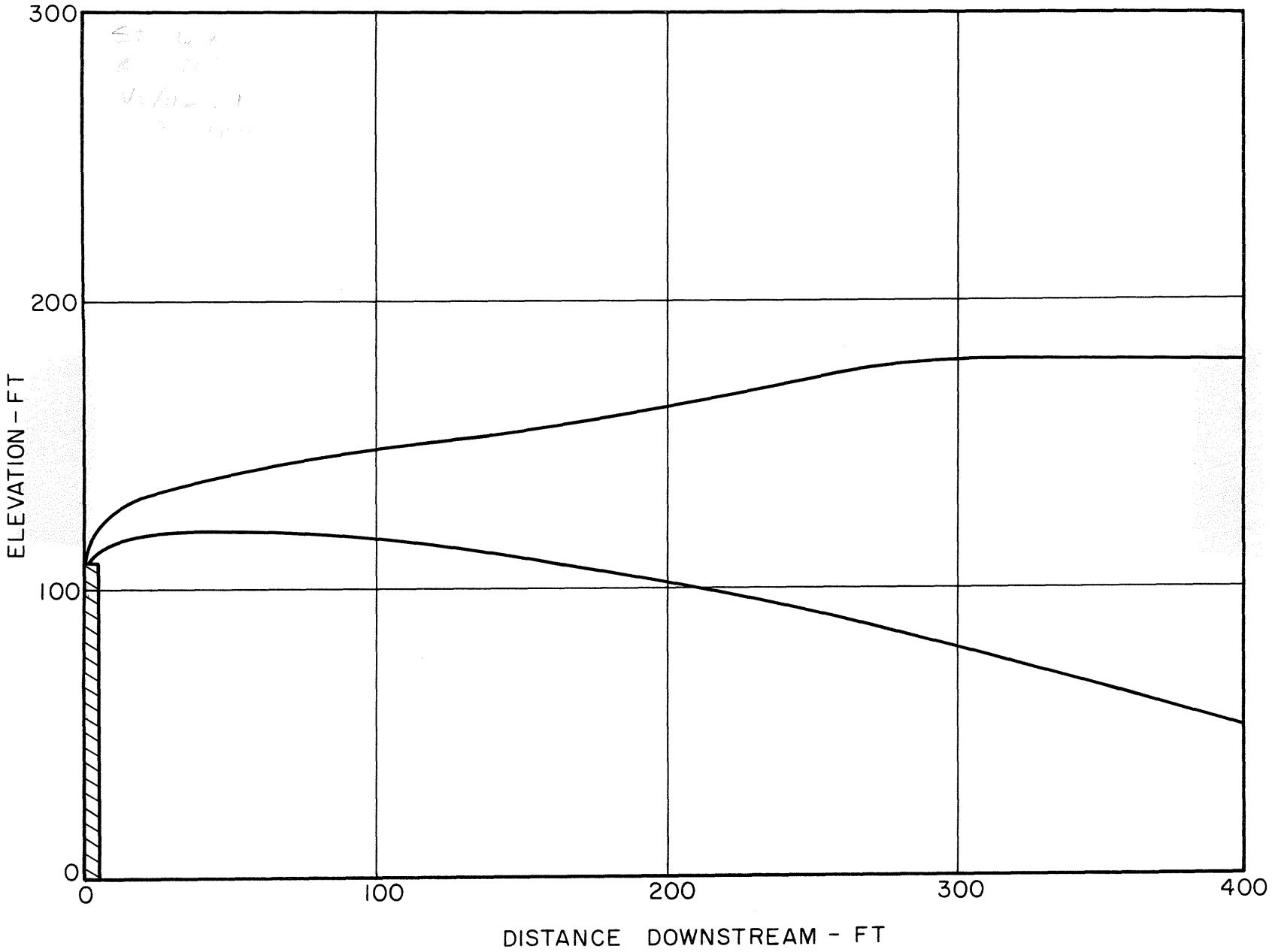

Figure 18 Stack 2, $\theta = 80°$, W/V = 1 , $\Delta T = 100°F$

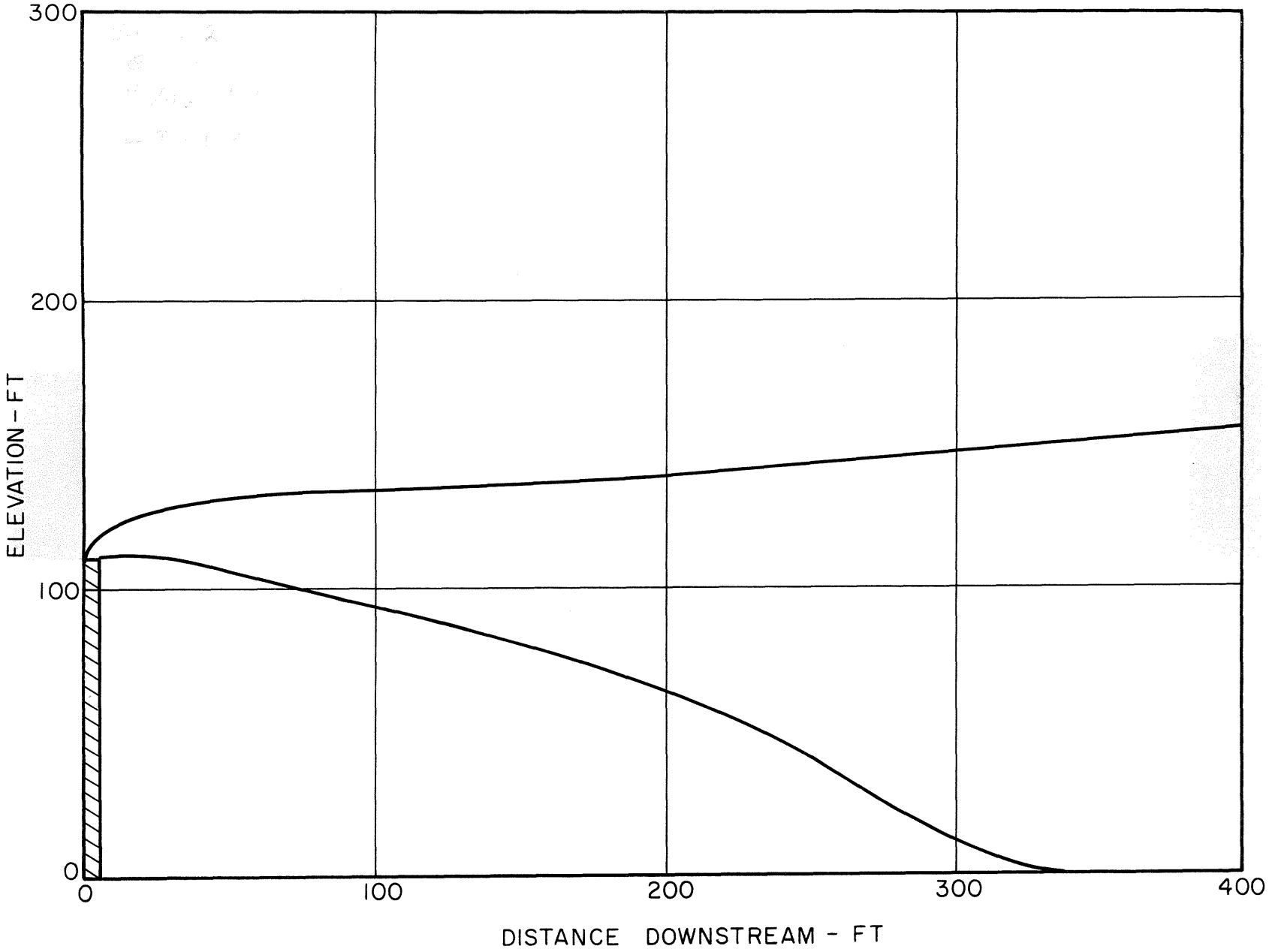

Figure 19 Stack 2, $\theta = 80°$, $W/V = 0.5$, $\Delta T = 100°F$

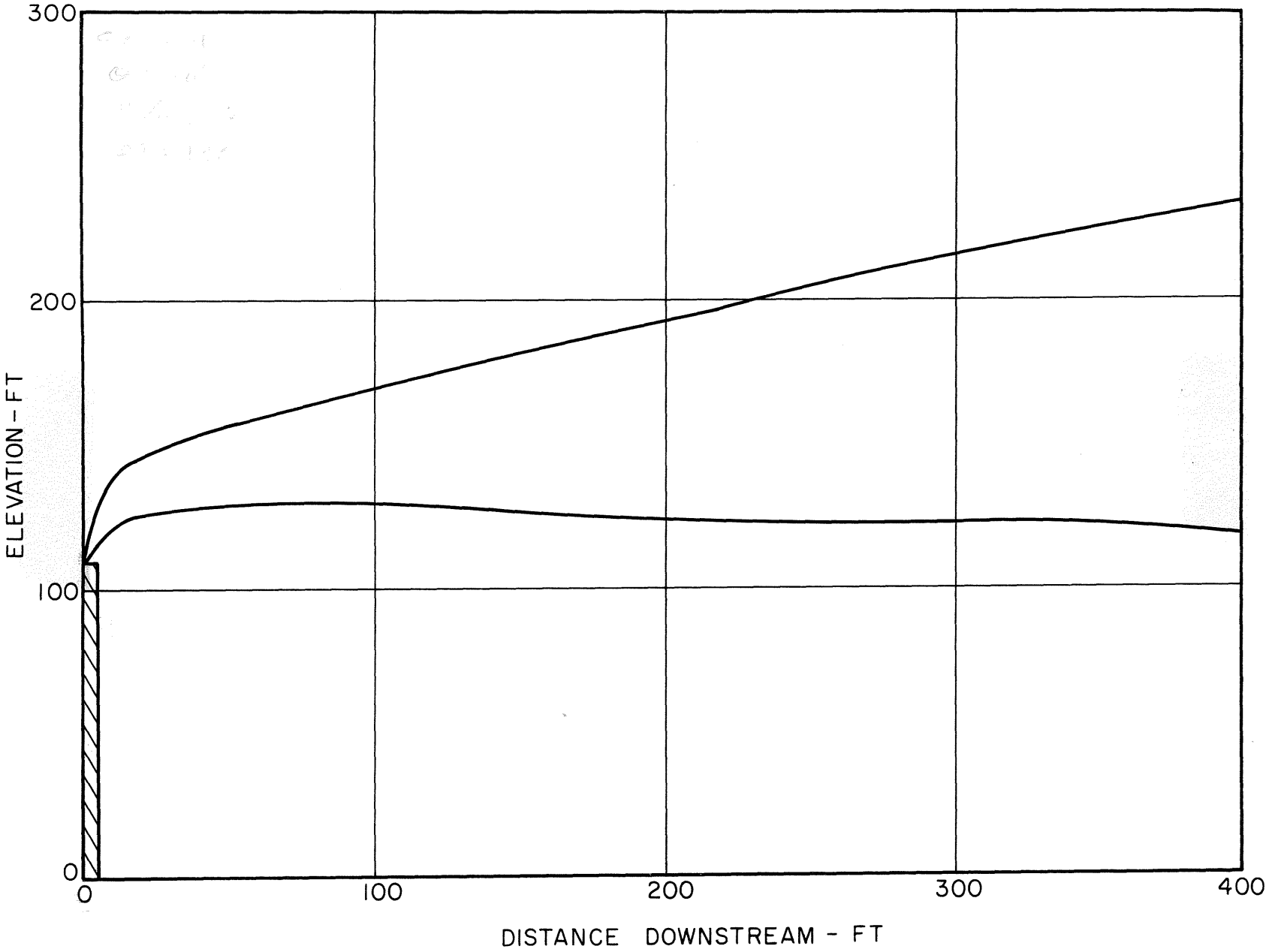

Figure 20 Stack 4, $\theta = 80°$, W/V = 2 , $\Delta T = 100°F$

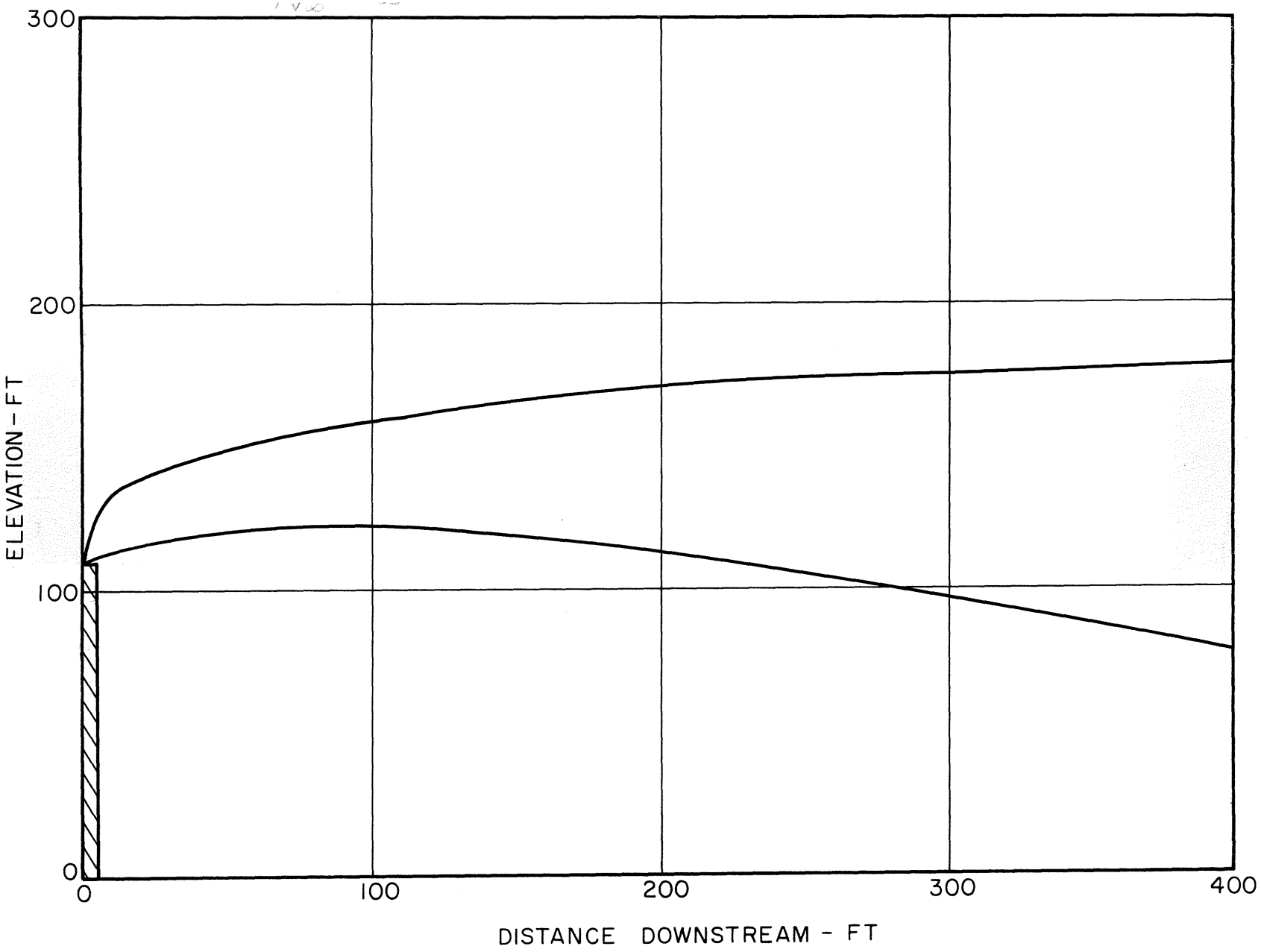

Figure 21 Stack 4, $\theta = 80°$, W/V = 1 , $\Delta T = 100°F$

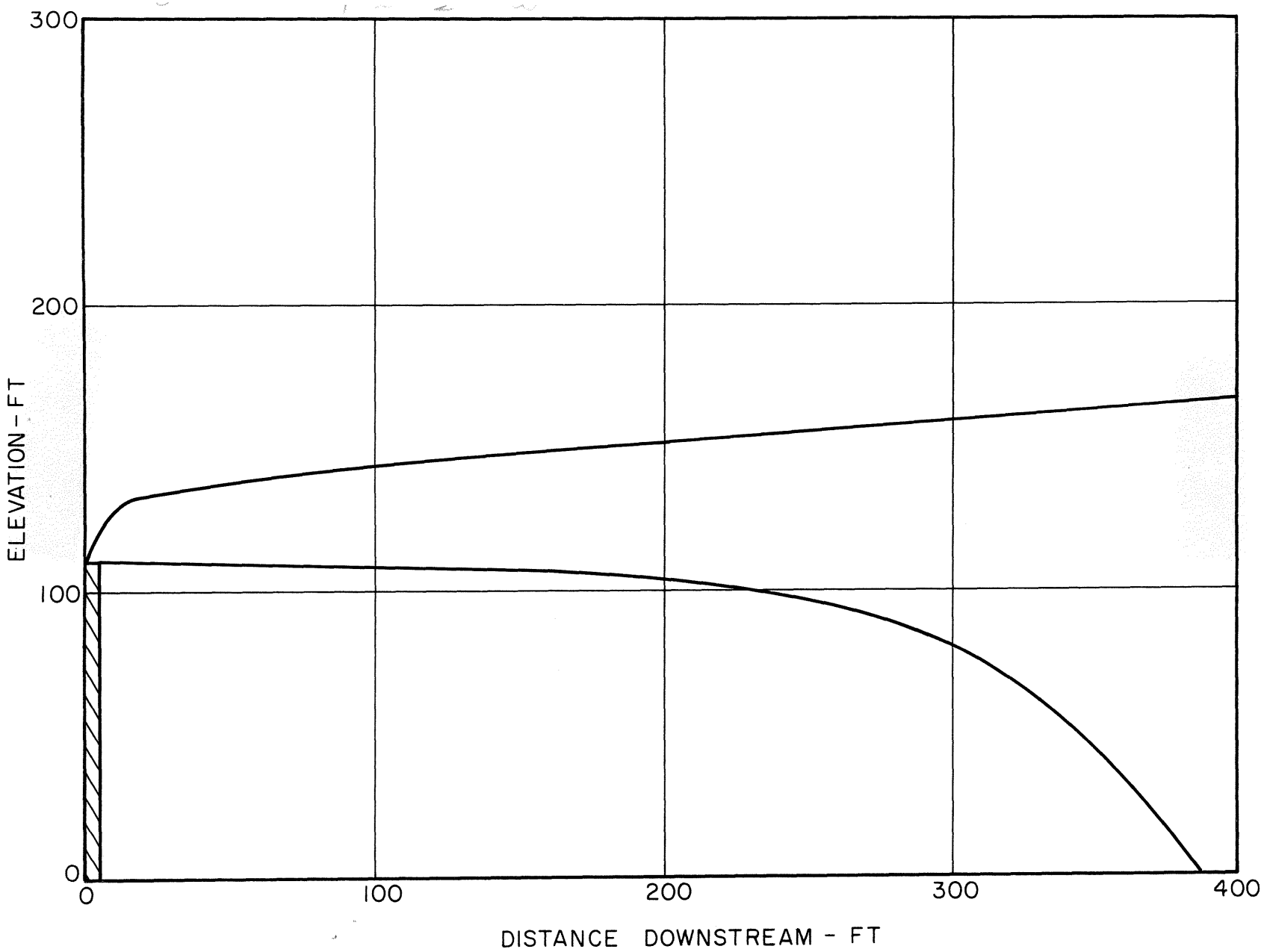

Figure 22 Stack 4, $\theta = 80°$, W/V = 0.5, $\Delta T = 100°F$

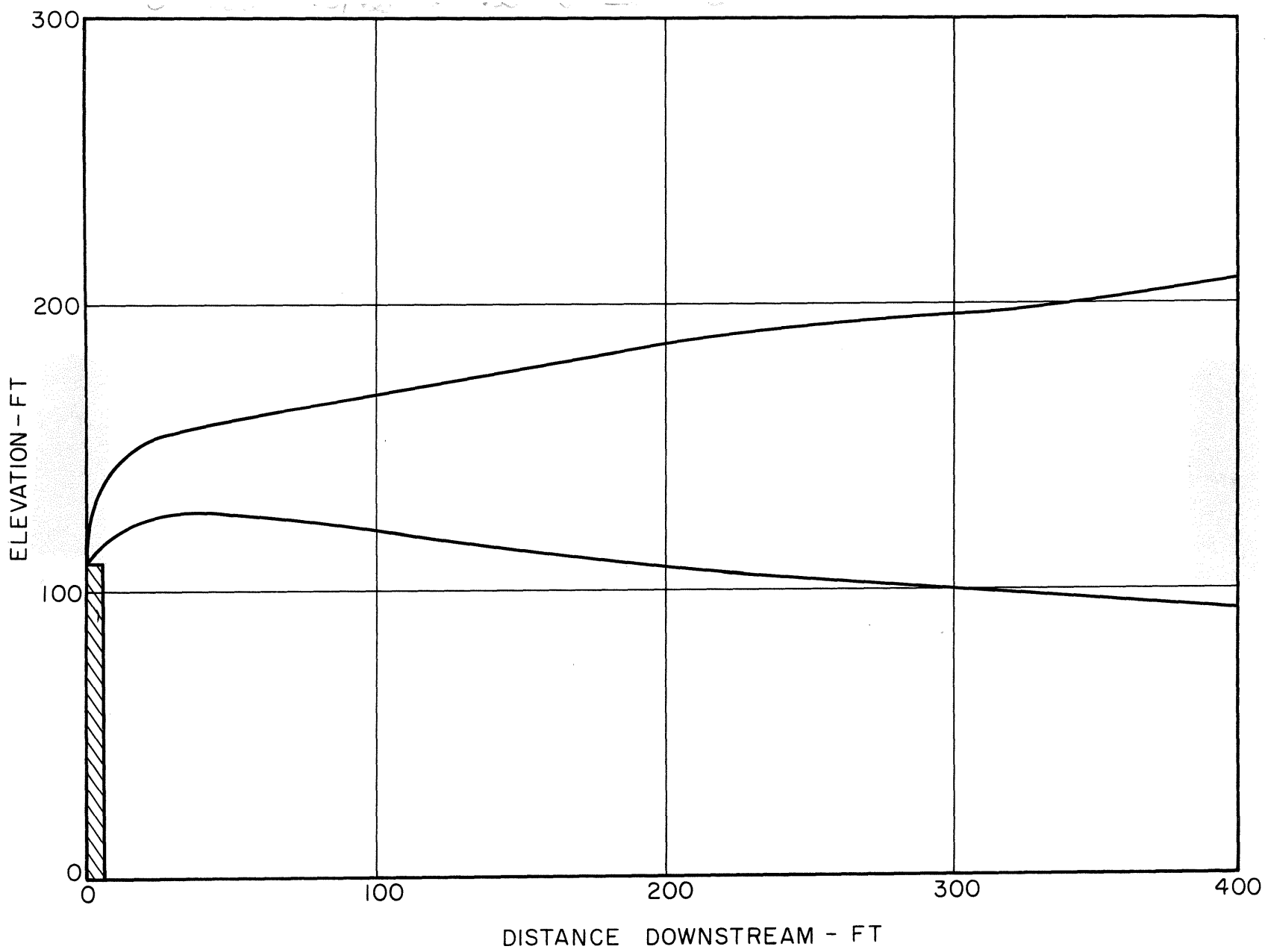

Figure 23 Stack 1, $\theta = 100^{\circ}$, W/V = 2, $\Delta T = 100^{\circ}F$

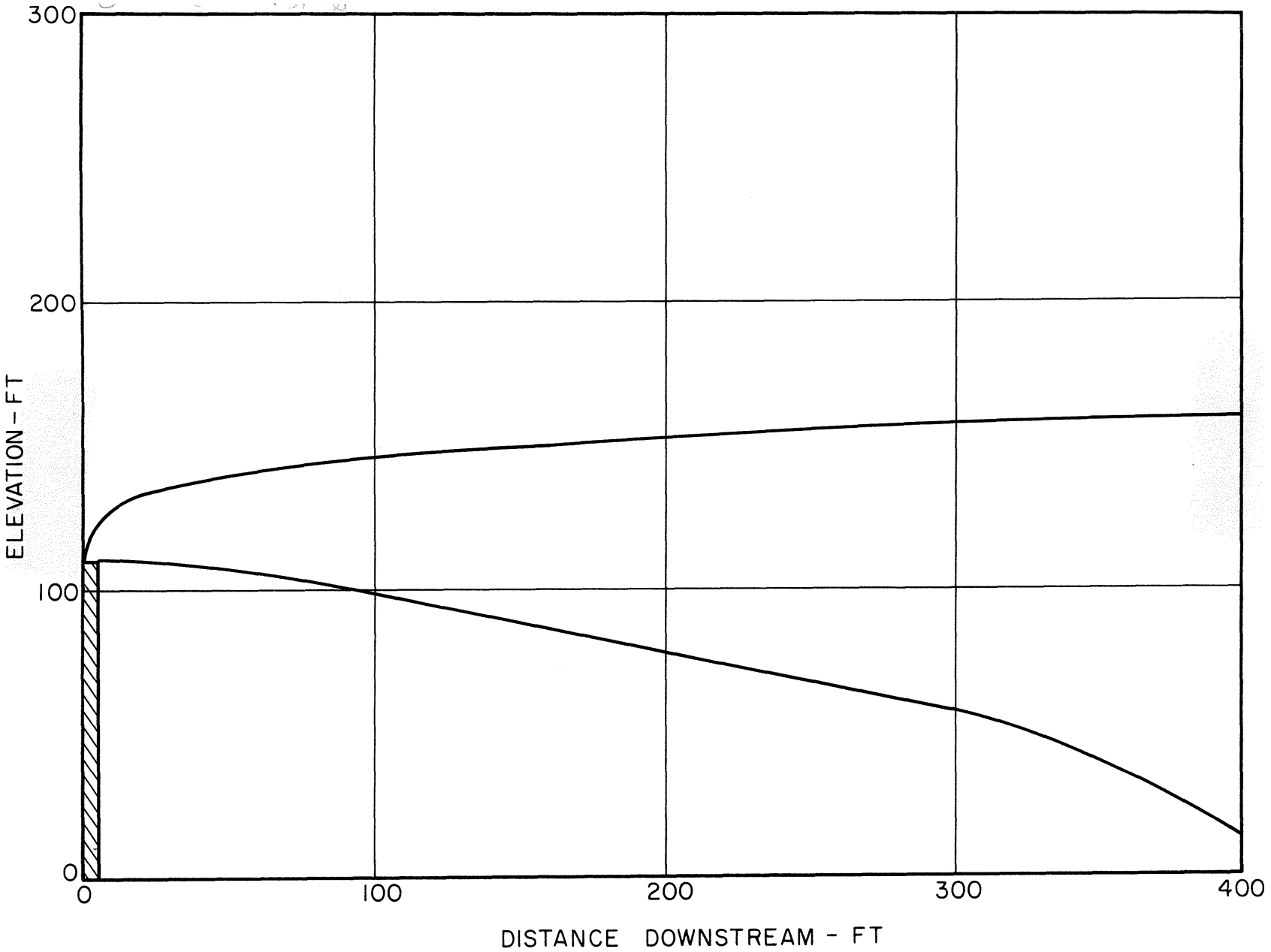

Figure 24 Stack 1, $\theta = 100°$, W/V = 1 , $\Delta T = 100°F$

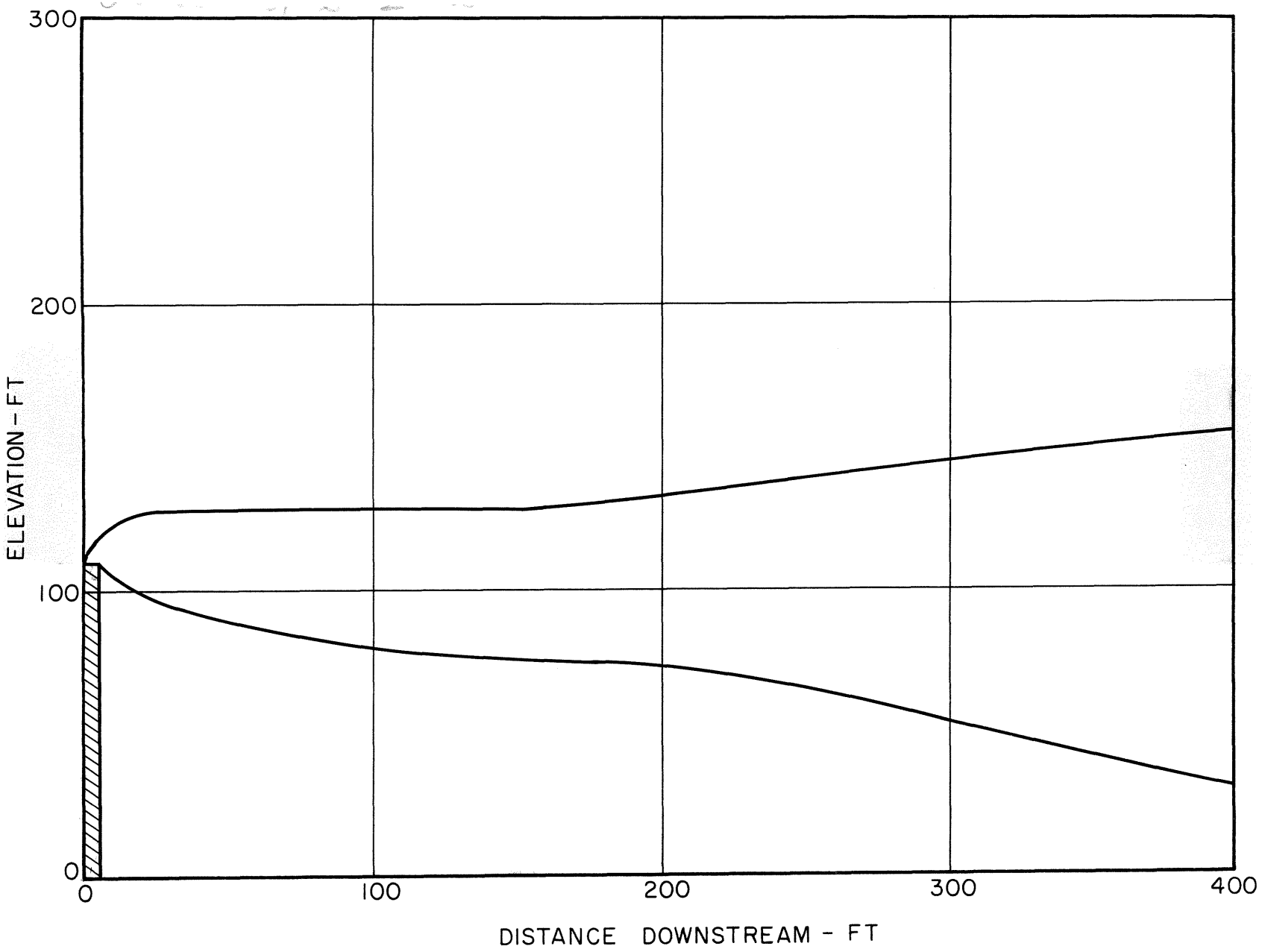

Figure 25 Stack 1, $\theta = 100^{\circ}$, W/V = 0.5, $\Delta T = 100^{\circ}F$

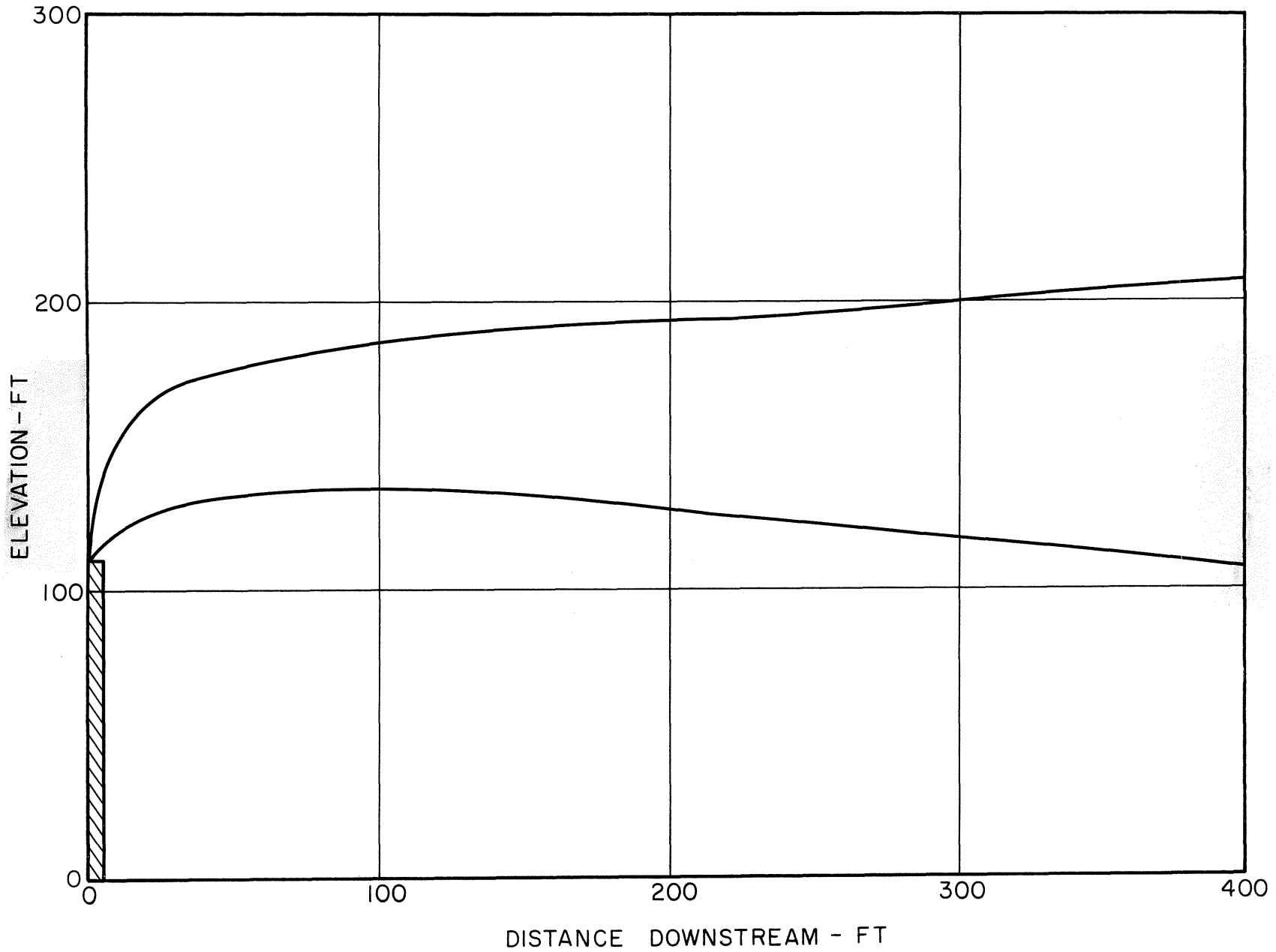

Figure 26 Stack 2, θ = 100°, W/V = 2 , ΔT = 100°F

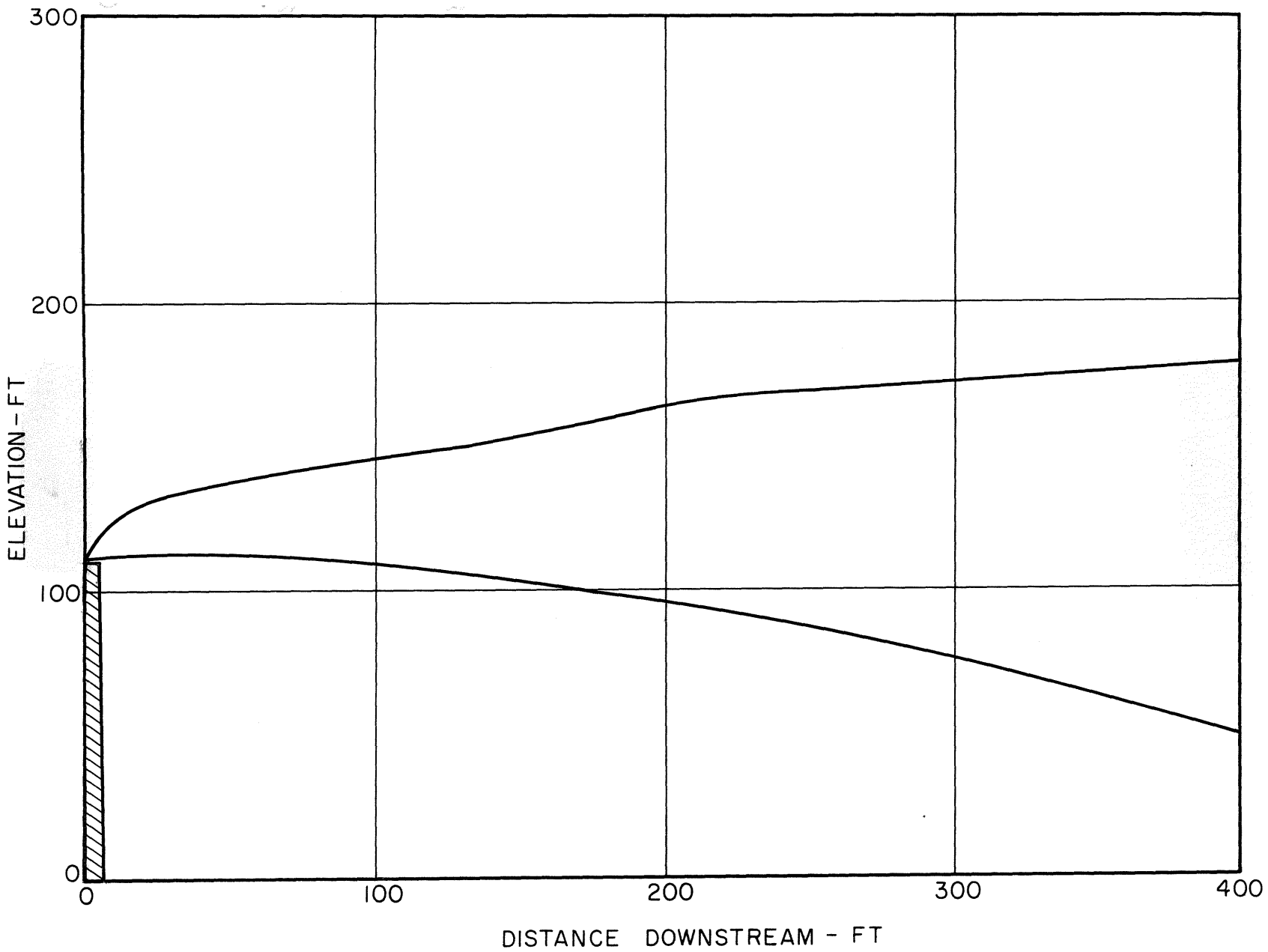

Figure 27 Stack 2, $\theta = 100°$, W/V = 1 , $\Delta T = 100°F$

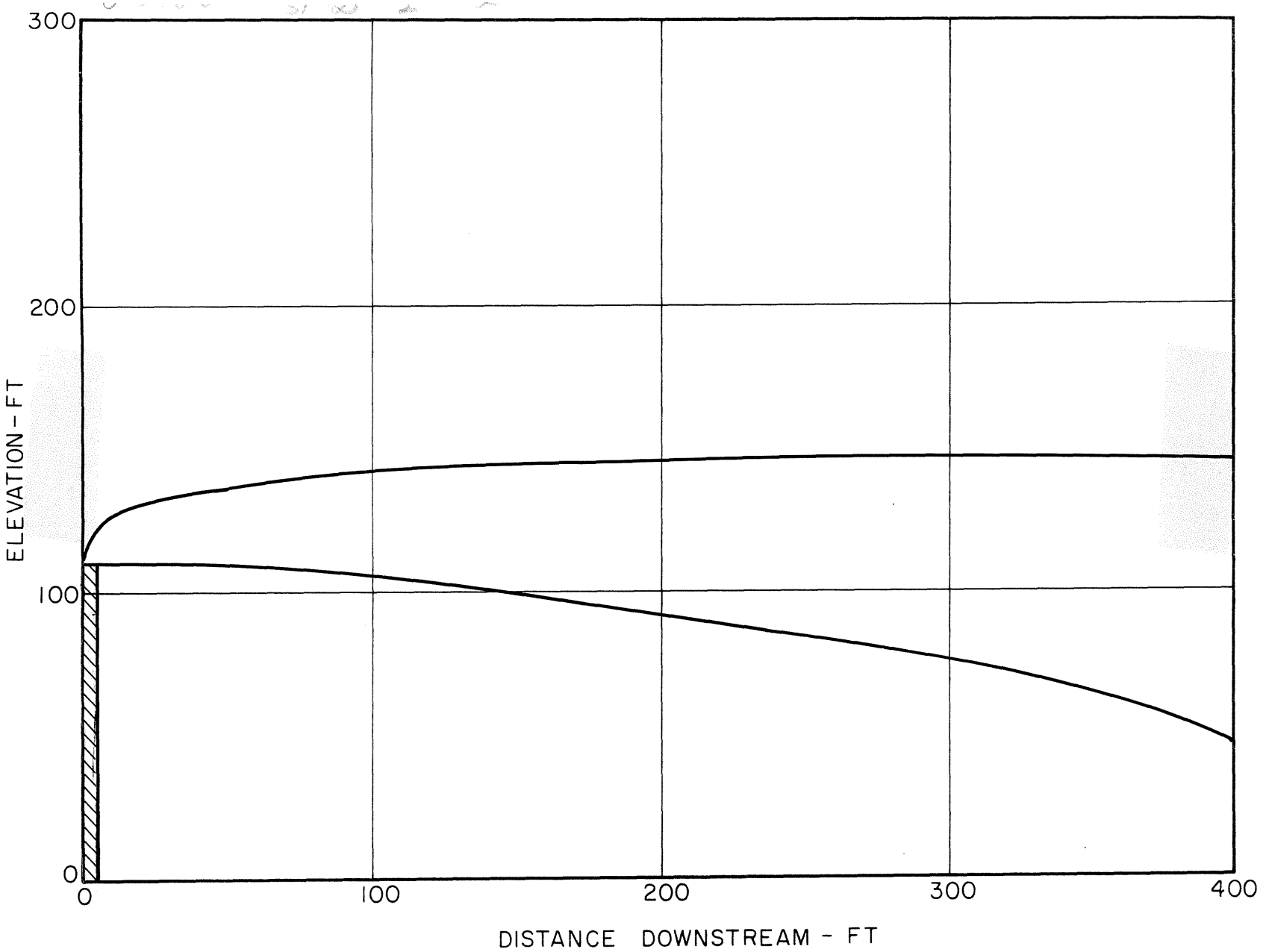

Figure 28 Stack 2, $\theta = 100°$, $W/V = 1/2$, $\Delta T = 100°F$

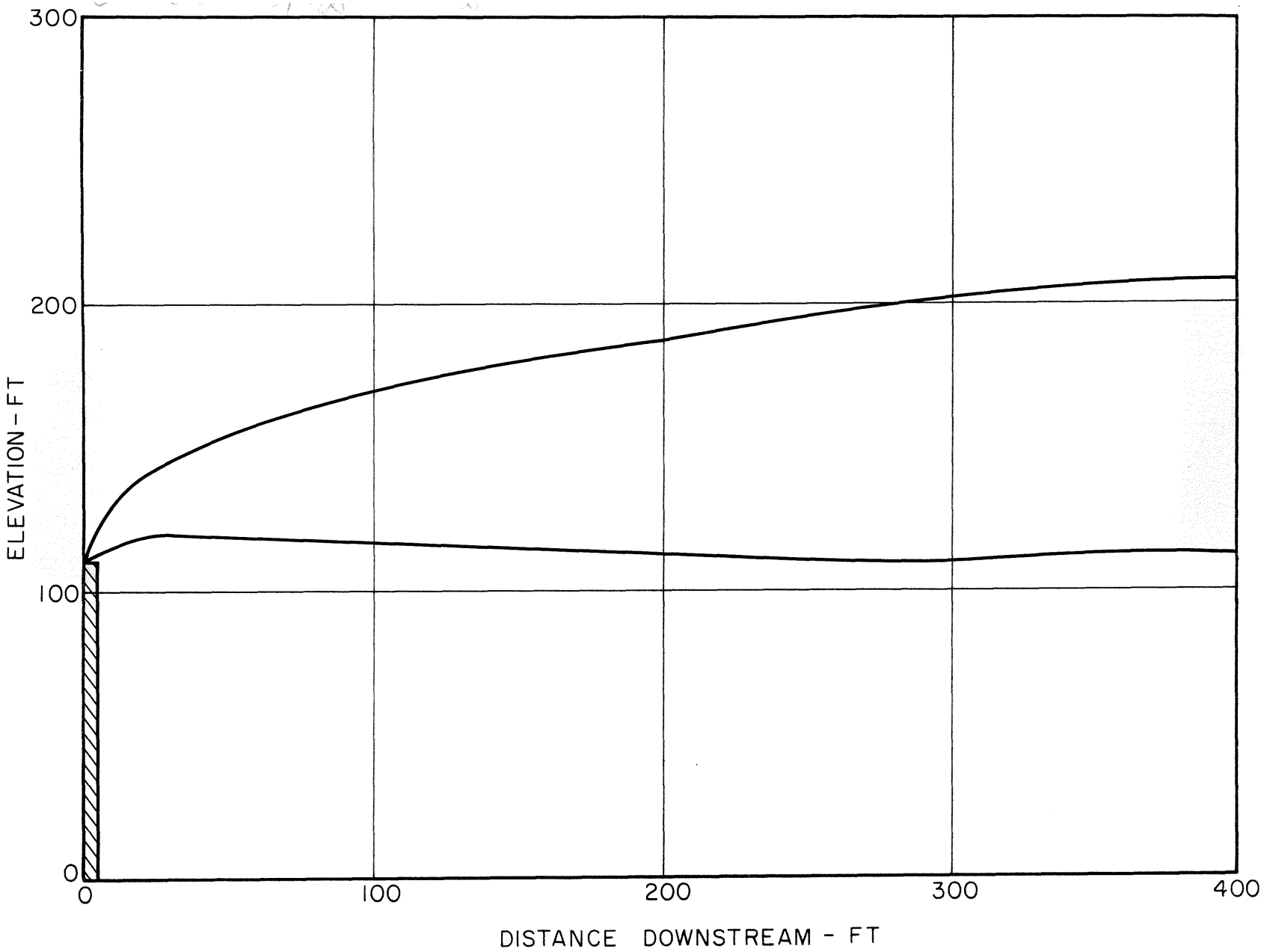

Figure 29 Stack 4, $\theta = 100°$, W/V = 2 , $\Delta T = 100°F$

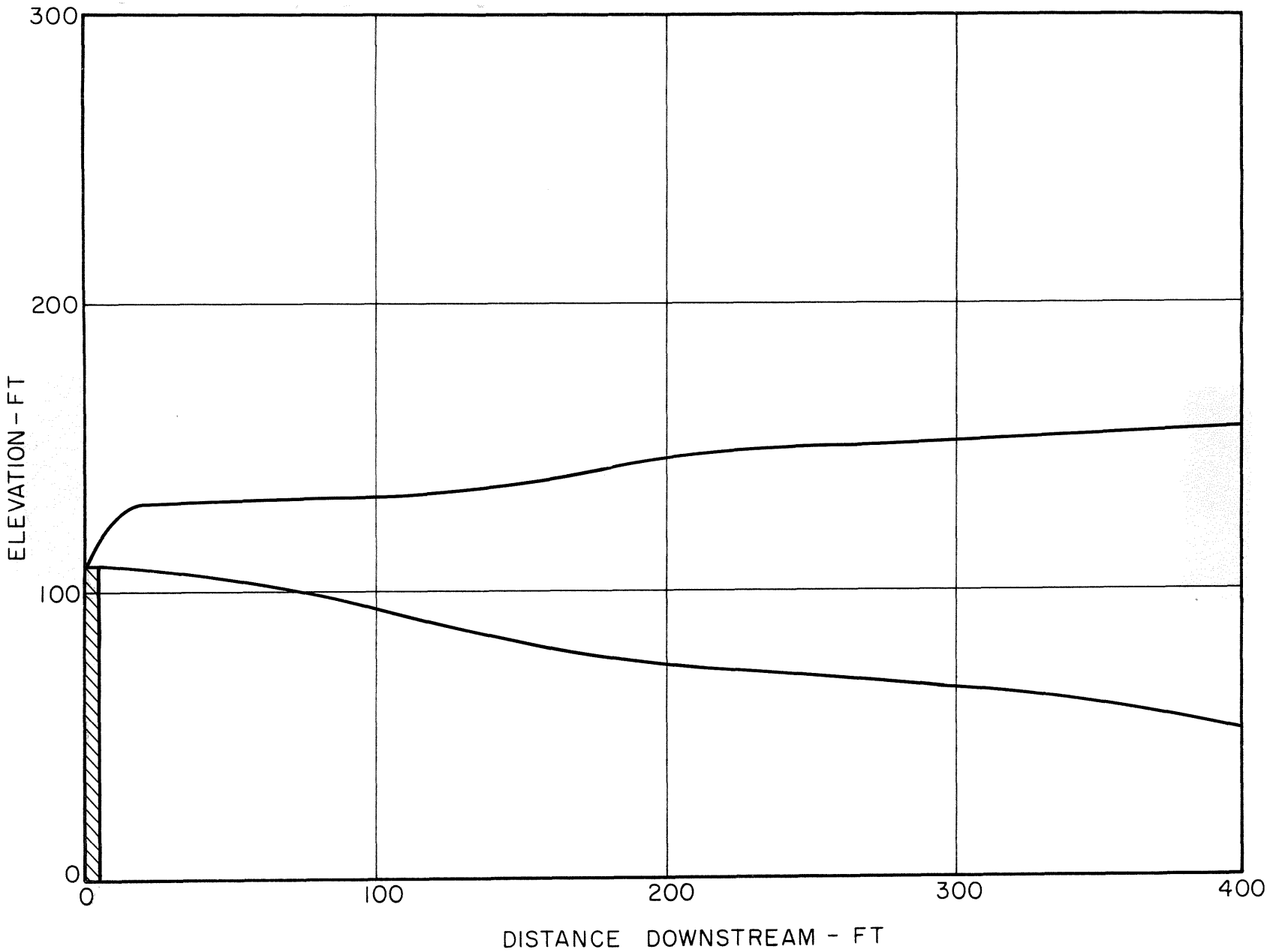

Figure 30 Stack 4, $\theta = 100°$, W/V = 1 , $\Delta T = 100°F$

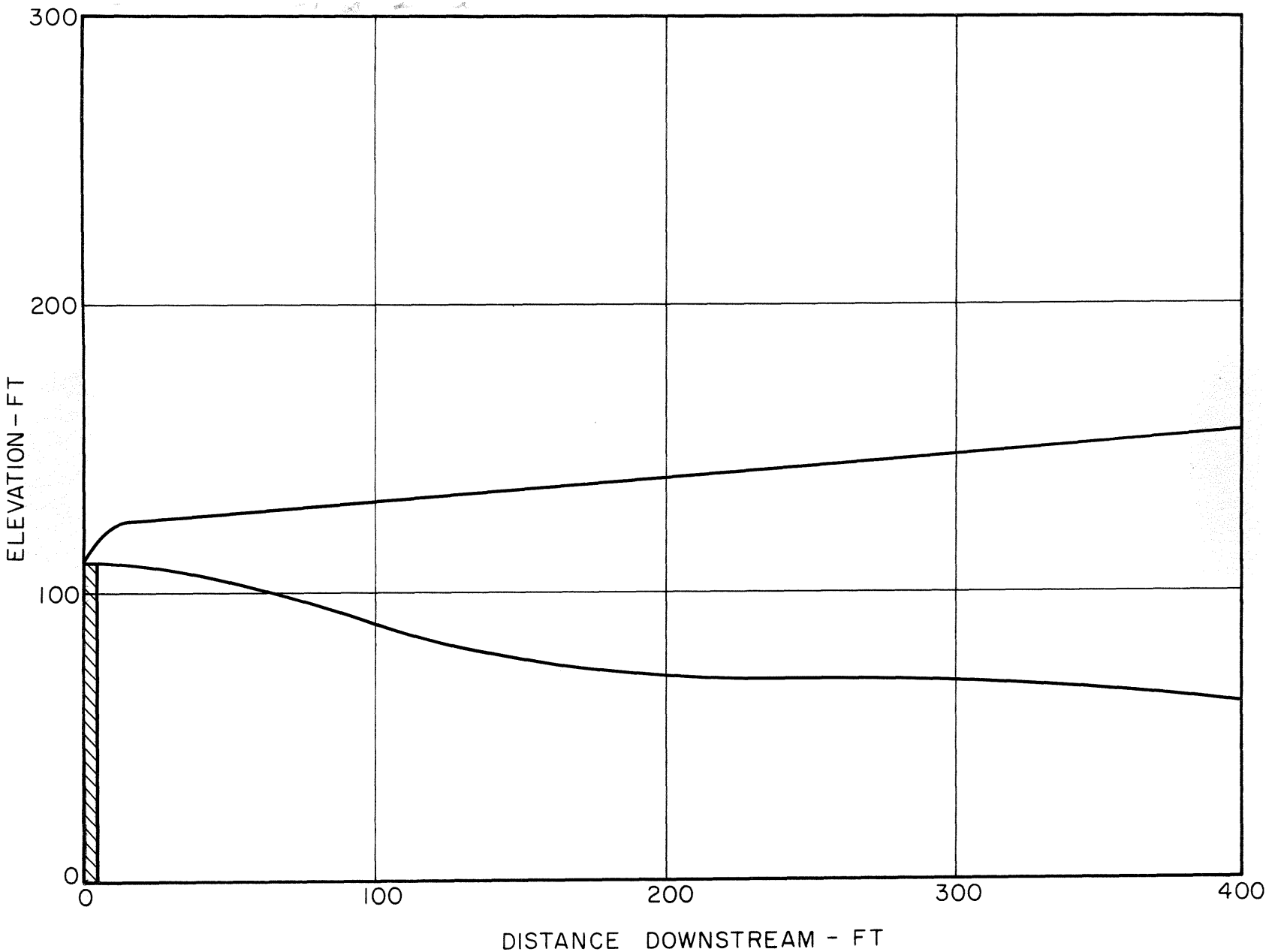

Figure 31 Stack 4, $\theta = 100°$, W/V = 1/2, $\Delta T = 100°F$

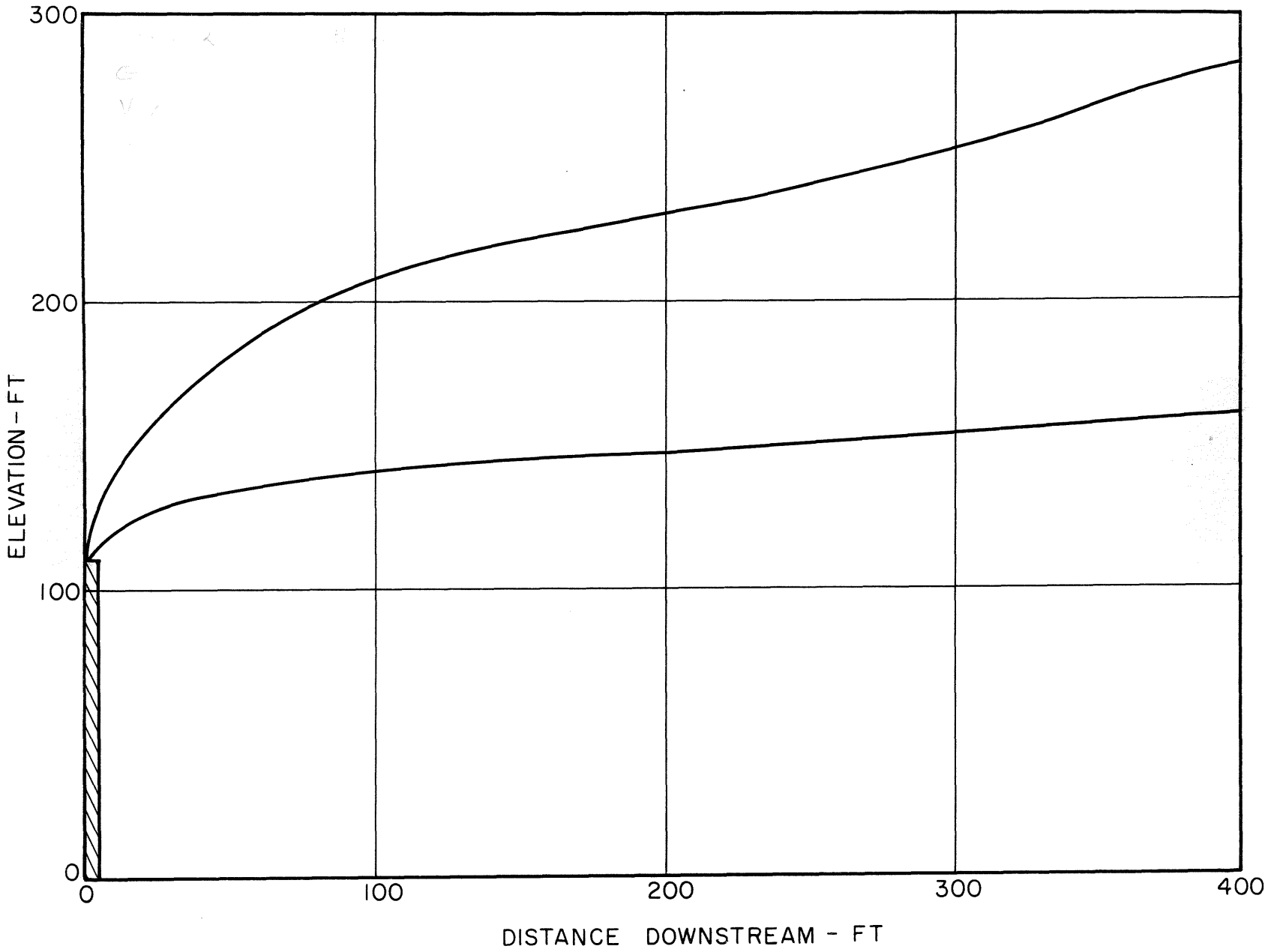

Figure 32 Stack 2 and others, $\theta = 80°$, $W/V = 2$, $\Delta T = 100°F$

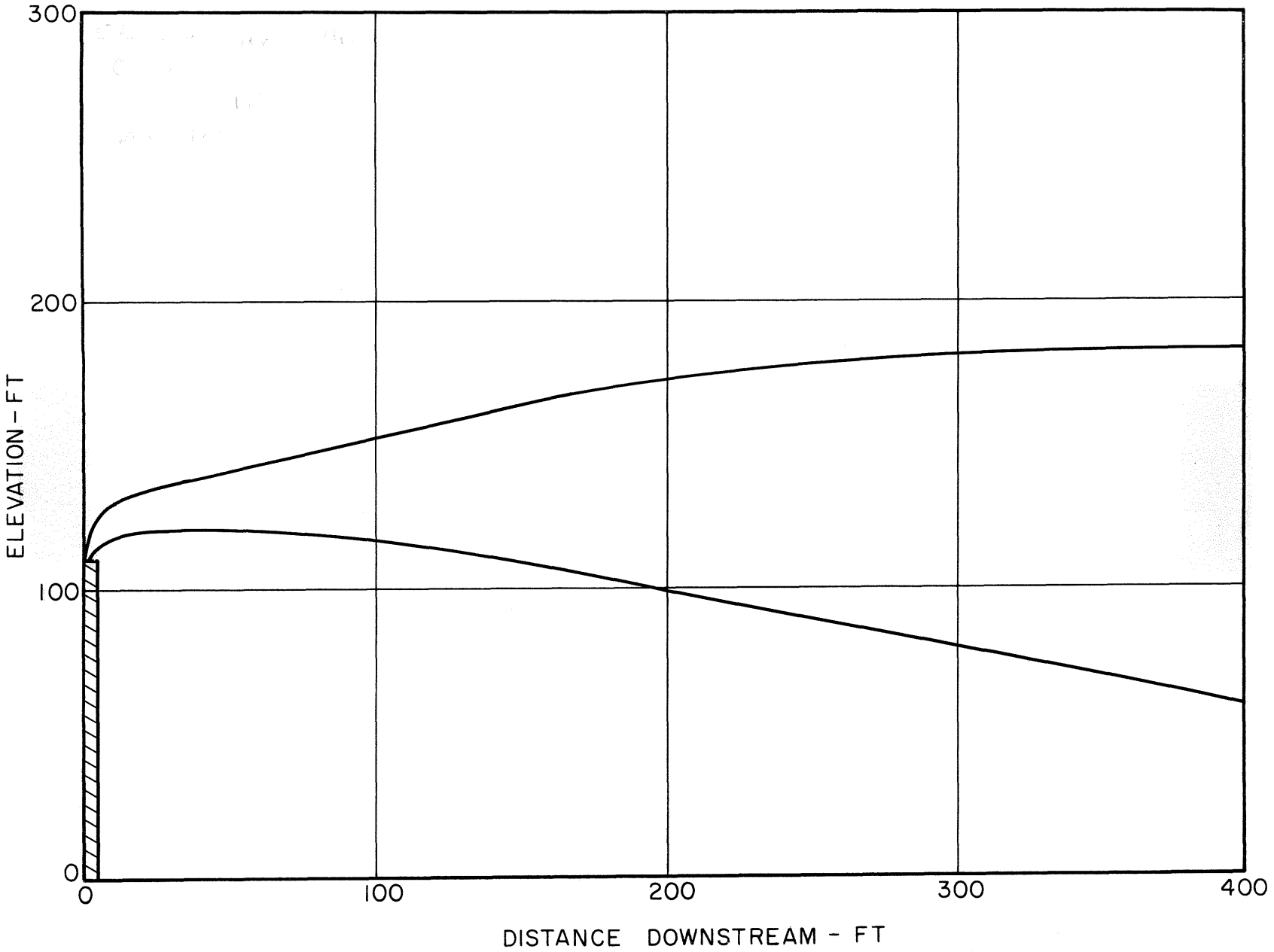

Figure 33 Stack 2 and others, $\theta = 80°$, W/V = 1 , $\Delta T = 100°F$

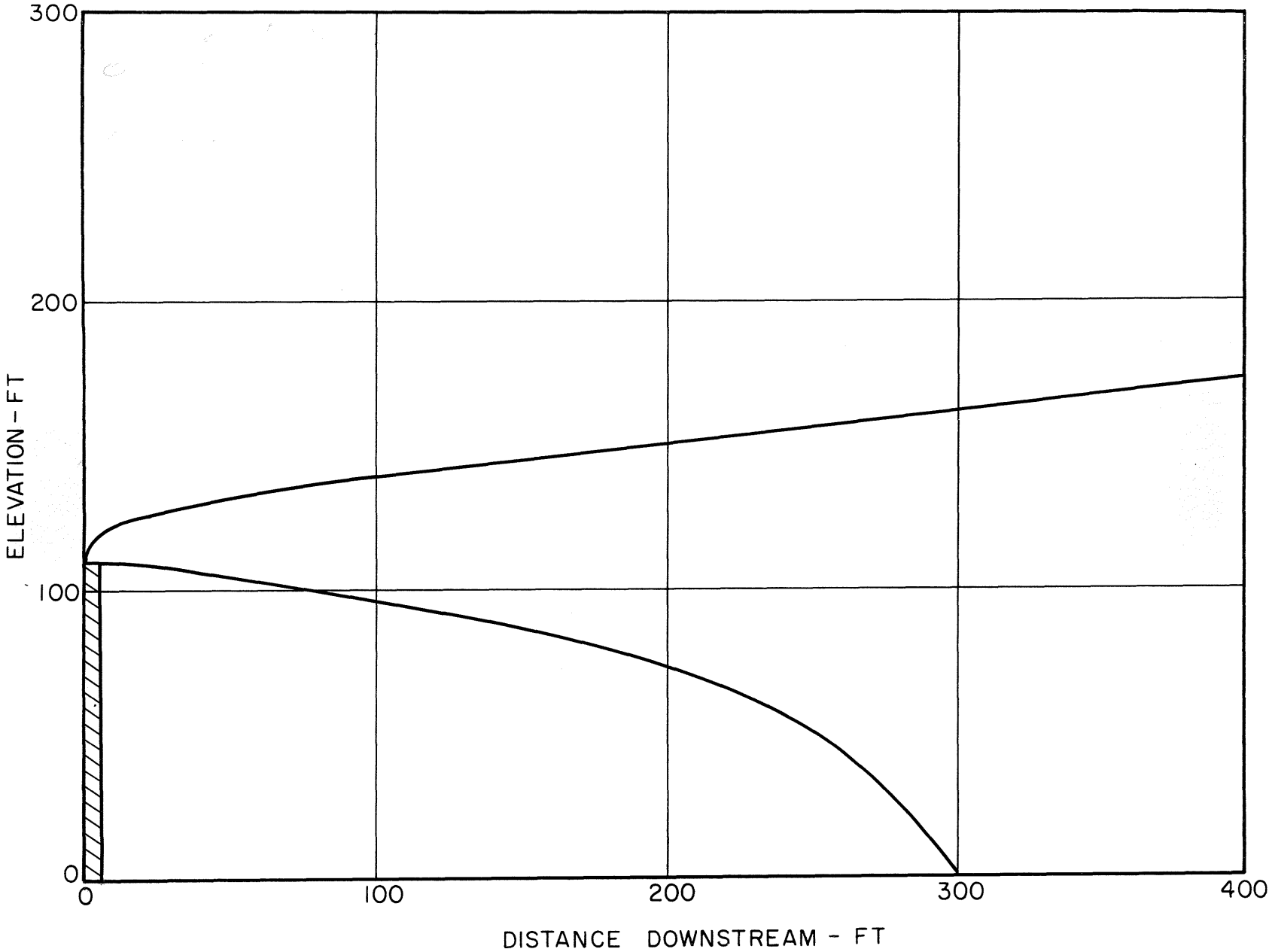

Figure 34 Stack 2 and others, $\theta = 80°$, $W/V = 0.5$, $\Delta T = 100°F$

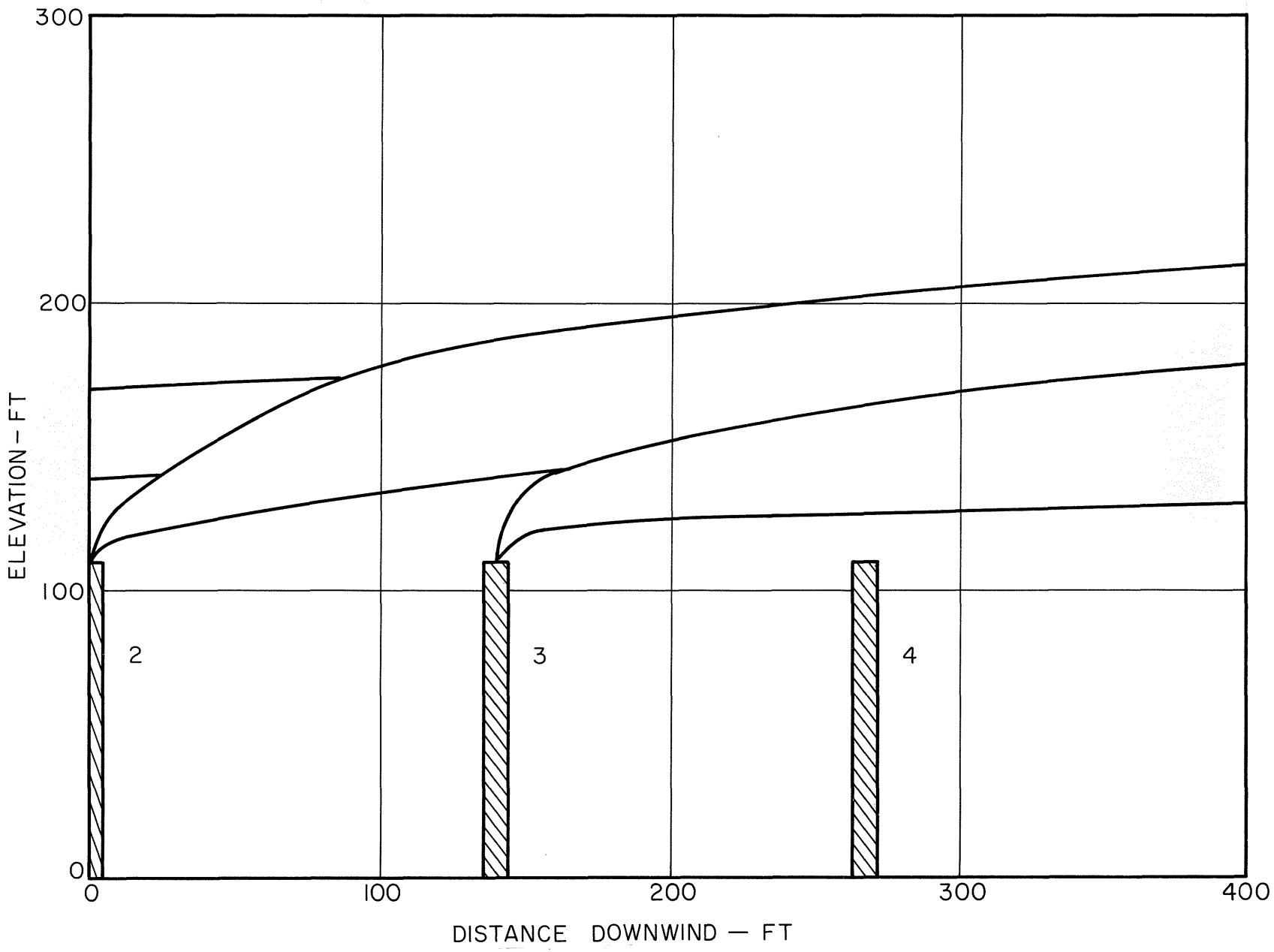

Figure 35 Stacks 1,2, & 3, $\theta = 180°$, W/V = 2.75, $\Delta T = 0.0°F$

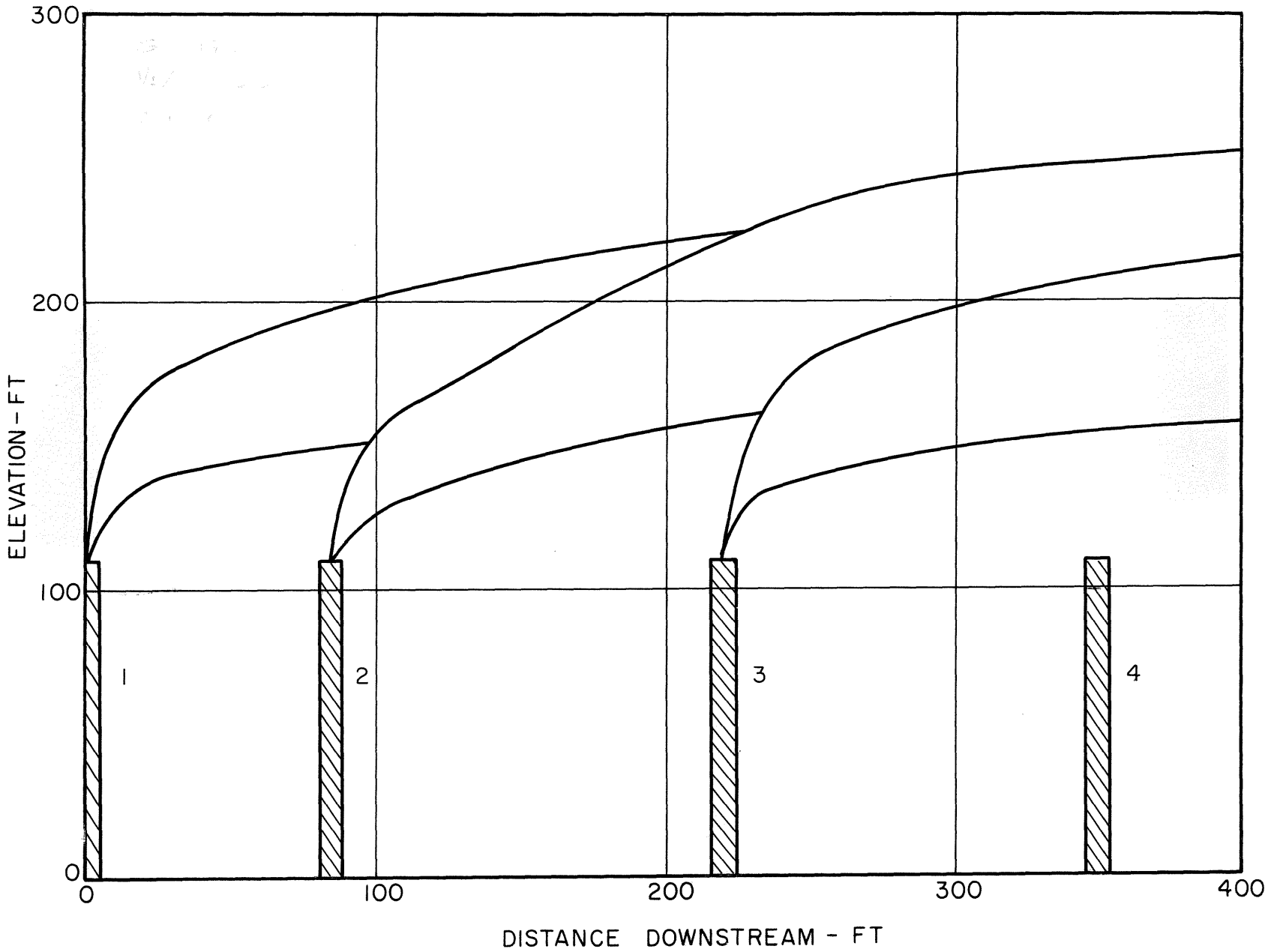

Figure 36 Stacks 1, 2, & 3, $\theta = 180°$, W/V = 5.5, $\Delta T = 0.0°F$

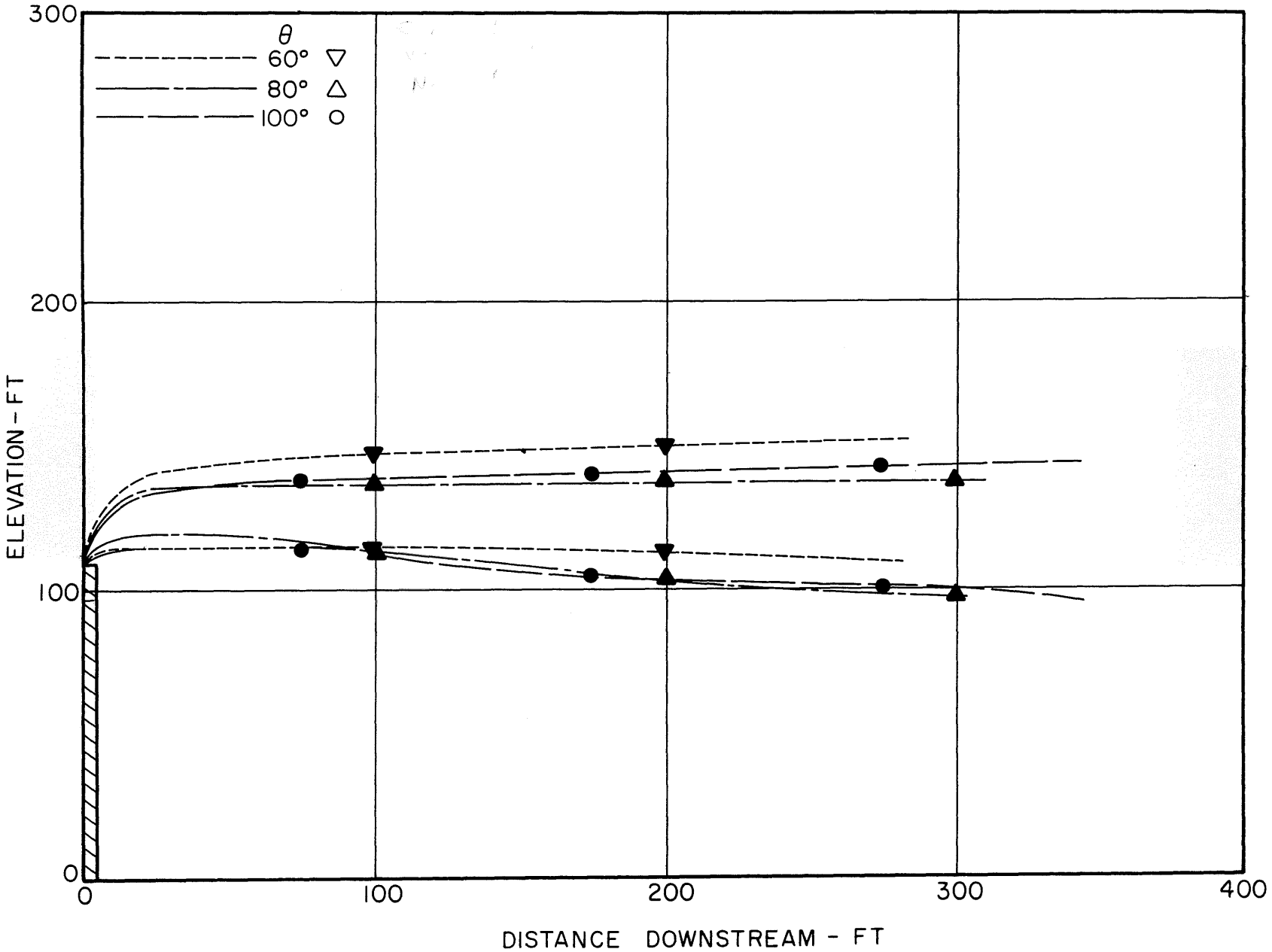

Figure 37 Comparison of the effect of angle variation, Stack 1, W/V = 0.95, ΔT = 0°F

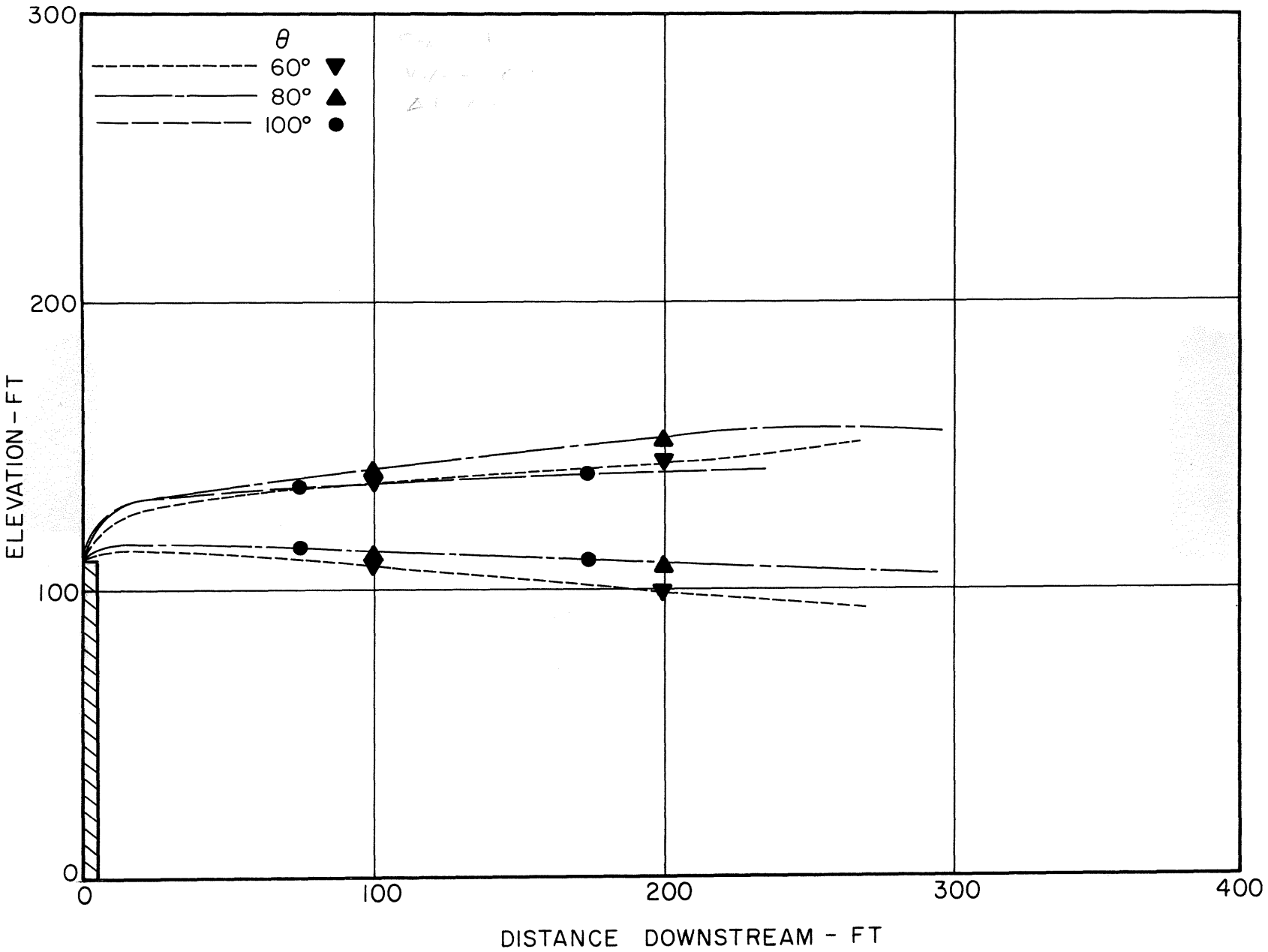

Figure 38 Comparison of the effect of angle variation, Stack 4, W/V = 0.95, $\Delta T = 0^{\circ}F$

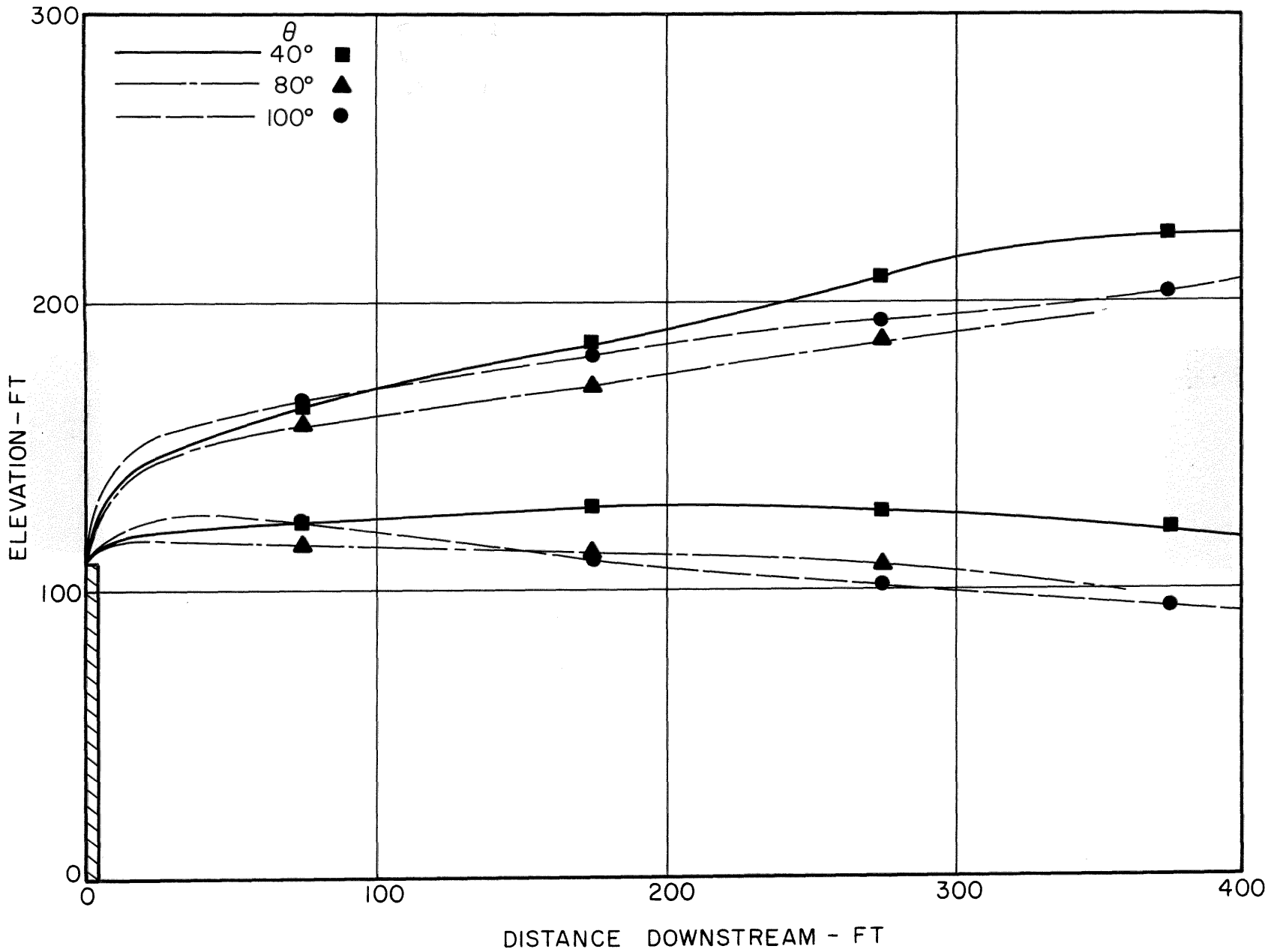

Figure 39 Comparison of the effect of angle variation, Stack 1, W/V = 2 , $\Delta T = 100^{\circ}F$

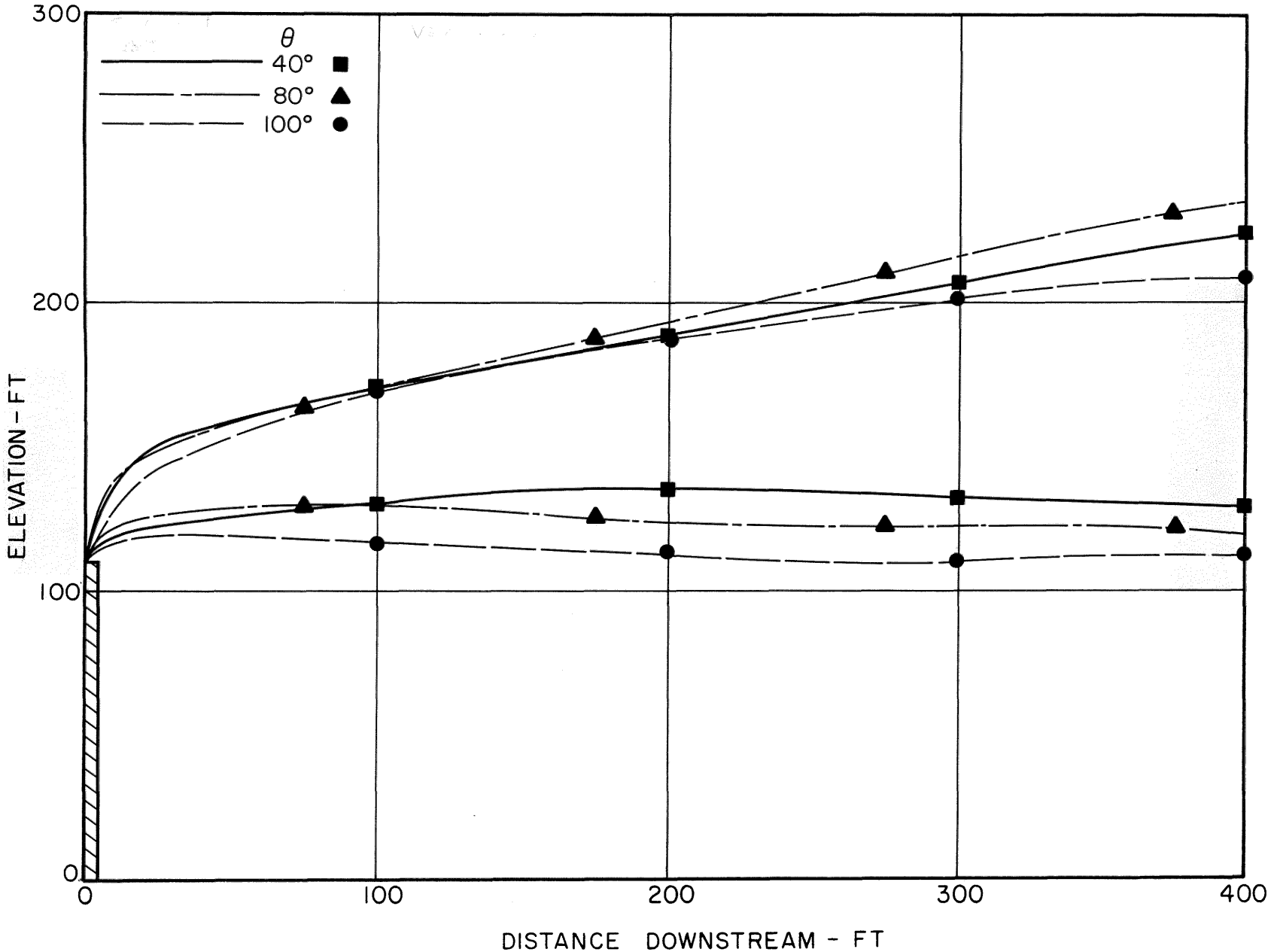

Figure 40 Comparison of the effect of angle variation, Stack 4, W/V = 2 , $\Delta T = 100^{\circ}F$

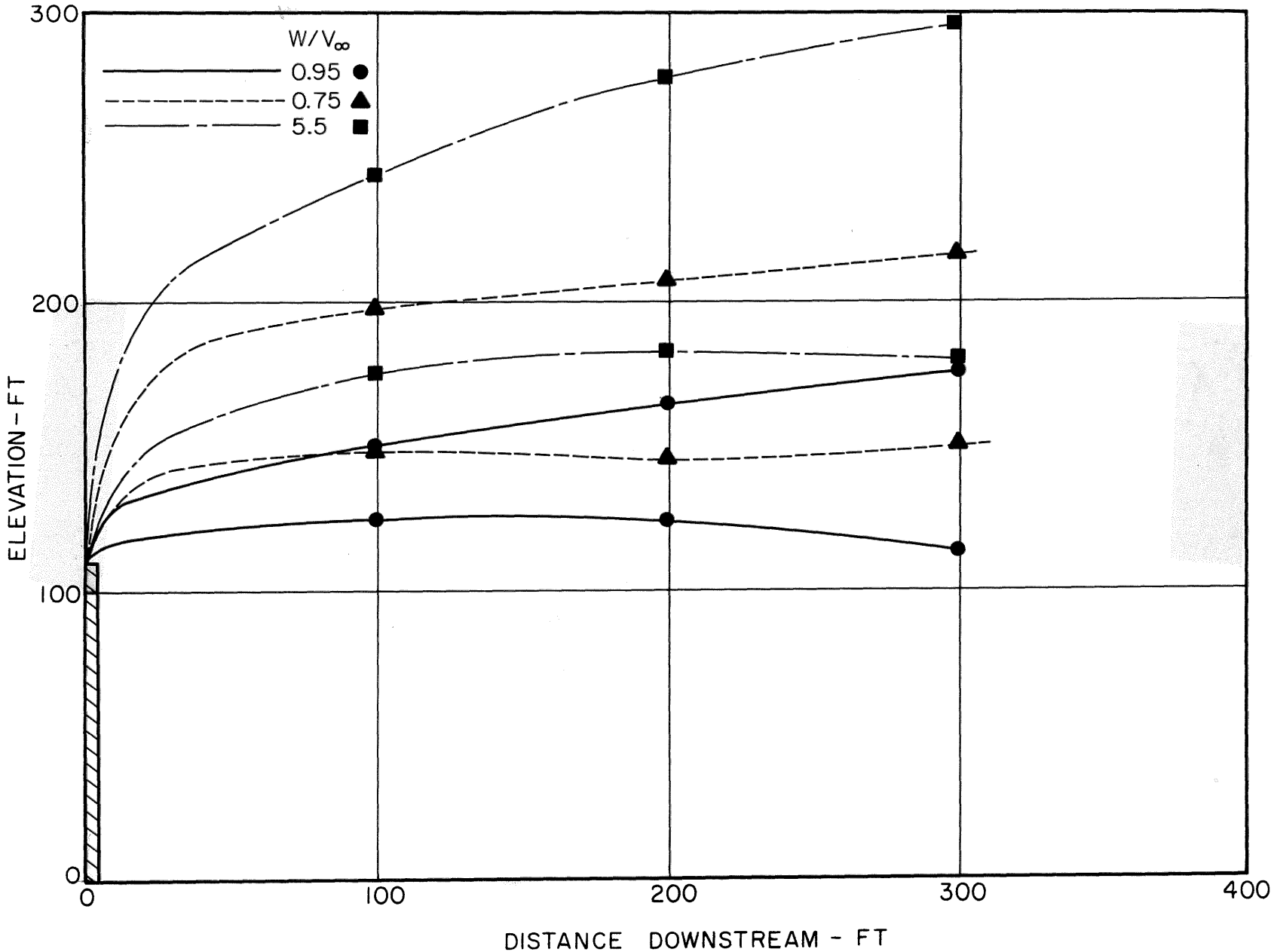

Figure 41 Comparison of variation in velocity ratios, Stack 2, $\theta = 80°$, $\Delta T = 0°F$

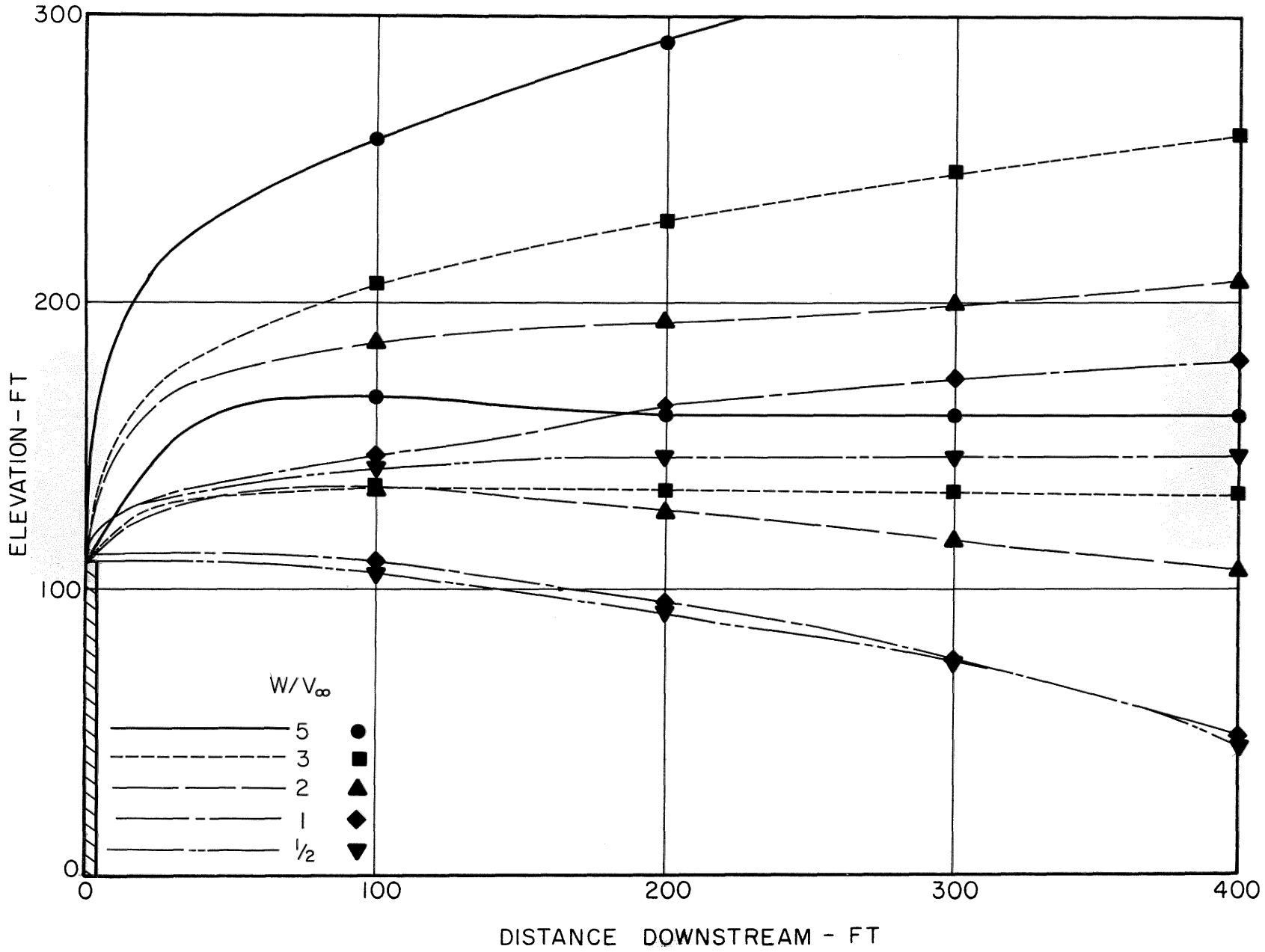

Figure 42 Comparison of variation in velocity ratios, Stack 2, $\theta = 80°$, $\Delta T = 100°F$

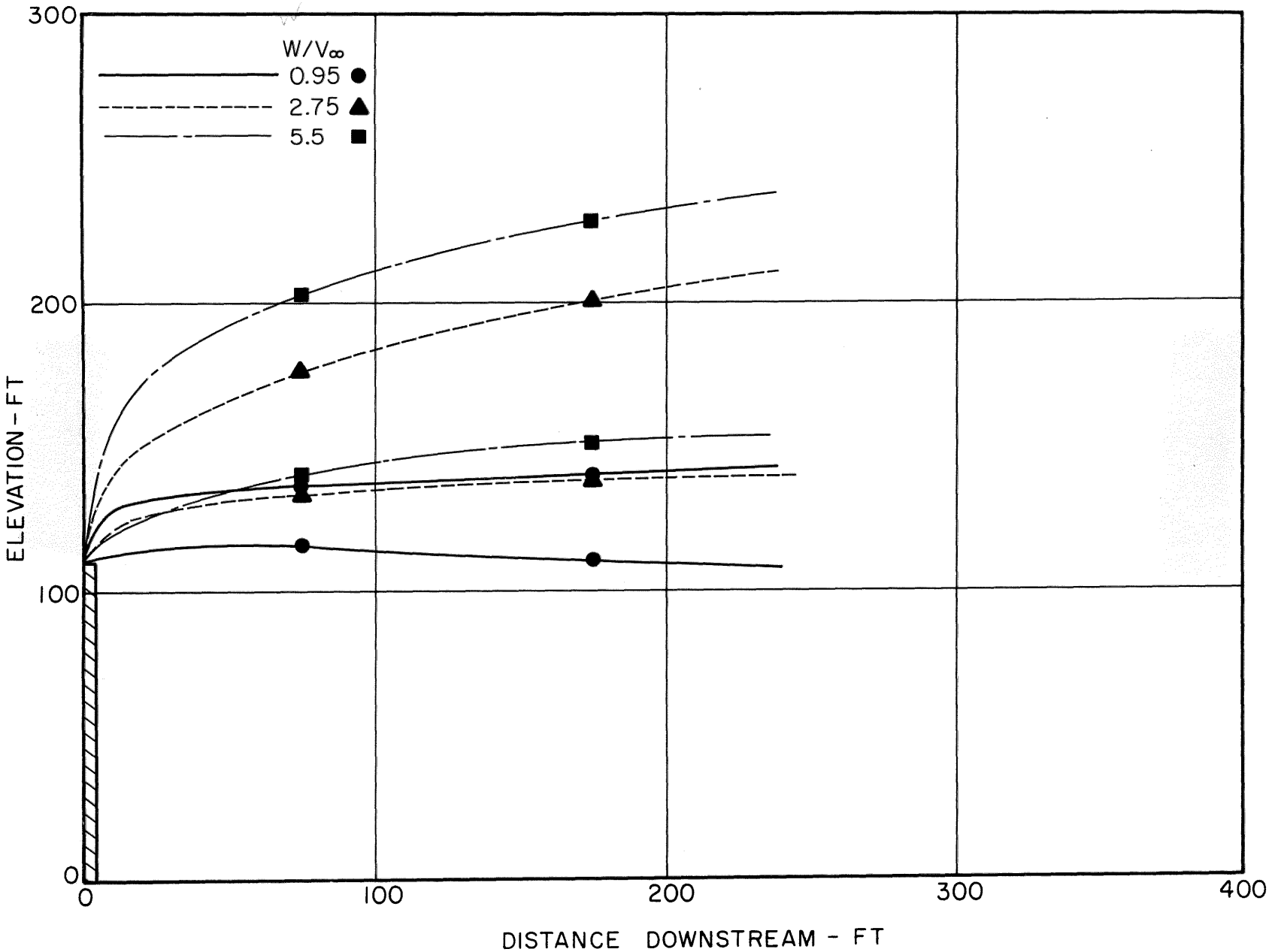

Figure 43 Comparison of variation in velocity ratios, Stack 4, $\theta = 100°$, $\Delta T = 0°F$

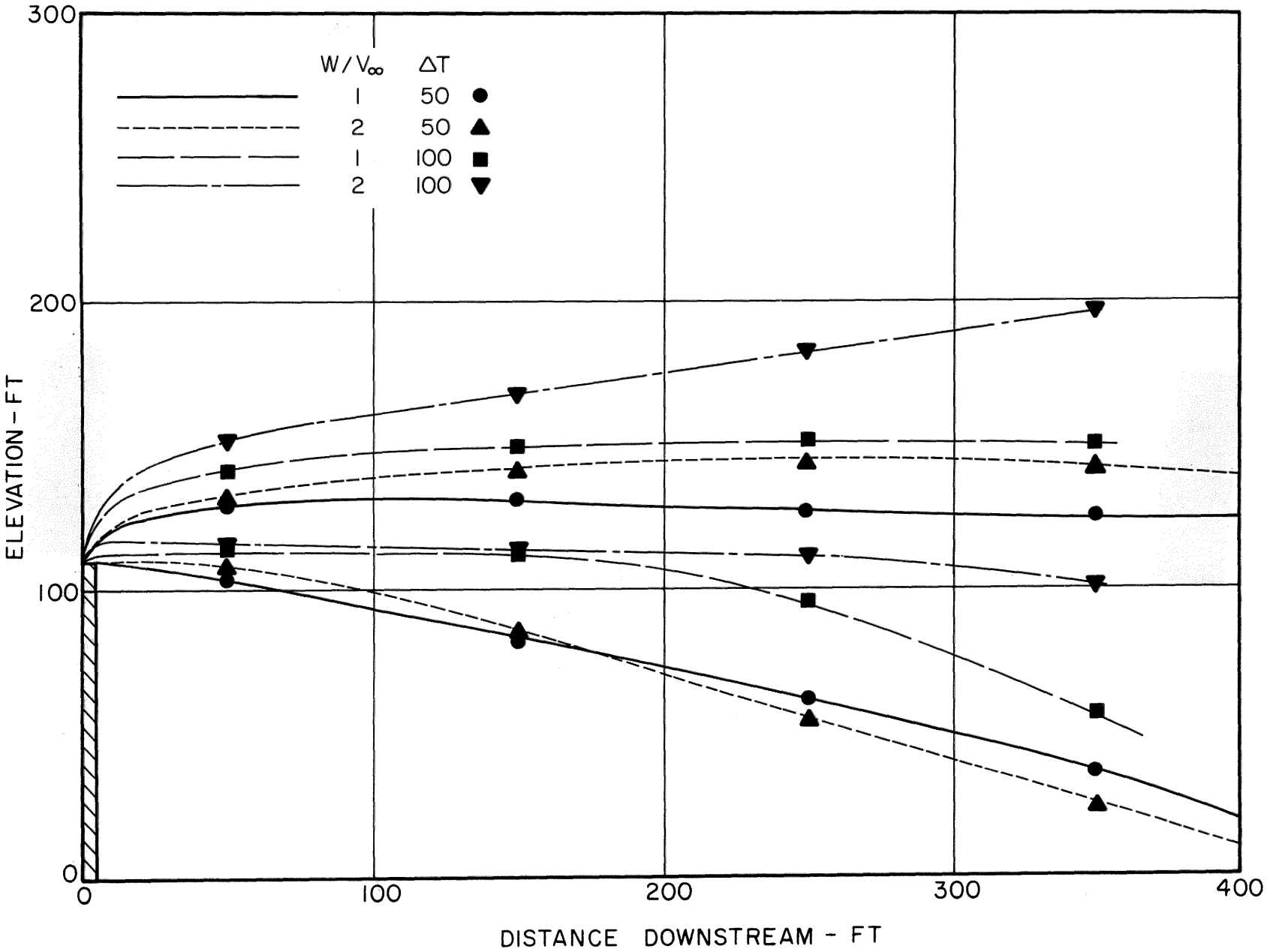

Figure 44 Comparison of variation in ΔT, Stack 1, θ = 80°

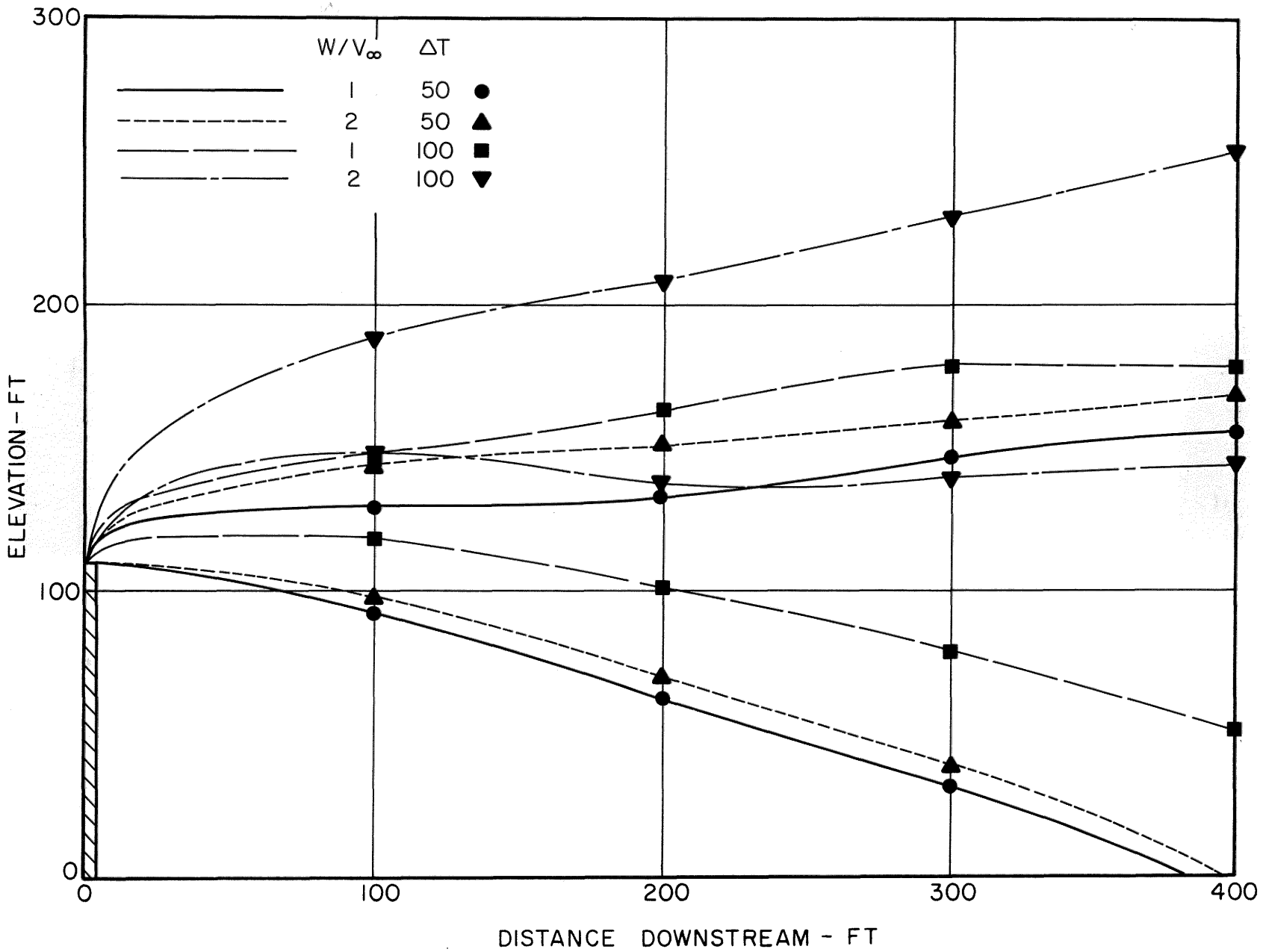

Figure 45 Comparison of variation in ΔT, Stack 2, θ = 80°

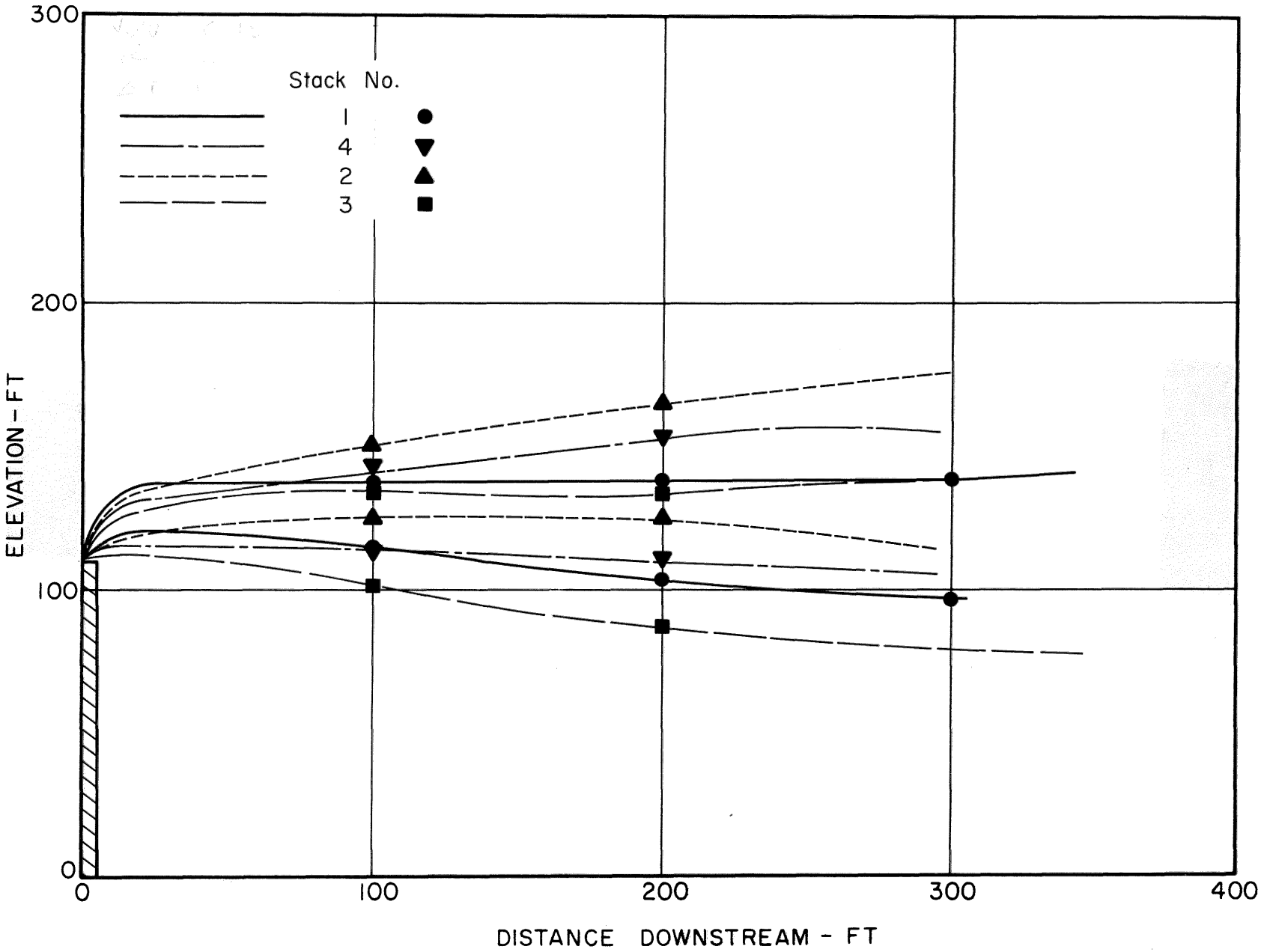

Figure 46 Comparison of Stack site release number, W/V = 0.95, θ = 80°, ΔT = 0°F

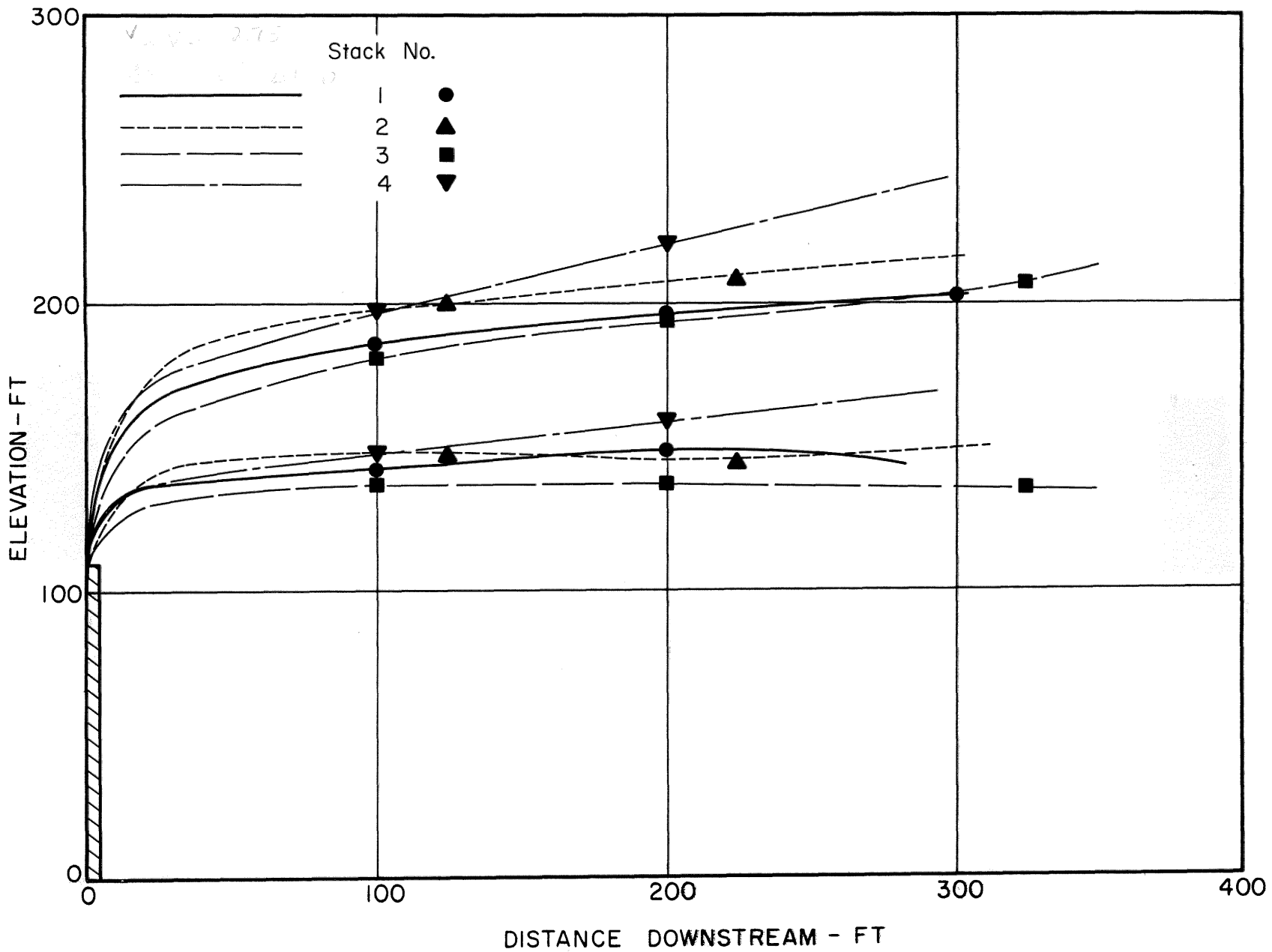

Figure 47 Comparison of Stack site release number, W/V = 2.75, θ = 80°, ΔT = 0°F

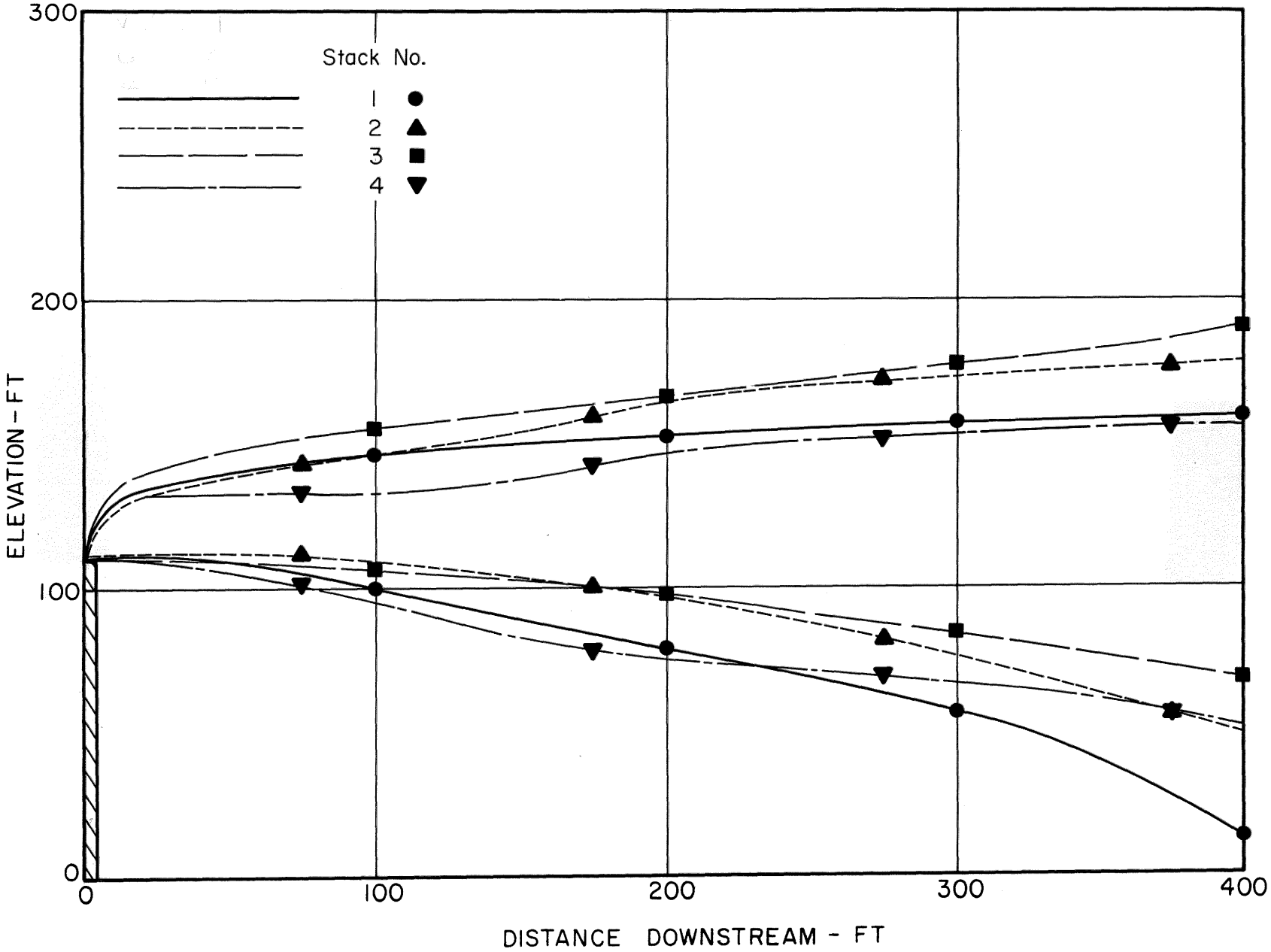

Figure 48 Comparison of Stack site release number, W/V = 1 , θ = 80°, ΔT = 100°F

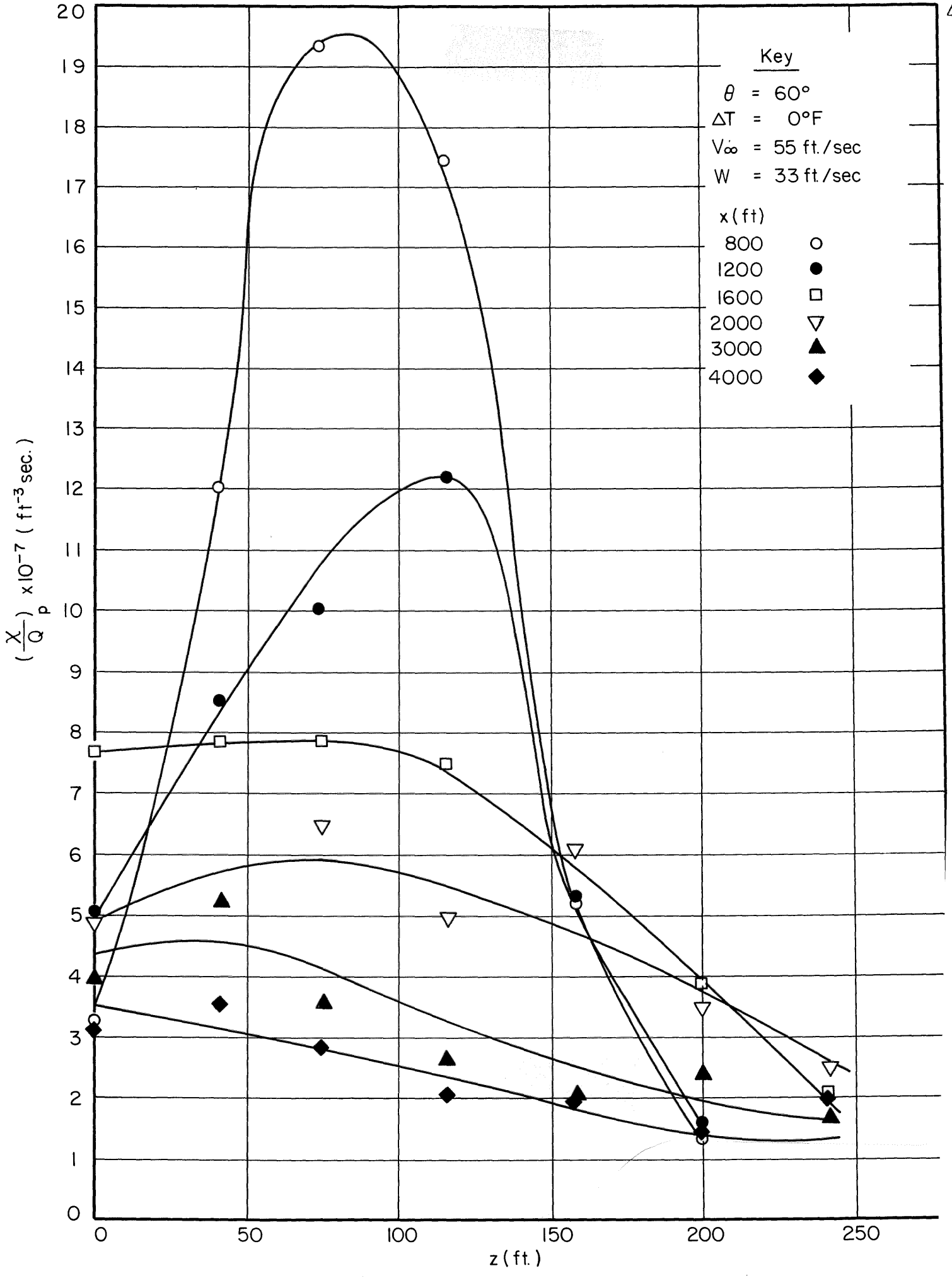

Figure 49 Vertical concentration distributions
W/V = 0.6, θ = 60°, ΔT = 0°F

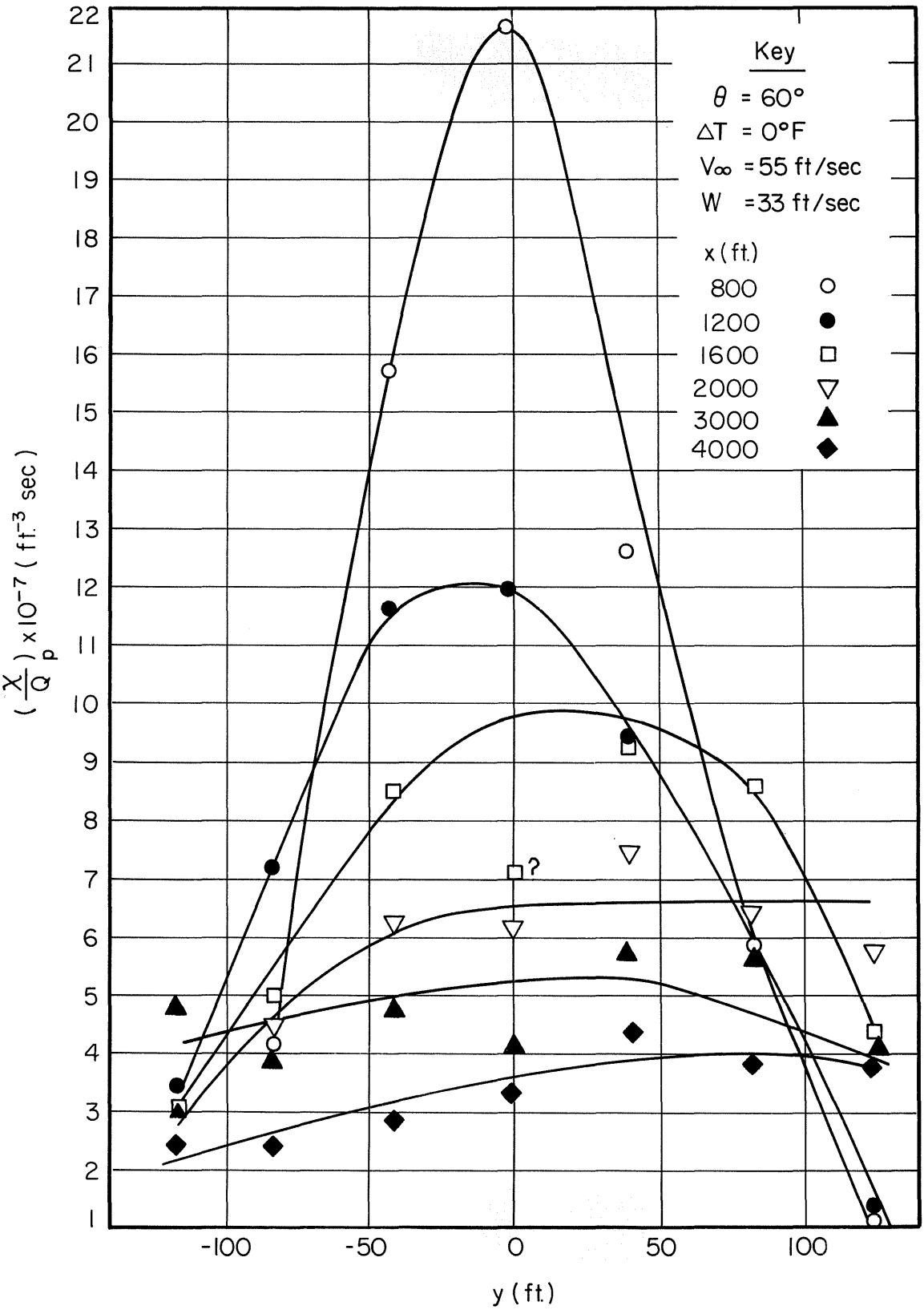

Figure 50 Horizontal concentration distributions
W/V = 0.6, θ = 60°, ΔT = 0°F

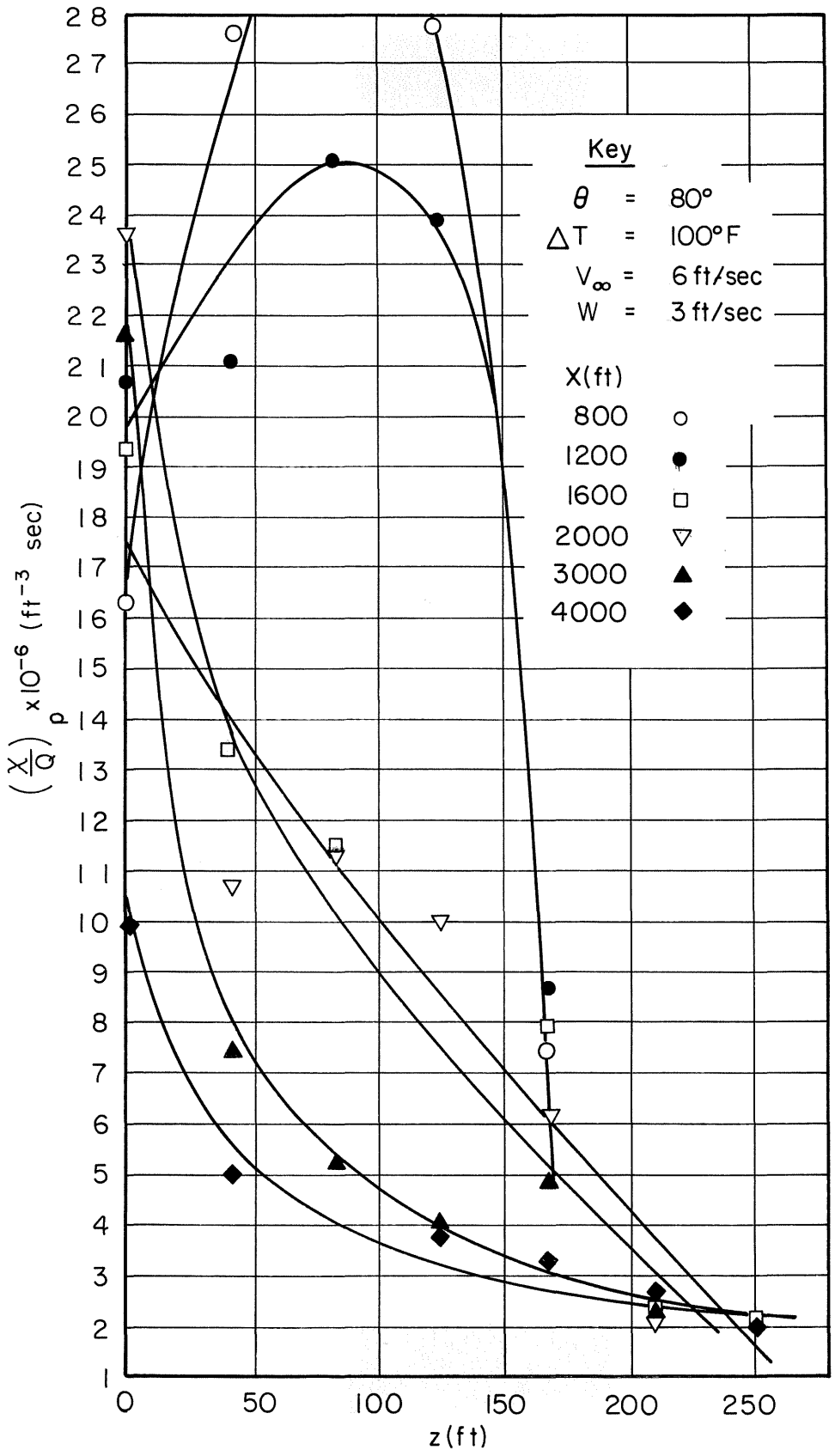

Figure 51 Vertical concentration distributions
W/V = 0.6, θ = 80°, ΔT = 100°F

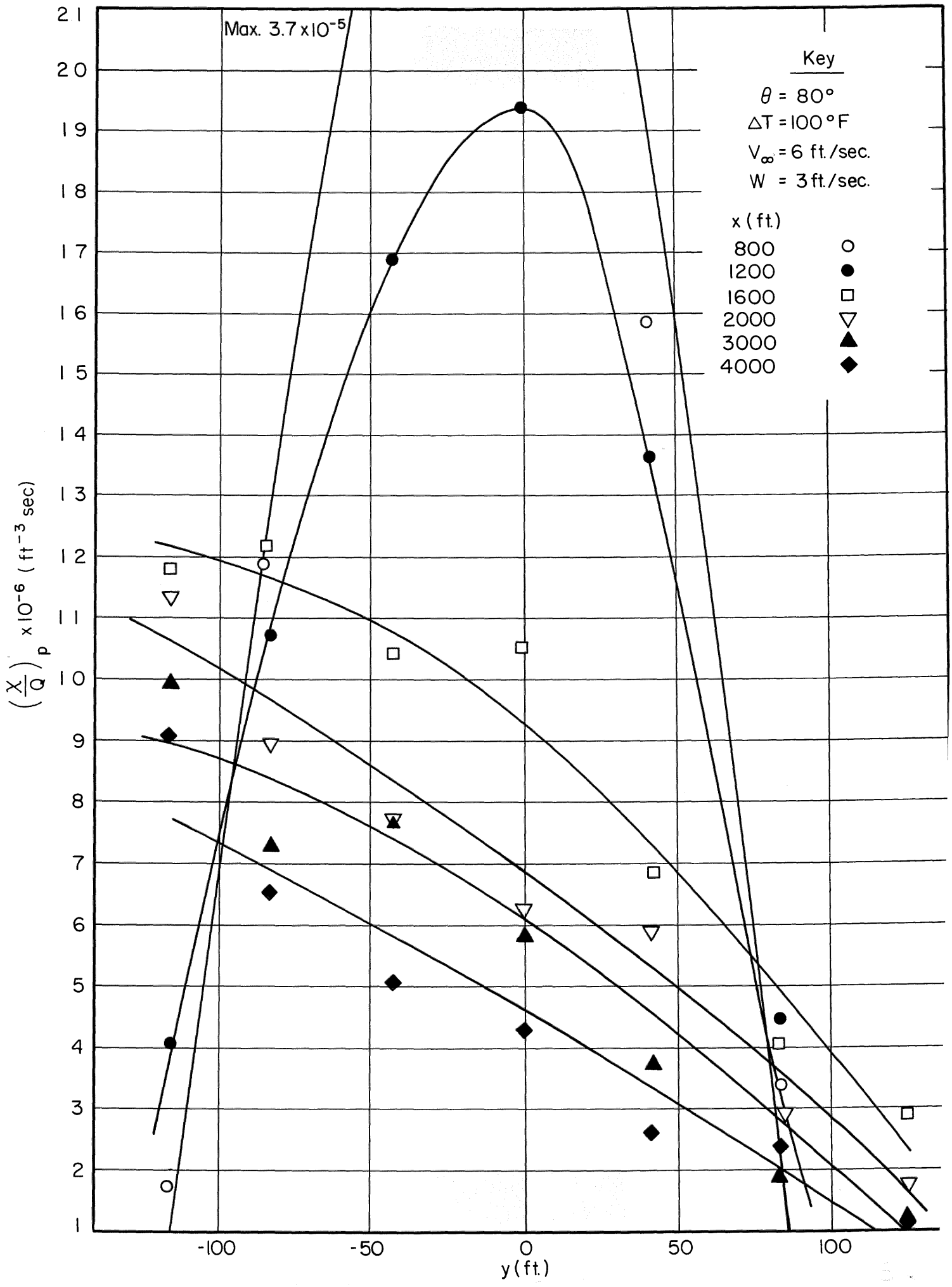

Figure 52 Horizontal concentration distributions
W/V = 0.6, θ = 80°, ΔT = 100°F

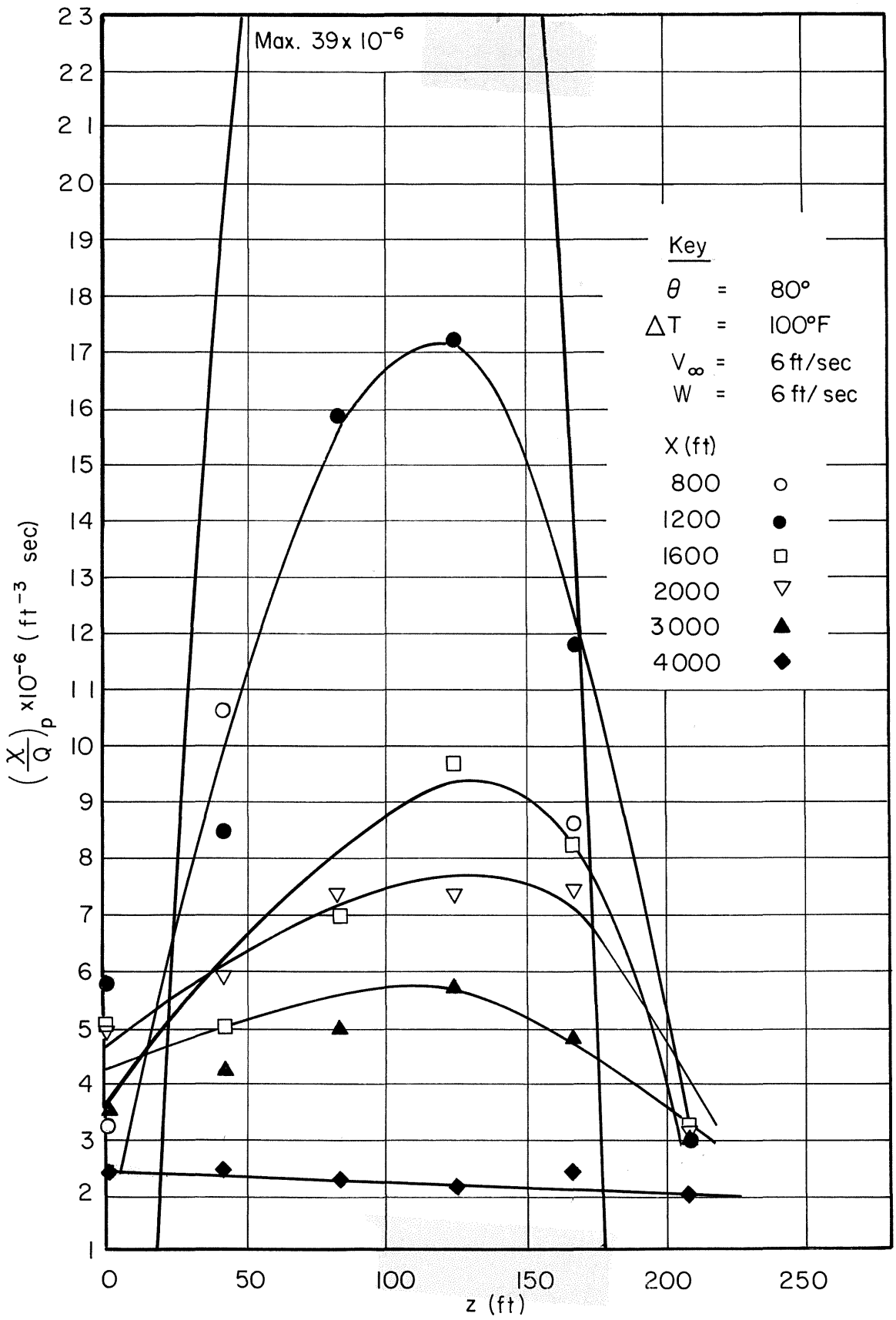

Figure 53 Vertical concentration distributions
W/V = 1, θ = 80°, ΔT = 100°F

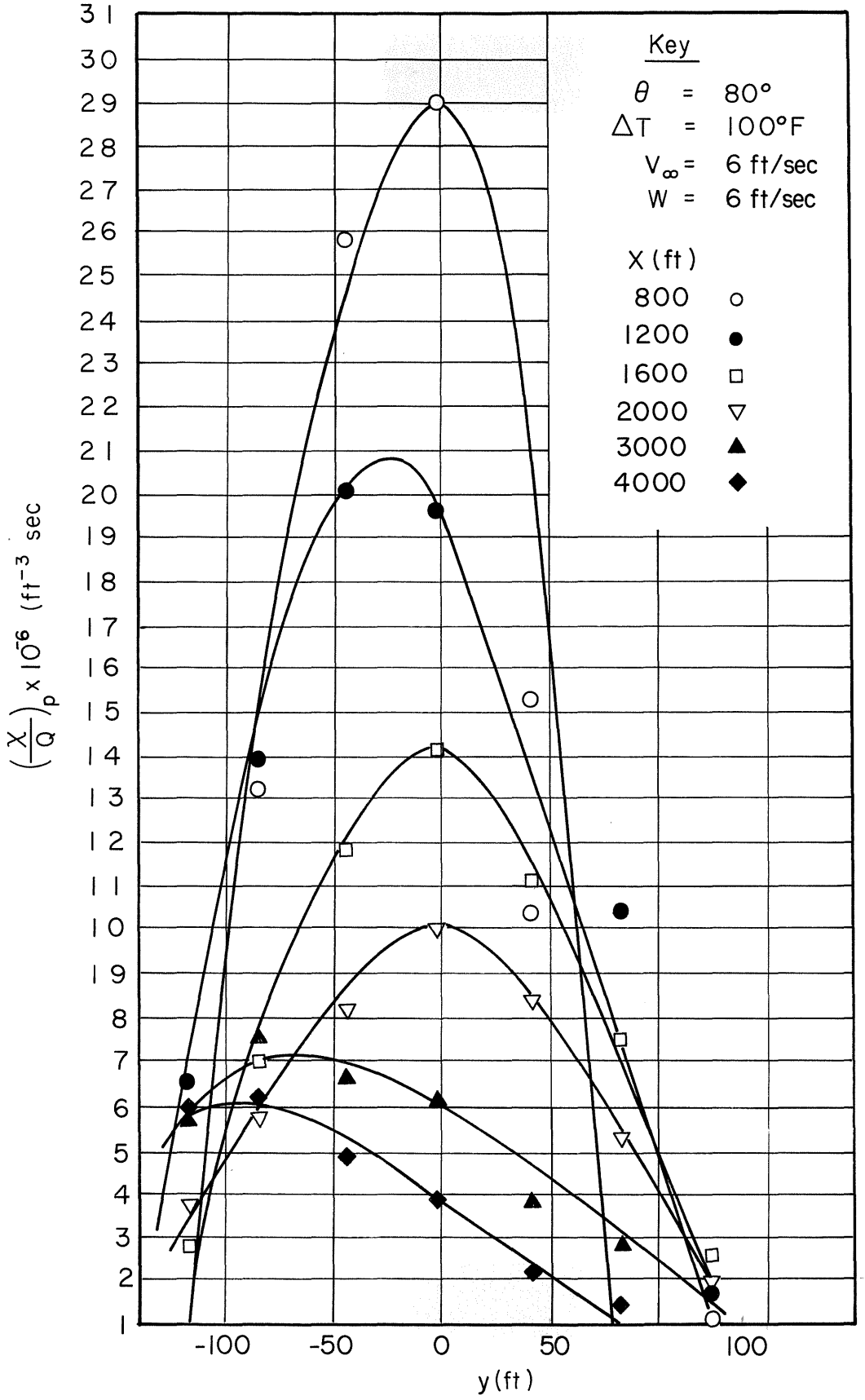

Figure 54 Horizontal concentration distributions
W/V = 1, θ = 80°, ΔT = 100°F

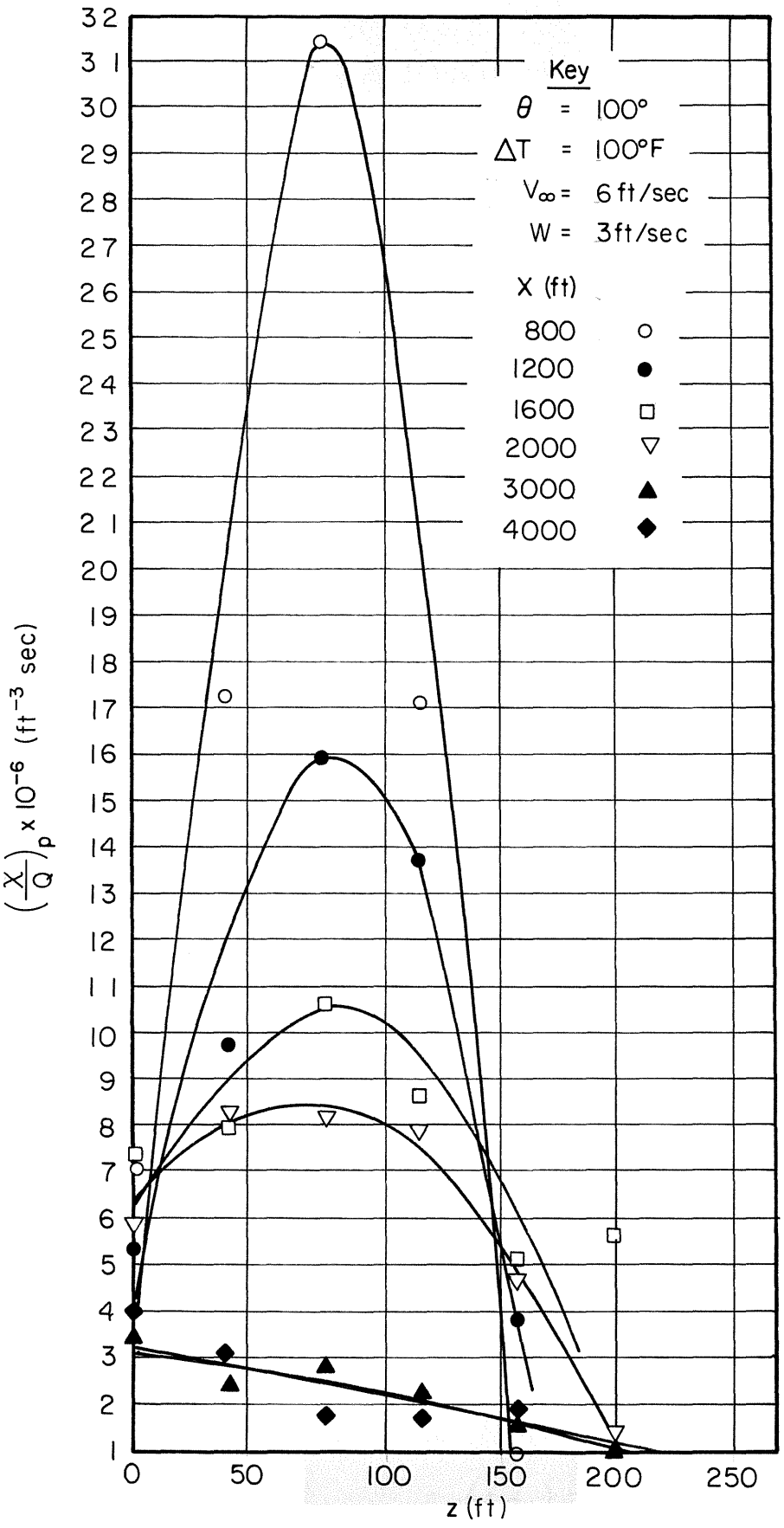

Figure 55 Vertical concentration distributions
W/V = 0.6, θ = 100°, ΔT = 100°F

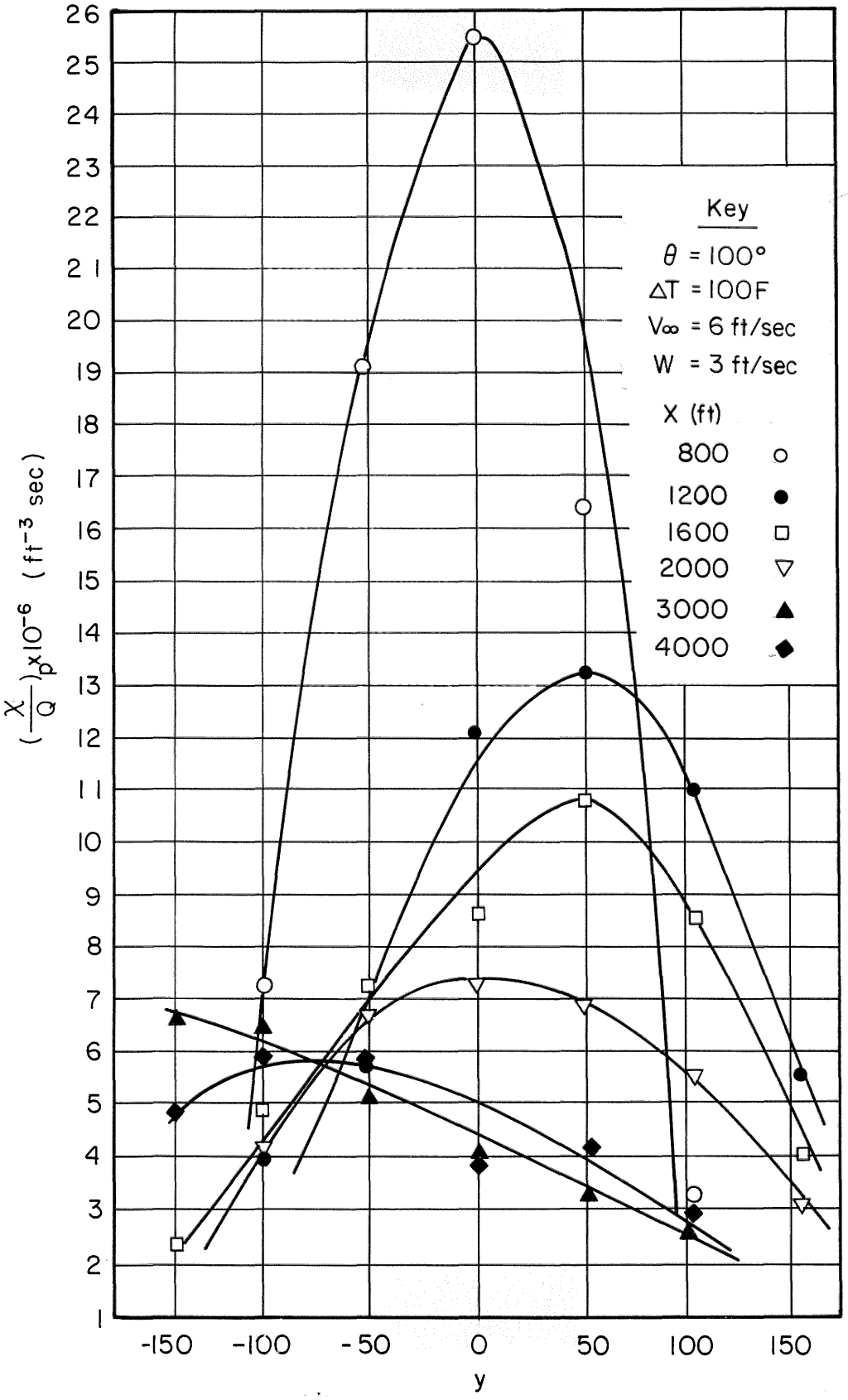

Figure 56 Horizontal concentration distributions
W/V = 0.6, θ = 100°, ΔT = 100°F

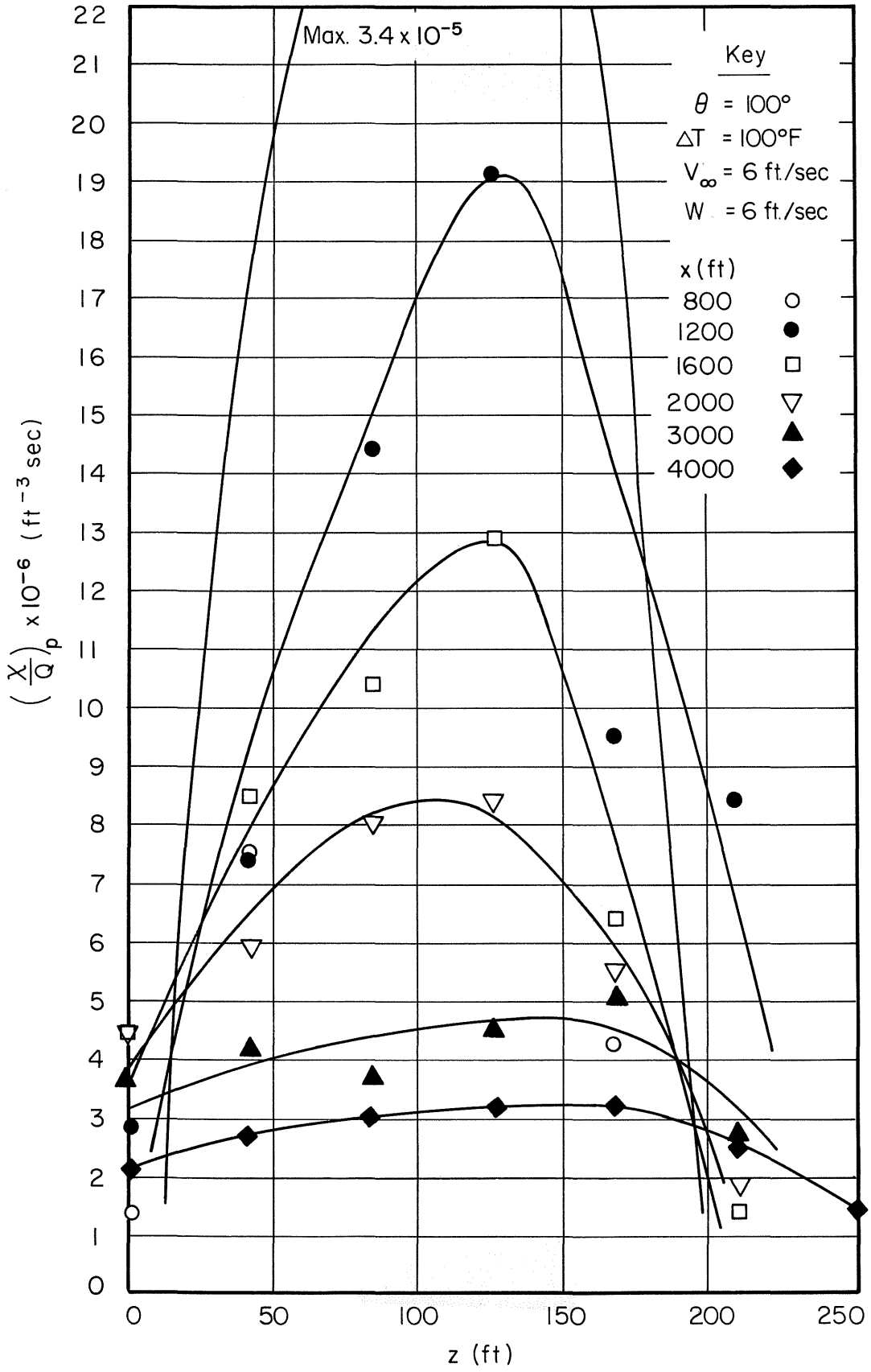

Figure 57 Vertical concentration distributions
W/V = 1, θ = 100°, ΔT = 100°F

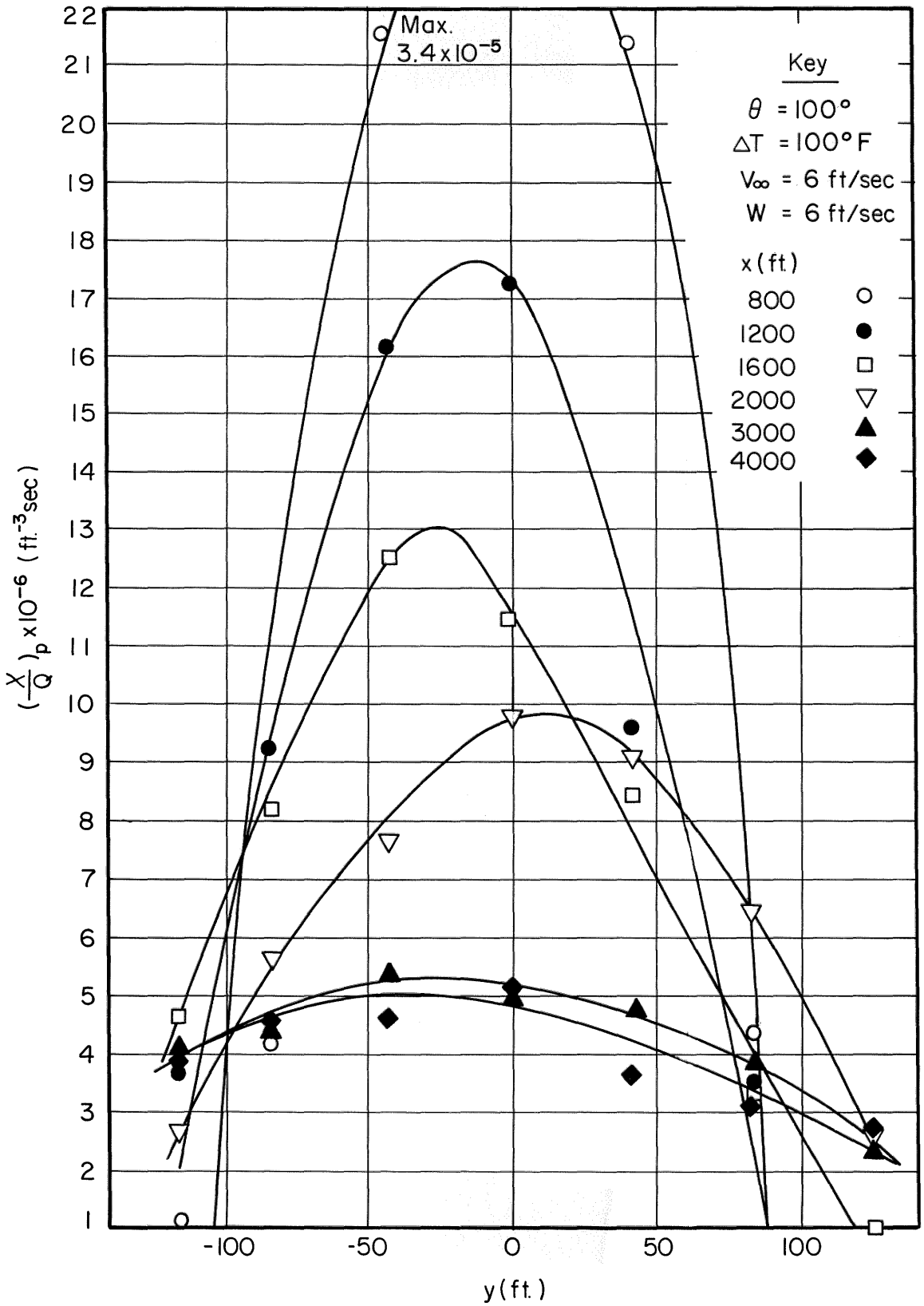

Figure 58 Horizontal concentration distributions
W/V = 1, θ = 100°, ΔT = 100°F

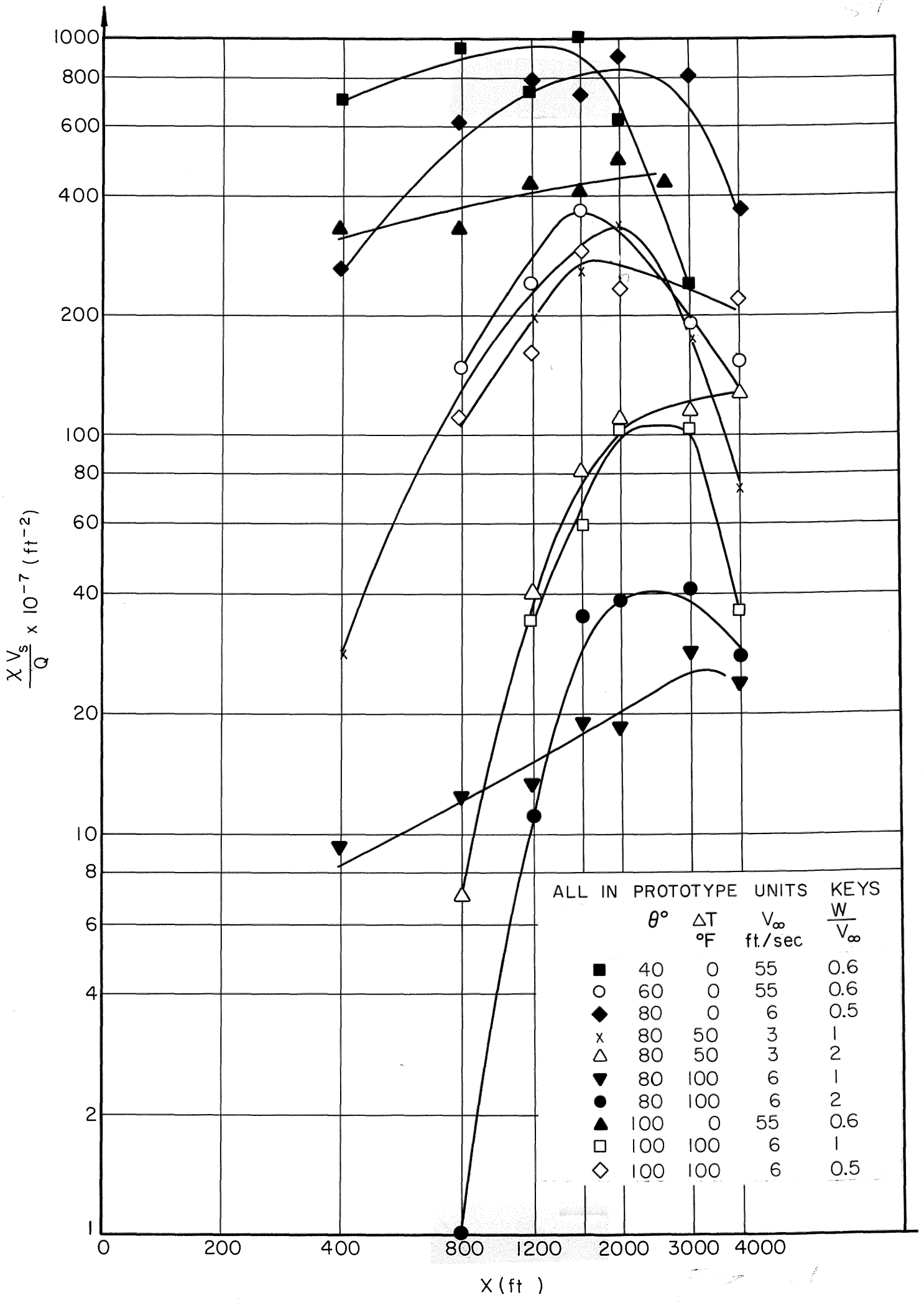

Figure 59 Maximum ground concentration vs downwind distance

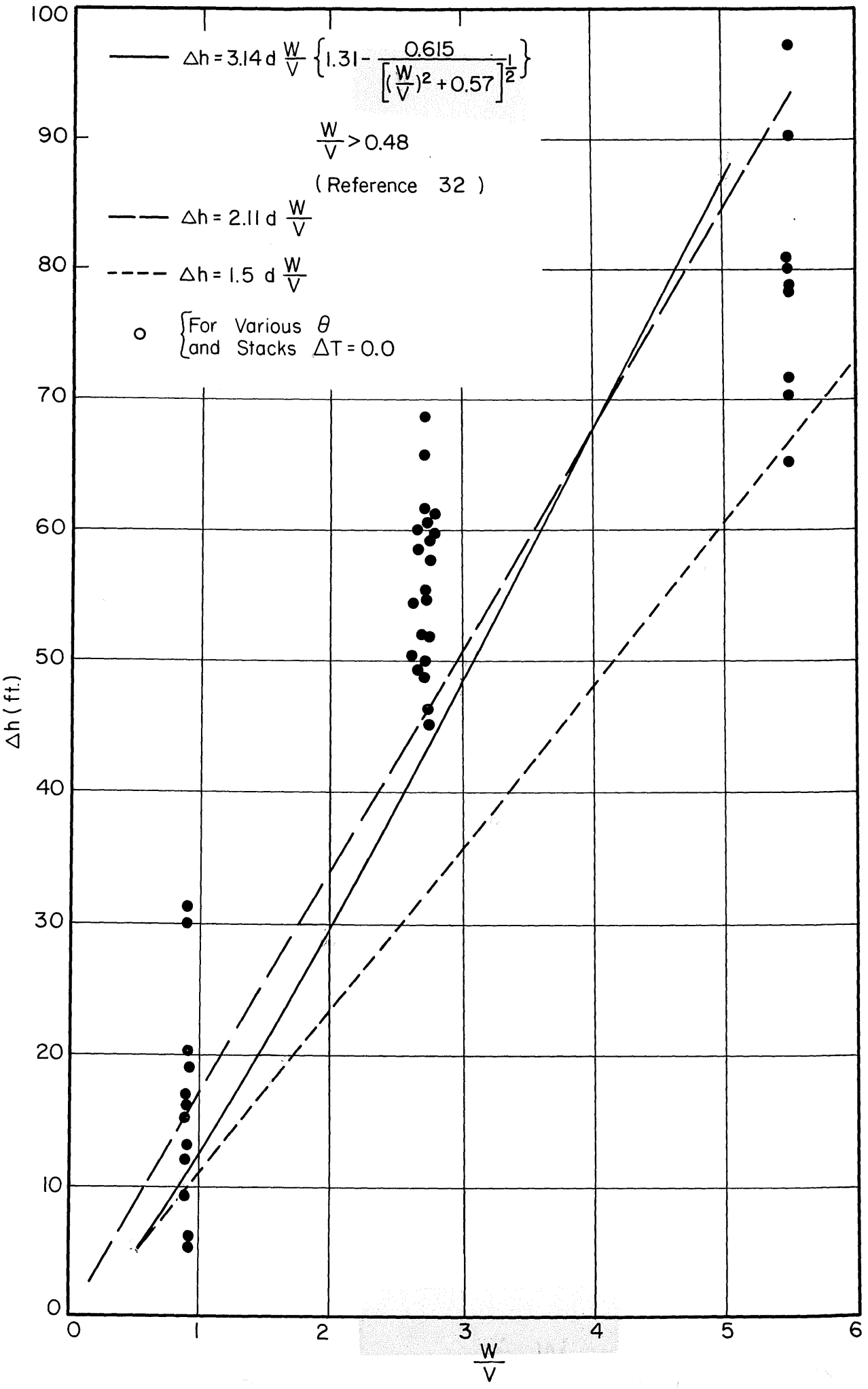

Figure 60 Plume rise vs velocity ratio

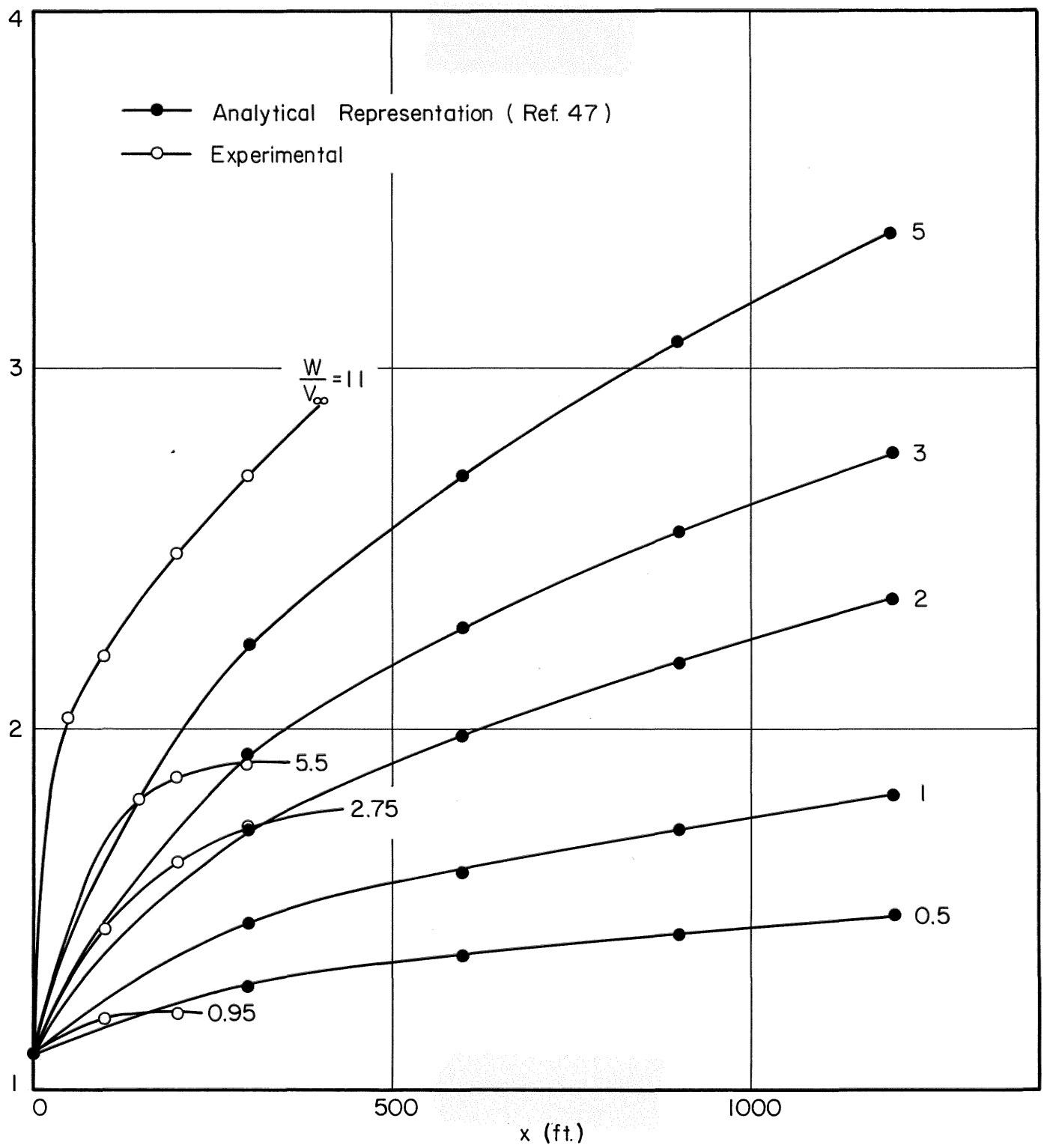

Figure 61 Plume trajectory near Stack, neutral buoyancy

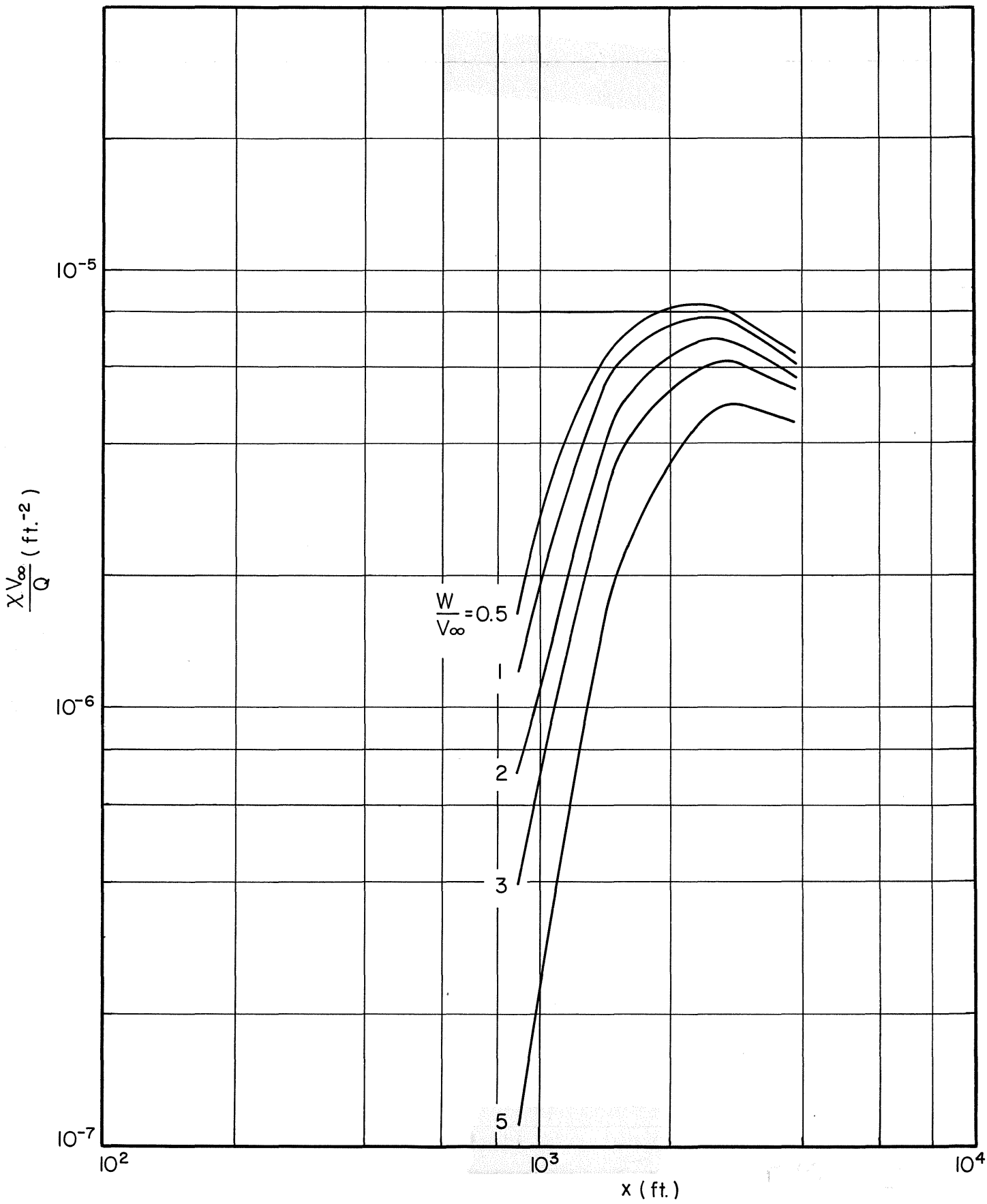

Figure 62 Analytical calculation of maximum ground concentration

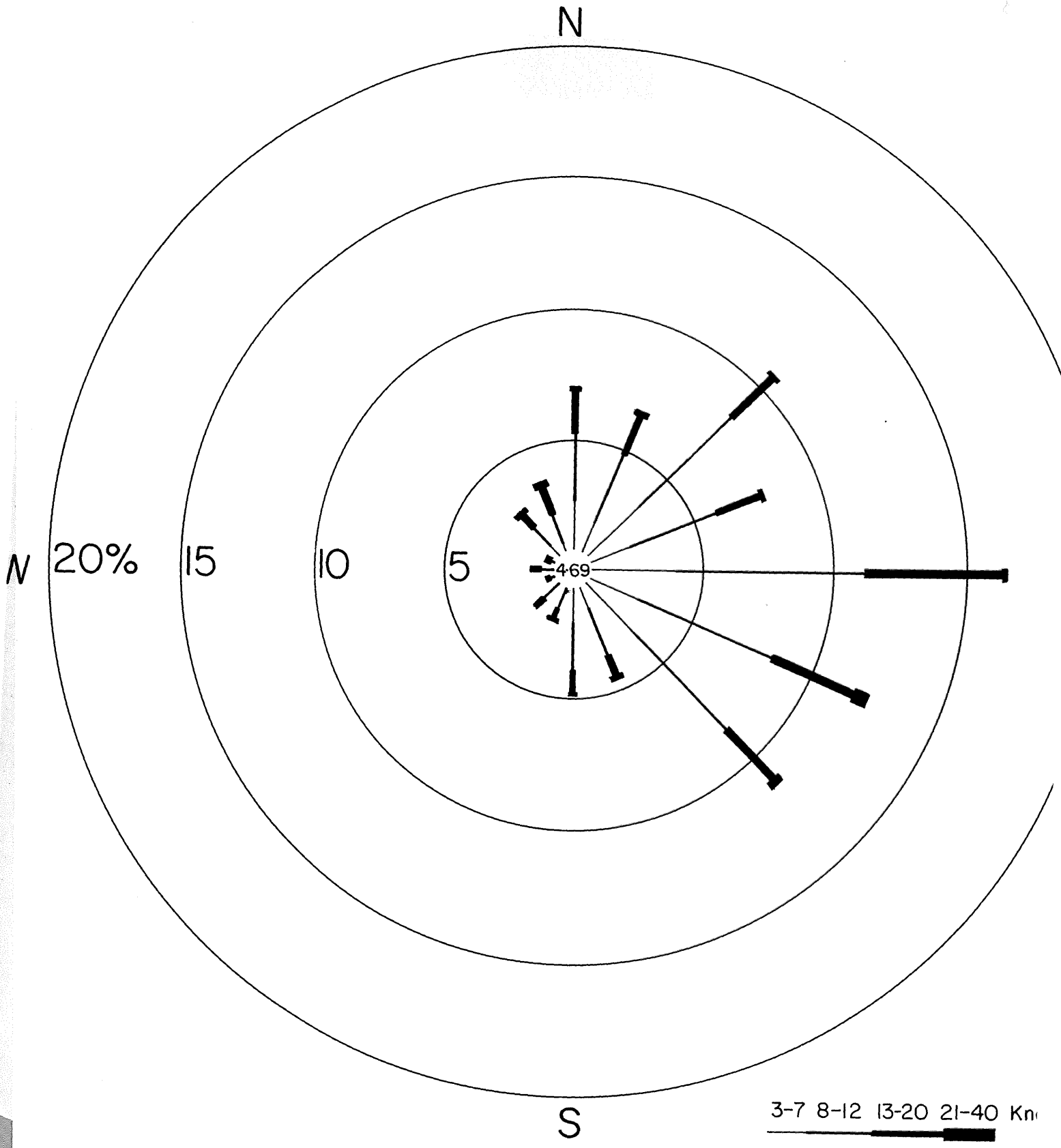

Figure A-1 Wind rose - Key West, Florida

Jan. 1949 to Dec. 1965

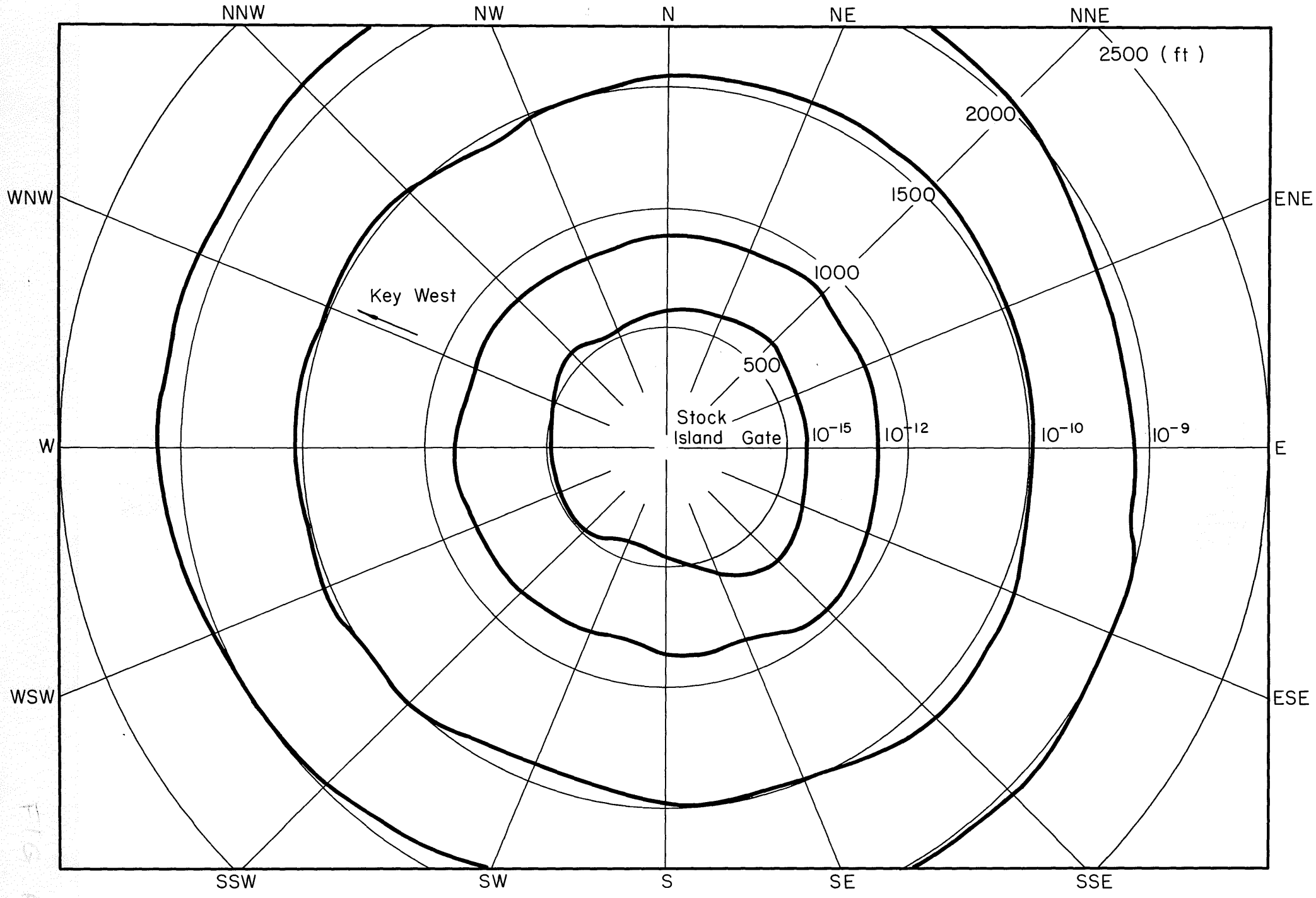

Figure A-2 Average annual concentration distribution χ/Q (sec/ft^3)

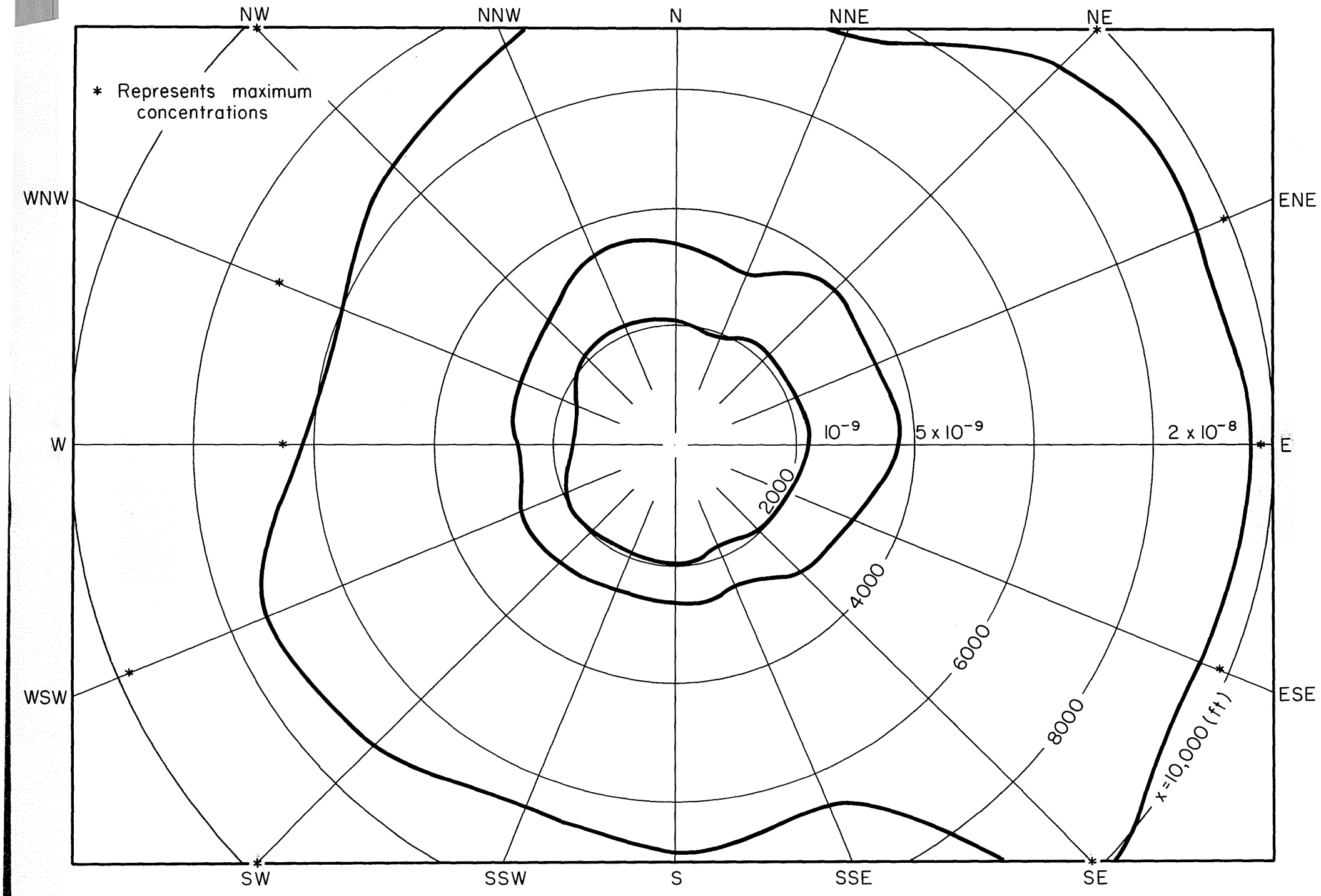

Figure A-3 Average annual concentration distribution χ/Q (sec/ft^3)